Nanoencapsulation of Ferrocene Incorporated Thiourea and Doxorubicin for Treatment of Acute Myeloid Leukemia.

Author

Nimra Idrees

Registration Number

0000326867

Supervisor

Dr. Nosheen Fatima Rana

DEPARTMENT OF BIOMEDICAL ENGINEERING & SCIENCES

SCHOOL OF MECHANICAL & MANUFACTURING ENGINEERING

NATIONAL UNIVERSITY OF SCIENCES AND TECHNOLOGY

ISLAMABAD

2023

Nanoencapsulation of Ferrocene Incorporated Thiourea and Doxorubicin for Treatment of Acute Myeloid Leukemia.

Author

Nimra Idrees

Registration Number

0000326867

A thesis submitted in partial fulfilment of the requirements for the degree of

MS Biomedical Sciences

Thesis Supervisor:

Dr. Nosheen Fatima Rana
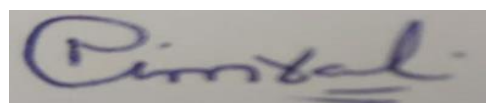
Thesis Supervisor's Signature:

DEPARTMENT OF BIOMEDICAL ENGINEERING & SCIENCES

SCHOOL OF MECHANICAL & MANUFACTURING ENGINEERING

NATIONAL UNIVERSITY OF SCIENCES AND TECHNOLOGY,

ISLAMABAD

2023

Declaration

I certify that this research work titled **Nanoencapsulation of Ferrocene Incorporated Thiourea and Doxorubicin for Treatment of Acute Myeloid Leukemia** is my own work. The work has not been presented elsewhere for assessment. The material that has been used from other sources it has been properly acknowledged / referred.

Signature of Student

Nimra Idrees

2020-NUST-MS-BMS-326867

THESIS ACCEPTANCE CERTIFICATE

Certified that final copy of MS/MPhil thesis written by **Regn No. 00000326867 Nimra Idrees** of **School of Mechanical & Manufacturing Engineering (SMME) (SMME)** has been vetted by undersigned, found complete in all respects as per NUST Statues/Regulations, is free of plagiarism, errors, and mistakes and is accepted as partial fulfillment for award of MS/MPhil degree. It is further certified that necessary amendments as pointed out by GEC members of the scholar have also been incorporated in the said thesis titled. **Nanoencapsulation of ferrocene incorporated thiourea and doxorubicin for treatment of acute myeloid leukemia.**

Signature: _____

Name (Supervisor): Nosheen Fatima Rana

Date: 16 - Nov - 2023

Signature (HOD): _____

Date: 16 - Nov - 2023

Signature (DEAN): _____

Date: 16 - Nov - 2023

Copyright Statement

- Copyright in text of this thesis rests with the student author. Copies (by any process) either in full, or of extracts, may be made only in accordance with instructions given by the author and lodged in the Library of NUST School of Mechanical & Manufacturing Engineering (SMME). Details may be obtained by the Librarian. This page must form part of any such copies made. Further copies (by any process) may not be made without the permission (in writing) of the author.

- The ownership of any intellectual property rights which may be described in this thesis is vested in NUST School of Mechanical & Manufacturing Engineering, subject to any prior agreement to the contrary, and may not be made available for use by third parties without the written permission of the SMME, which will prescribe the terms and conditions of any such agreement.

- Further information on the conditions under which disclosures and exploitation may take place is available from the Library of NUST School of Mechanical & Manufacturing Engineering, Islamabad.

Acknowledgments

Praise to be Allah Almighty, the most benevolent and the most merciful. Without His will, nothing is possible. My ideas and dreams regarding this research work would not have materialized, had it not been for Allah's blessings on me.

I acknowledge and thanks my Supervisor, **Dr. Nosheen Fatima** whose support and guidance helped me through every problem I faced in research as well as in my life. Thank you for being the best mentor.

I truly dedicate this degree to my Parents **Mr. and Mrs. Muhammad Idrees Aftab** without them I'm nothing in this world. They are the reason for my successful life, and I can't thank them enough for everything they did for me, I'll always be in debt. I would really like to say thanks to all my siblings for the constant support they provided me throughout this degree and for all the advice which helped me in my life.

And off course I'm very grateful to my friends **Urooba, Laiba, Sahar, Jannat, Osama, Amna** (my sister too) for supporting me, for encouraging me, for making this journey memorable and best years of my life. This degree was not possible without them. They are the reason I'm a better, more thankful, and more cheerful person.

Lastly, I would like to thank all the individuals who supported me throughout this degree.

Nimra Idrees

Abstract

Acute myeloid leukaemia (AML) is a type of hematologic malignancy that is distinguished by a malfunction in stem cell differentiation, which results in an accumulation of immature cells in the bone marrow and peripheral circulation. Individuals with AML require constant monitoring and novel treatment options; thus, the condition is viewed as a severe problem in the health system. The International Agency for Research on Cancer (IARC) has classified benzene as a category I carcinogen since 1987. According to the findings, benzene causes acute myeloid leukaemia (AML) and acute non-lymphocytic leukaemia (ANL). Doxorubicin (DOX) is a common first-line treatment for many malignancies. However, its therapeutic efficacy is restricted by undesired side effects such as gonadotoxicity, cardiotoxicity, and renal toxicity. The nonspecific action, poor distribution, and limited solubility of DOX are some of its drawbacks. Ferrocenyl compounds with amide or amine moieties were found to be anticancer in the lymphocytic leukaemia P-388. The activity of ferrocene integrated thiourea can be seen by focussing on the DNA, topoisomerase II, and cell membrane. They bind to DNA with great affinity via covalent or non-covalent bonds. Intercalation, groove binding, and electrostatic forces are commonly used to damage or break DNA. DNA damage causes cell cycle arrest, which leads to apoptosis and irreversible damage to the cell genome. Drug-resistant cancer cells and chemotherapeutic medicines with insufficient stability and solubility for optimal efficacy at the target location are two major difficulties in conventional cancer treatment. Liposomal nanoparticles were created for ferrocene-incorporated thiourea drug (FITU), DOX, and their combination to test their activity against benzene-induced acute myeloid leukaemia (AML) in wistar rats, and their free drug activity was compared. Before undertaking in-vivo testing, the developed nanoparticles were

characterised and evaluated in-vitro. Liposomal nanoparticles outperformed free drug in terms of reduced adverse effects and higher bioavailability due to tailored distribution via liposomal nanoparticles.

Table of Contents

List of Figures

List of Tables

Table of Abbreviations

AML	Acute Myeloid Leukemia
IARC	International Agency for Research on Cancer
DOX	Doxorubicin
FITU	Ferrocene-Incorporated Thiourea
ALL	Acute Lymphoblastic Leukemia
CLL	Chronic Lymphocytic Leukemia
CML	Chronic Myelogenous Leukemia
Np	Nanoparticles
UV-Vis spectroscopy	Ultraviolet–visible spectroscopy
XRD	X-ray Diffraction
FTIR	Fourier Transform Infrared
EDX	Energy Dispersive X-Ray Analysis
SEM	Scanning Electron Microscopy
ER	Estrogen Receptor
ROS	Reactive Oxygen Species
DOPC	1,2-Dioleoyl-sn-glycero-3-phosphocholine
DPPC	Dipalmitoyl phosphatidyl choline
PEG	Polyethylene glycol

Chapter 1: Introduction

1.1 Cancer

Cancer is defined as a condition marked by the unregulated growth of atypical cells, which possess the ability to spread to distant sites within the body (Rupapara et al., 2022). Presently, it is regarded as a substantial worldwide contributor to mortality. In the year 2020, an estimated 19.3 million individuals received a new diagnosis of cancer, leading to around 10 million fatalities. There is variation in the mortality rates among different types of cancer. In 2020, liver, stomach, and breast cancer exhibited mortality rates of 8.3%, 7.7%, and 6.9%, respectively. During the corresponding year, the mortality rate for lung cancer was observed to be 18%, whereas colorectal cancer demonstrated a mortality rate of 9.4% (Sung et al., 2021). Furthermore, blood cancer constituted around 10% of the total newly diagnosed cancer cases (Eid et al., 2021).

1.2 Hallmarks of Cancer

The identification of precise etiological variables contributing to the development of cancer is a considerable challenge. However, there exist well-documented risk factors that have been established, including alcohol intake, exposure to radiation, obesity, tobacco use, and leading a sedentary lifestyle. The term "cancer" embraces a diverse range of disorders, although a shared and defining feature is the proliferation of aberrant cells. Hanahan and Weinberg (2000) identified six cancer hallmarks in their seminal work, which collectively represent the fundamental principles that drive the proliferation and metastasis of cancer (Hanahan & Weinberg, 2000). The phenomenon of tumour development involves a series of sequential phases during which healthy cells undergo a gradual transformation into malignant cells, acquiring distinct

capabilities that facilitate their progression towards tumorigenesis (Hanahan & Weinberg, 2011). These hallmarks are:

1.2.1 Sustain Proliferative Signaling

Cancer cells can conduct unregulated proliferation, even in the absence of external stimulation. In contrast to regular cells, which effectively control the synthesis of growth factors to uphold adequate cell quantities, tissue organisation, and functionality, tumour cells display disrupted signalling pathways that confer autonomy from proliferation cues, resulting in unrestrained development. (1) Tumour cells can attain autonomy through a variety of processes. The ability to produce endogenous growth factors and their accompanying receptor sites enables the phenomenon of autocrine stimulation. (2) Tumour cells can induce neighbouring normal cells through paracrine signalling mechanisms, hence promoting the secretion of several growth factors that facilitate the proliferation of cancerous cells. (3) Cancer cells can augment their sensitivity by upregulating the quantity of growth factor receptors. (4) Self-sufficiency is attained through the disruption of negative feedback mechanisms or the activation of downstream signalling pathways, resulting in a reduced dependence on external growth stimuli (Gutschner & Diederichs, 2012).

1.2.2 Evading Growth Suppressors

 Multiple genes that encode proteins responsible for suppressing tumour growth exhibit distinct mechanisms in inhibiting cell proliferation. Notable examples include RB, TP53, and PTEN. These genes possess the capability to be activated by a range of external and internal stimuli, hence potentially initiating cell cycle arrest, senescence, or apoptosis. The activation of tumour suppressor genes is dependent on the existence of internal or external signals and can result in various biological consequences,

including senescence, cell cycle arrest, or apoptosis. In order to evade the activation or manifestation of these genes responsible for suppressing tumour growth, cancer cells utilise distinct tactics. Frequently, this process entails the full deletion of a tumour suppressor gene or the occurrence of mutations that result in the gene's inactivation. For example, a majority of human tumours display genetic alterations such as mutations or deletions in the TP53 gene.Tumour suppressor genes have the ability to interact with other proteins that are produced within tumour cells, therefore causing their inactivation or facilitating their fast destruction. The interaction between the human papillomavirus (HPV) oncogenes E6 and E7 and the tumour suppressors TP53 and RB is a significant factor in the development of HPV-associated malignancies, particularly cervical cancers This interaction leads to the inactivation of TP53 and RB (Subramanya & Grivas, 2008). Moreover, it has been observed that Mdm2, which functions as a ubiquitin ligase, is involved in the process of TP53 degradation via the proteasome route (Brooks & Gu, 2011).

1.2.3 Enabling Replicative Immortality

Cancer cells exhibit a remarkable capacity for nearly unrestricted reproduction, which stands in stark contrast to the limited number of cell division cycles observed in normal cells. The variation in replicative capacity is determined by the existence of telomeres situated at the ends of chromosomes. After every instance of cell division, the telomeric repeats undergo a gradual reduction in length, so establishing the maximum number of division cycles that a cell can undergo. Therefore, the loss of these protective telomeric ends leads to the acquisition of replicative immortality in cells (Blasco, 2005). Tumour cells have evolved two separate mechanisms to circumvent telomere attrition and sustain their proliferation. The initial strategy is the activation of telomerase, a specialised enzyme with the ability to append telomeric repeats to the ends of

chromosomes. Significantly, this phenomenon is present in nearly 90% of all human malignancies. In contrast, approximately 10% of neoplastic cells choose to engage in an alternate mechanism referred to as ALT, which stands for alternate Lengthening of Telomeres. The alternative lengthening of telomeres (ALT) is a non-conservative mechanism characterised by the redistribution of telomere tandem repeats between the sister chromatids of a chromosome (Henson et al., 2009).

1.2.4 Activating Invasion and Metastasis

Cancer cells exhibit significant alterations in their morphology and modulate their interactions with adjacent cells and the extracellular matrix, hence facilitating the initiation of intricate invasion and metastasis mechanisms. This process entails a series of modifications, commencing with the breach of intact tissue barriers, subsequently leading to intravasation into the lymphatic and circulatory systems. Upon entering these circulatory systems, cancer cells demonstrate anchorage-independent proliferation and employ tactics to elude detection by the immune system. Subsequently, extravasation becomes necessary, as the cells depart the vasculature and infiltrate certain tissues, leading to the eventual production of micrometastases and the subsequent growth of secondary tumours. (Yilmaz & Christofori, 2009).

1.2.5 Inducing Angiogenesis

The uncontrolled multiplication of cancer cells leads to an increase in tumour size and bulk. However, the growth of these cells can be limited due to a deficiency in crucial nutrients and oxygen. Nevertheless, cancer cells possess the capability to overcome these constraints by the initiation of angiogenesis, a biological process characterised by the creation of novel blood vessels. Tumor-induced angiogenesis performs a dual function, encompassing the provision of oxygen and nutrients to support tumour

growth, as well as facilitating the onset of hematogenous metastasis and the elimination of metabolic waste. In order to accomplish this, cancer cells secrete pro-angiogenic factors or, in certain instances, inhibit antiangiogenic signals to facilitate the proliferation of neovascularization. (Baeriswyl & Christofori, 2009).
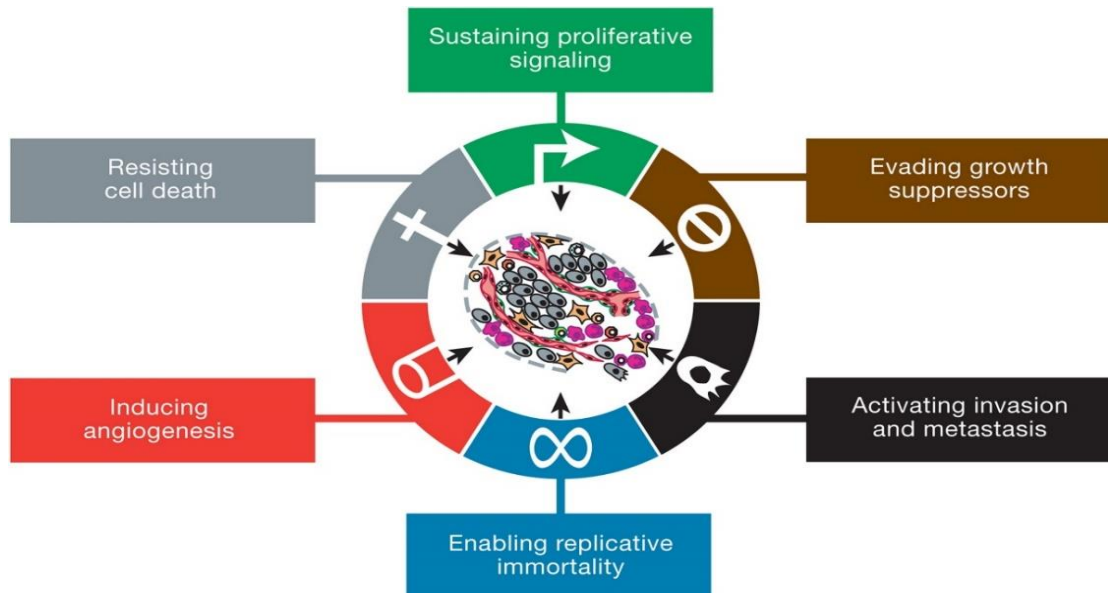
Figure 1: The Hallmarks of Cancer (Hanahan & Weinberg, 2011)

1.2.6 Resisting Cell Death

Normal cells possess three essential pathways that can lead to cell death. However, in cancer cells, the regulation of these processes is of utmost significance. Apoptosis, a regulated cellular process, can be initiated by a multitude of endogenous and exogenous stimuli. Numerous research have provided evidence indicating that tumours with a high level of aggressiveness possess the ability to inhibit apoptosis, hence developing resistance against therapeutic interventions. One approach to triggering apoptosis is the induction of DNA damage, typically accomplished through the administration of chemotherapeutic agents. This process activates the TP53 pathway, resulting in the upregulation of pro-apoptotic proteins, including NOXA and PUMA. Ultimately, this cascade of events culminates in cellular demise. On the other hand, tumours commonly

have an elevated production of anti-apoptotic proteins such as Bcl-2 and Bcl-xL, hence facilitating their survival and impeding cell death mechanisms (Adams & Cory, 2007). Autophagy is a cellular process characterised by regulated cell death, which generally occurs at a basal level within cells. Nevertheless, a range of cellular stressors, such as insufficiency in nutrients, have the potential to initiate the activation of this particular biological mechanism. Autophagy functions as a cellular recycling process, wherein cellular components and organelles are broken down to supply the cell with necessary building blocks for diverse biosynthetic pathways or to produce energy. The involvement of autophagy in cancer is multifaceted, as it can either facilitate the viability and proliferation of cancerous cells or impede the progression of carcinogenesis. In instances of significant cellular stress, the process of autophagy can induce a reversible state of cellular dormancy, enabling cells to endure unfavourable circumstances. The potential for cancer recurrence may be influenced by this survival strategy, as quiescent cells have the ability to subsequently reawaken and resume their proliferative activity. (Levine & Kroemer, 2008). Necrosis, commonly known as "uncontrolled" cell death, shares similarities with autophagy in its dual function pertaining to the proliferation of cancer cells. Necrosis has the potential to either impede or facilitate the proliferation of malignant cells. When cellular death occurs through necrosis, it leads to the production of signals that can attract proinflammatory cells. These cells with inflammatory properties can initiate several biological processes, including cell proliferation, angiogenesis, and invasion. Consequently, they provide a favourable environment that promotes the growth and dissemination of cancer cells. (Galluzzi & Kroemer, 2008).

Over the course of the previous ten years, significant progress in the field of cancer research has yielded a greater understanding of these fundamental characteristics. Consequently, this enhanced comprehension has facilitated the modification and improvement of the initial notion.

1.3 Leukemia

Leukaemia is characterised by the abnormal proliferation of leukemic cells in the bone marrow, resulting in an increased presence of precursor cells in the circulatory system. inside the realm of lymphoid malignancies, there exists an additional component characterised by anomalous cellular proliferation occurring inside lymphatic tissues (Bispo et al., 2020). Leukaemia comprises around 3% of the total cases of cancer in adults and is the most common form of cancer among children between the ages of 0 and 14. Typically, the aggregate five-year survival rate for haematological malignancies in the teenage and young adult population is approximately 50%. Despite advancements in the rates of survival for childhood cancer, it is noteworthy that blood cancer remains the primary cause of cancer-related fatalities among paediatric patients (Chulián et al., 2022).

1.3.1 Types of Leukemia

Leukaemia can be classified into two primary subtypes: myeloid (also known as myelogenous) and lymphoid (including lymphoblastic or lymphocytic). Moreover, the classification can also be determined according to the developmental stage of the cells that are impacted. Acute leukaemias are distinguished by the presence of rapidly proliferating blast cells, which are immature and undeveloped lymphocytes and myelocytes. On the other hand, chronic leukaemias are characterised by the progressive

accumulation of fully differentiated cells and manifest as a malignancy with a relatively indolent growth rate. Therefore, there are four discrete categorizations of leukaemia:

i. **Acute Lymphoblastic Leukemia (ALL):** Acute Lymphoblastic Leukaemia (ALL) is distinguished by the occurrence of B and T cells that have suffered blastic alteration. Childhood leukaemia is the prevailing form of leukaemia, accounting for approximately 80% of occurrences within this demographic, whereas adults comprise a mere 20% of instances. The management of young adults diagnosed with acute lymphoblastic leukaemia (ALL) frequently relies on paediatric treatment protocols, given their proven efficacy in achieving higher rates of survival.

ii. **Chronic Lymphocytic Leukemia (CLL):** Chronic Lymphocytic Leukaemia (CLL) is characterised by the clonal expansion of lymphoid cells and predominantly affects persons between the ages of 60 and 70.

iii. **Acute Myeloid Leukemia (AML):** Acute Myeloid Leukaemia (AML) is distinguished by the existence of a myeloid blast count exceeding 20% and is the predominant manifestation of acute leukaemia in the adult population. Acute Myeloid Leukaemia (AML) is characterised by its notable degree of behaviour that is aggressive, and the prognosis might exhibit substantial variation contingent upon the molecular subtypes implicated.

iv. **Chronic Myelogenous Leukemia (CML):** Chronic Myeloid Leukaemia (CML) typically arises because of the fusion and reciprocating translocation event involving the BCR gene located on chromosome 22 and the ABL1 gene situated on chromosome 9. The occurrence of this genetic phenomenon leads to the development of an aberrant tyrosine kinase on chromosome 22, commonly

referred to as the Philadelphia chromosome. The establishment of a monoclonal population of defective granulocytes, particularly neutrophils, eosinophils, and basophils, is attributed to the existence of the Philadelphia chromosome (Arber et al., 2016).

1.4 Acute Myeloid leukemia (AML)

Acute Myeloid Leukaemia (AML) is a malignancy distinguished by the invasion of the bone marrow, blood, and several organs by a clonal and vigorously proliferating population of haematological cells. These cells frequently demonstrate inadequate differentiation and may sporadically display suboptimal differentiation (Döhner et al., 2022).The primary categorizations of Acute Myeloid Leukaemia (AML) include subtypes such as AML with recurrent genetic abnormalities, AML with myelodysplasia-related alterations, therapy-related AML, and AML not otherwise described (Hartmut Döhner, 2015).

1.4.1 Epidemiology of Acute Myeloid leukemia (AML)

The prevalence of Acute Myeloid Leukaemia (AML) is estimated to be around 4.2 cases per 100,000 individuals in both genders, leading to an annual occurrence of over 20,000 new cases in the United States. Acute myeloid leukaemia (AML) is frequently detected in individuals of non-Hispanic white ethnicity, and males demonstrate a higher prevalence compared to females, with a ratio of 5 to 3. At the time of diagnosis, the typical age is roughly 65. Acute myeloid leukaemia (AML), a disease previously deemed as untreatable, has witnessed substantial advancements in therapeutic efficacy. At now, it has been seen that a cure can be achieved by approximately 35-40% of adult patients who are below the age of 60, whereas a lower percentage of 5-15% of older patients have been found to attain the same outcome. (Sung et al., 2021).

1.4.2 Symptoms

The clinical signs of Acute Myeloid Leukaemia (AML) span a spectrum of symptoms, which include anaemia, propensity for bruising, excessive bleeding, bone pain, recurrent infections, and headaches. The physical examination has the potential to identify various indicators, including pallor, bruising, hepatomegaly (the enlargement of the liver), and splenomegaly (the enlargement of the spleen). Patients diagnosed with acute myeloid leukaemia (AML) have an increased susceptibility to the development of disseminated intravascular coagulation (DIC), a pathological condition characterized by abnormal blood clotting throughout the body. This illness, if left untreated, can result in the invasion of organs by these blood clots. Although fatigue and shortness of breath are shared symptoms between Chronic Lymphocytic Leukaemia (CLL) and Acute Myeloid Leukaemia (AML), CLL is characterized by lymphadenopathy (enlarged lymph nodes), cough, and hypertension, while AML is distinguished by nosebleeds, bleeding gums, fever, flu-like symptoms, abdominal pain, chest pain, vomiting, and nausea (Shephard et al., 2016).

1.4.3 Prognostic Factors

The prognostic factors for Acute Myeloid Leukaemia (AML) can be classified into two categories: patient-associated factors and disease-related factors. Various patient-related characteristics, such as advanced age and the coexistence of comorbidities, frequently exhibit a positive association with an elevated likelihood of premature mortality. On the other hand, disease-related characteristics, such as specific genetic alterations inside cells that are leukemic and the leukemic-cell count, can function as indications of resistance to conventional therapy. Several factors can influence treatment results and responsiveness to therapy in leukaemia. These include previous

cytotoxicity therapy for a different condition, an elevated white cell count, and specific genetic abnormalities in leukaemia cells (Hartmut Döhner, 2015).

1.4.4 Genomic Landscape

Various genes have been discovered as playing a role in the development of different types of cancer, with mutations in these genes being a contributing factor. These mutations exert their influence through a range of ways. As an illustration, alterations in signalling genes such as FLT3 have the potential to augment cellular proliferation through the modulation of signalling pathways. Disruptions in gene expression and blood cell differentiation can occur because of mutations in transcription factors, such as RUNX1, and specific chromosomal rearrangements. Mutations occurring in the nucleophosmin (NPM1) gene have the potential to induce aberrant protein localization.
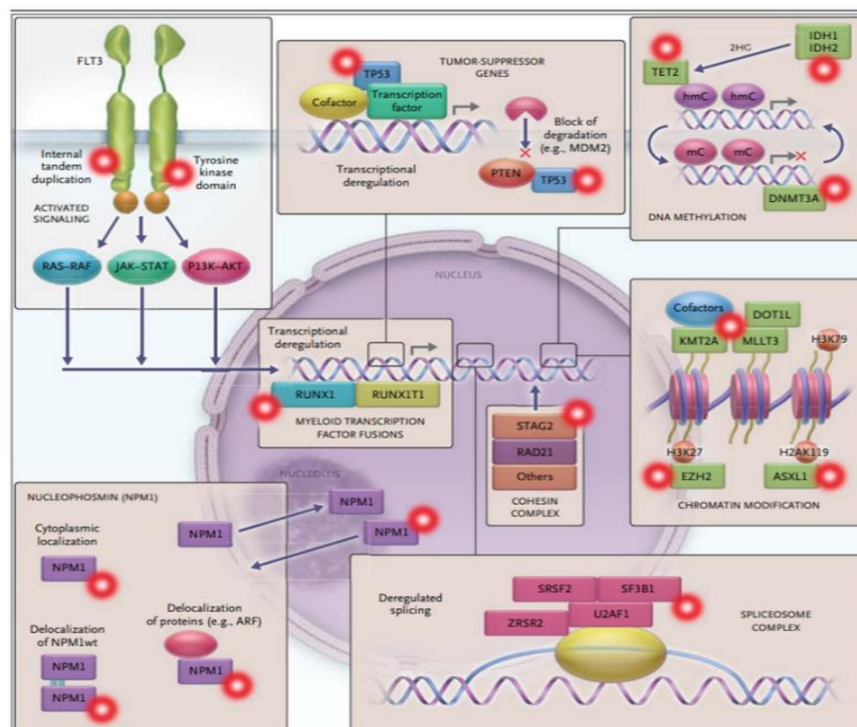
Figure 2 Genes That Are Mutated In AML(Hartmut Döhner, 2015)

Furthermore, disruptions in the genetic makeup of spliceosome complex-related genes, such as SRSF2 and SF3B1, have the potential to impede the proper processing of RNA

molecules. Genetic modifications are known to exert a substantial influence on the initiation and advancement of cancer (Cancer Genome Atlas Research et al., 2013).

Disruptions in chromosomal segregation and transcriptional control can occur because of mutations in genes associated with the cohesin complex, including STAG2 and RAD21. Dysregulation of chromatin modification can occur because of mutations in genes associated with epigenetic processes, such as ASXL1 and EZH2. DNA methylation anomalies can occur due to mutations in genes such as DNMT3A, TET2, IDH1, and IDH2. Moreover, alterations in tumour suppressor genes, such as TP53, can result in the dysregulation of gene expression and impairments in degradation processes due to interactions with proteins such as MDM2 and PTEN. The presence of these mutations together influences the initiation and advancement of cancer by impacting crucial biological mechanisms (Christiansen et al., 2005).

1.4.5 Risk Factors

There is a notable correlation between smoking and the increased susceptibility of individuals to acquire Adult Acute Myeloid Leukaemia (AML). Multiple meta-analytic studies have consistently demonstrated an increased susceptibility to acute myeloid leukaemia (AML) among individuals who engage in smoking behaviour. An investigation conducted by Ugai et al. examined data from nine cohort studies in Japan, revealing that persons with a smoking history above 30 pack-years had a 66% elevated risk of acquiring acute myeloid leukaemia (AML) in comparison to non-smokers. Individuals who are presently engaged in smoking activities shown an approximately 40% elevated susceptibility to acute myeloid leukaemia (AML). The results of this study highlight the significant correlation between smoking behaviour and the likelihood of developing acute myeloid leukaemia (AML) in the adult population.(Ugai et al., 2017).

While the available information about the association between environmental chemical exposures and Acute Myeloid Leukaemia (AML) may not be as extensive, it is important to note that benzene exposure has been identified as a recognised risk factor. The International Agency for Research on Cancer (IARC) has established a link between benzene exposure and AML. Benzene is frequently utilised within the United States, with those employed in various industries such as rubber manufacture, oil refining, shoe manufacturing, and gasoline-related jobs experiencing the greatest occupational exposure to this chemical. Consequently, these individuals are at an increased vulnerability to acute myeloid leukaemia (AML).(Khalade et al., 2010; Raaschou-Nielsen et al., 2018).

1.4.6 Role of Benzene in Acute Myeloid Leukemia

Benzene is an aromatic liquid that exhibits flammability, possessing a chemical formula of C6H6 and having a molecular weight of 78.11. It is identifiable by its pale yellow hue and distinctive odour. The substance exhibits limited solubility in water, while demonstrating solubility in solvents that are organic and oils. Benzene exhibits a pronounced reactivity towards oxidizing chemicals and possesses a notable propensity for vaporization.
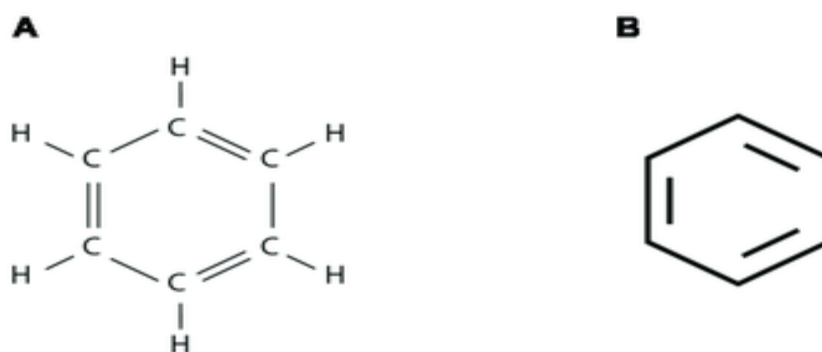
Figure 3 Structure of Benzene *(Hameroff, 2022)*

Benzene can be encountered through various routes of exposure, including inhalation, dermal contact, or ingestion. Research conducted on animals has demonstrated that over

50% of benzene that is breathed is taken in by the body. Upon entering the human body, benzene undergoes rapid metabolism in the liver, resulting in the conversion of benzene into water-soluble molecules. These chemicals are subsequently eliminated from the body through urine within a timeframe of 48 hours. Certain metabolites have the ability to translocate to the bone marrow as well. Although benzene is generally considered non-toxic, its metabolites, specifically benzoquinone and mucoaldehyde, have the potential to cause detrimental effects on the bone marrow (Ross, 2000).

Benzene has been designated as a Group I carcinogen by the International Agency for Research on Cancer (IARC) since 1987. The Enforcement Decree of Industrial Accident Compensation Insurance Acts in 2003 specified precise conditions. According to these criteria, the presence of benzene at a concentration of 1 part per million (ppm) or more for a period of 10 years or more is deemed significant enough to result in occupational illnesses such as leukaemia and multiple myeloma. In instances where the overall duration of exposure falls below 10 years, it is important to note that a cumulative exposure over 10 ppm-years is still regarded as an adequate level of exposure. The International Agency for Research on Cancer (IARC) has shown that benzene has low association with other haematological malignancies, with the exception of acute non-lymphocytic leukaemia (ANLL) and acute myeloid leukaemia (AML) (Yoon et al., 2018).

i.   **Metabolism of Benzene:** The metabolic processes associated with benzene encompass multiple sequential reactions. The first stage involves the process of oxidation mediated by cytochrome P450 (CYP), leading to the production of benzene oxide and its tautomeric form, oxepin. Benzene oxide undergoes subsequent spontaneous rearrangement, resulting in the formation of phenol (PH). Phenol can be excreted or further metabolised into 1,4-benzoquinone (HQ) and 1,4-

benzoquinone (1,4-BQ). The benzene oxide that remains has the potential to undergo hydrolysis, resulting in the formation of catechol (CA) and 1,2-benzoquinone (1,2-BQ). Alternatively, it can also undergo a reaction with glutathione, leading to the production of S-phenylmercapturic acid (SPMA). The metabolic process of oxepin can result in the generation of reactive muconaldehydes and E,E-muconic acid (MA) by means of the aromatic ring's opening. The aforementioned metabolites, including benzene oxide, BQs, muconaldehydes, and benzene diol epoxides, exhibit electrophilic properties that enable them to engage in reactions with proteins within cells, so disrupting their regular functionality. The complete understanding of the specific function of these metabolites in the carcinogenicity of benzene remains incomplete. However, it is widely acknowledged that the conversion of hydroquinone (HQ) into benzoquinones (BQs) through the activity of myeloperoxidase in the bone marrow is regarded as a crucial stage.

There exists empirical data suggesting that this particular pathway plays a substantial role in the genesis of BQ. The protective effects of the enzyme NQO1 against benzene-induced myelodysplasia and hematotoxicity have been demonstrated in studies conducted on both mice and humans. Nevertheless, it is crucial to acknowledge that potential negative consequences arising from alternative metabolites within the benzene metabolic pathway cannot be disregarded, and the precise processes responsible for benzene's ability to cause cancer are still an area of active investigation. (Henderson et al., 2005; Iskander & Jaiswal, 2005; Waidyanatha & Rappaport, 2005).

Research has indicated that in laboratory conditions, benzene and its metabolites, such as hydroquinone and 1,4-benzoquinone, might accelerate DNA cleavage and inhibit the

activity of topoisomerase II. The genotoxic effects of benzene are linked to this disruption of DNA activities. (Lindsey et al., 2005).
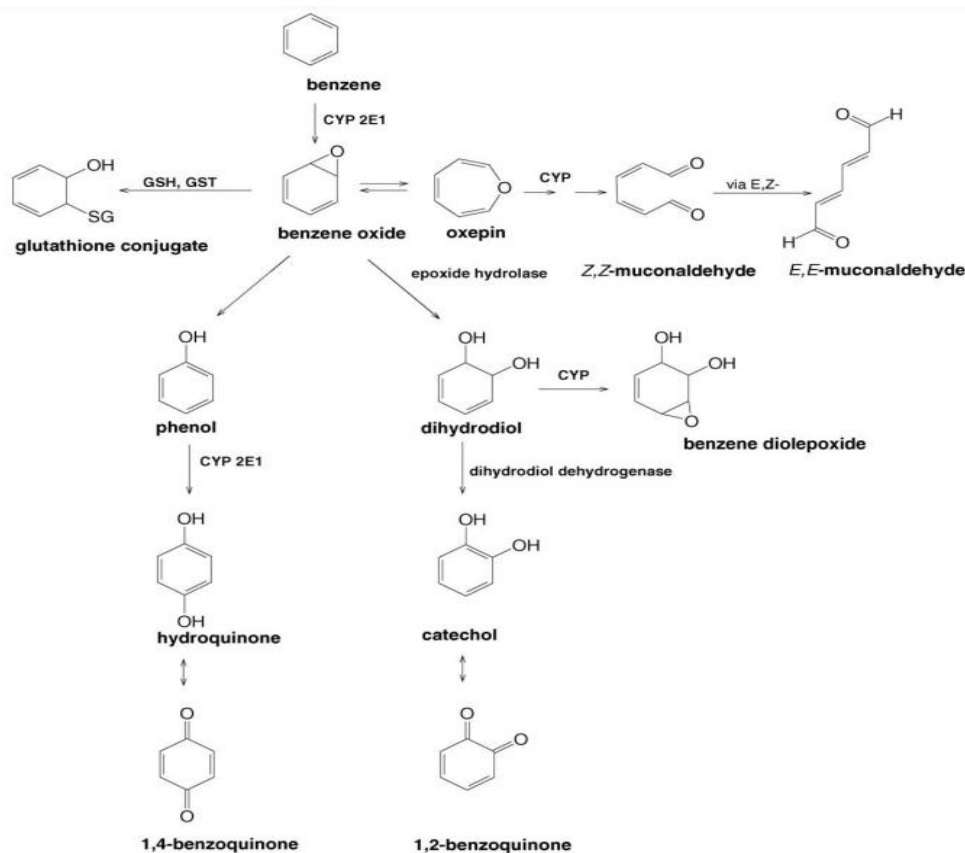
Figure 4 Metabolism of Benzene (Waidyanatha & Rappaport, 2005)

The intensity of topo II inhibition is increased when peroxidase converts hydroquinone (HQ) to 1,4-benzoquinone (BQ). In cell-free tests, BQ is a more powerful topo II inhibitor than HQ. Exposure to benzoene can alter the leukemogenic process in a number of ways, including immune system failure, oxidative stress, disruption of microtubules, and chromosomal damage (Rivedal & Witz, 2005). Specific microRNAs, DNA methylation, gap-junction-intercellular communication, and stem cell pools are all impacted by benzene hematotoxicity (Cho, 2008; Li et al., 2009). This intricate mechanism suggests that benzene's leukemogenic effects are complex and occur at different stages of the process. Background and hobby/occupational benzene exposures

28

have cumulative effects and comparable effects. It appears that there is no practical threshold and that the effects of individual benzene molecules accumulate linearly based on the frequency of ambient consumption of benzene as a combustion by-product (Smith, 2010).

1.4.7 Diagnosis of Acute Myeloid Leukemia

Finding evidence of anaemia, thrombocytopenia, leukopenia, or even leukocytosis in the patient's peripheral blood is usually the first step in the diagnosis of acute myeloid leukaemia (AML). A bone marrow aspirate and biopsy are usually carried out to confirm the diagnosis, and peripheral blood samples are taken for morphologic and genetic evaluations, immunophenotyping, flow cytometry, and other investigations. The diagnosis of acute myeloid leukaemia (AML) is confirmed by the results of the bone marrow aspirate and biopsy, which frequently show a hypercellular marrow with a reduced proportion of typical hematopoietic cell types and an extensive number of blasts, which are immature white blood cells (Rose-Inman & Kuehl, 2014). Several colours and chemical markers are used in flow cytometry to classify leukaemia cells. By using a technique called immunophenotyping, it is possible to distinguish between leukemic and healthy cells based on the pattern of surface proteins that are expressed on each type of cell. This method is useful for identifying and categorizing various forms of leukaemia (Severson, 2016). Differentiation levels and patterns of cell surface proteins are key factors in classification and diagnosis. (Arber et al., 2016).

A minimum of 20% myeloblasts must be present in a peripheral blood sample or bone marrow biopsy for AML to be diagnosed. Risk assessment is aided by additional diagnostic tests such as molecular investigations, cytogenetics, and flow cytometry. AML blasts frequently display the CD33 and CD13 antigens (Estey, 2016). Fluorescence in-situ hybridization (FISH) testing can be used to identify cytogenetic

anomalies such as t(15;17), t(8;21), t(6;16), and inv(16). Gene anomalies in NPM1, CEBPα, IDH1, IDH2, TP53, cKIT, or FLT3 ITD or TKD may be discovered using molecular testing. Furthermore, it is recommended to perform a full metabolic panel, liver function test, serum lactic acid dehydrogenase, and uric acid. In order to be considered for hematopoietic cell transplantation, patients must have a positive human leukocyte antigen type. A lumbar puncture or computed tomography scan may be necessary in addition to other diagnostic procedures, depending on the clinical symptoms and presentation of the patient (Blackburn et al., 2019).

1.4.8 Treatment of Acute Myeloid Leukemia

Establishing disease control and, when possible, achieving total eradication are the aims of AML treatment. This usually entails starting therapy with the goal of obtaining complete remission (CR), and then using consolidating and/or maintenance therapy to deepen the remission and prolong the duration of response. For those who qualify, allogeneic stem cell transplant is a possibility. When a patient is unable to receive either intensive or non-intensive treatment, supportive care and transfusions are used to improve the patient's quality of life and reduce problems connected to cytopenia. Services for palliative care are also offered when needed (Döhner et al., 2022). The high frequency of unfavorable genetic traits, the long-term consequences of prior treatment, and occasionally the persistence of the underlying disease all contribute to the generally poor survival percentage of AML patients with therapy-related disease (Kayser et al., 2011; Röllig et al., 2020). Generally, whether a patient is eligible for intensive or non-intensive treatment, their care should be guided by the same basic therapeutic concepts. (Jentzsch et al., 2021).

During the induction phase of intensive therapy, anthracycline and cytarabine combinations, also known as "7+3" regimens, are usually used. In 60% to 80% of cases,

younger persons experience complete remission (CR), whereas older adults (60 years of age and older) experience CR in 40% to 60% of cases. Consolidation is usually performed with regimens that include intermediate-dose cytarabine, ideally given consecutively on days 1 through 3 (Dumas et al., 2020; Jaramillo et al., 2017). While some centers continue to employ high-dose cytarabine (3000 mg/m2), its increased toxicity and lack of improvement in survival argue against its prolonged usage (Burnett et al., 2013).

After obtaining CR, maintenance therapy for AML attempts to lower the chance of relapse by offering a less hazardous course of treatment. The principal objective is to provide medication with minimum toxicities while effectively lowering the risk of leukemic recurrence. Given subcutaneously for up to 12 cycles, azacitidine maintenance therapy has been demonstrated in a randomized study involving newly diagnosed older patients in their first remission following two cycles of intense induction to improve disease-free survival when compared to no maintenance (Huls et al., 2019). Only when hematopoietic stem cell transplantation (HSCT) provides a longer predicted survival time and better quality of life than alternative treatments is it advised. It should also be carefully considered based on each patient's unique transplant outcomes and the most recent guidelines (Takami, 2018).

Even with the variety of therapy choices available, continued clinical research is necessary to investigate novel medicines and combinations in order to improve patient outcomes (Döhner et al., 2021).

Chapter 2: Literature Review

2.1 Doxorubicin

The drug falls within the category of nonselective class I anthracyclines, which consists of both aglyconic and sugar components. The aglycone is composed of a tetracyclic ring with adjacent quinone-hydroquinone groups, a short side chain containing a methoxy substituent, and a carbonyl group. The sugar component, known as daunosamine, is linked to one of the rings through a glycosidic bond and comprises a 3-amino-2,3,4-trideoxy-L-fucosyl moiety. (Hilmer et al., 2004).
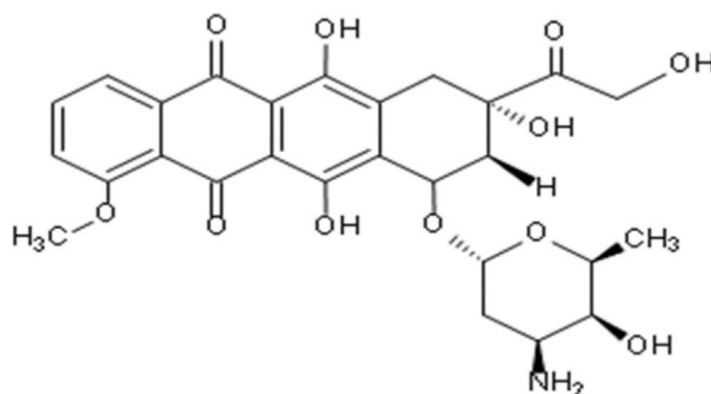
Figure 5 Structure of Doxorubicin (Ibrahim et al., 2022)

2.1.1 Mode of Action of Doxorubicin

There are a variety of drugs that can interfere with DNA, resulting in disturbances in the process of cell replication. These disruptions ultimately contribute to the increased effectiveness of these medications in combating cancer. The anticancer efficacy of doxorubicin can be ascribed to its quinone and amino group constituents, as evidenced by previous studies (Jawad et al., 2019; Moiseeva, September 2018). Although the exact mechanism by which doxorubicin exerts its effects is not completely understood,

it has been associated with several processes. These include DNA unwinding and separation, increased alkylation, the release of cytochrome c from mitochondria, the inhibition of topoisomerase II, intercalation within DNA, and the generation of free radicals. These actions collectively lead to oxidative stress, ultimately contributing to the cytotoxic effects of doxorubicin (Hanušová et al., 2011).
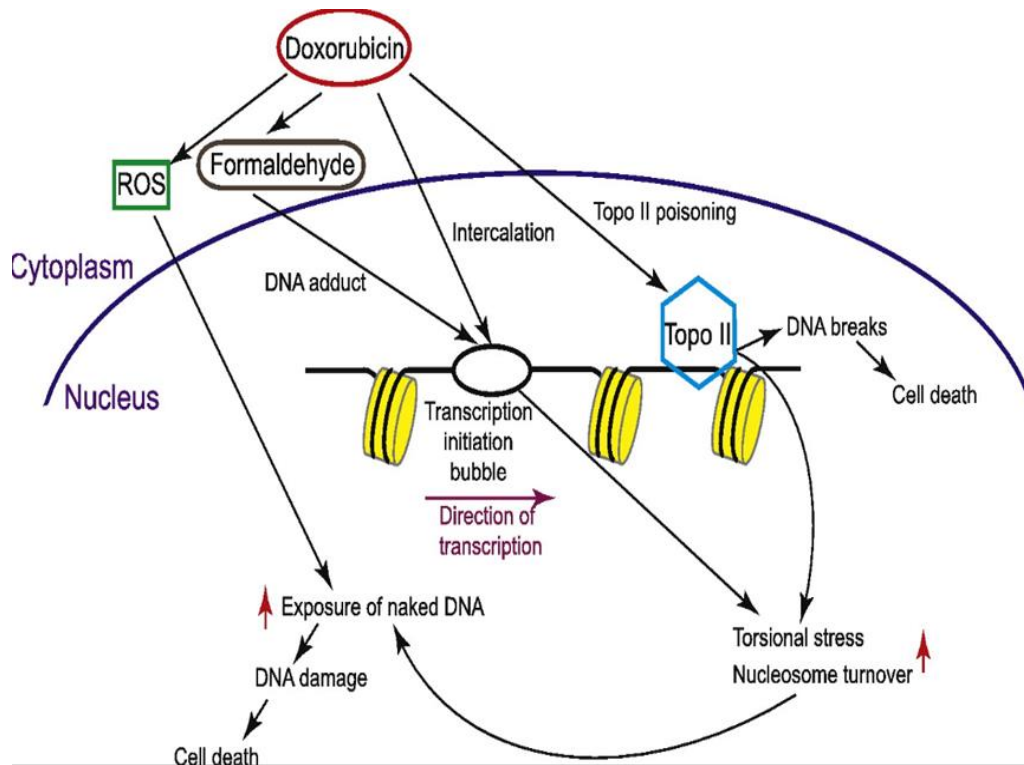
Figure 6 Mode of Action of Doxorubicin (Yang et al., 2014)

However, the primary mode of action of doxorubicin mostly revolves around the disruption or inhibition of the enzyme topoisomerase II. The interference described in the statement results in the occurrence of DNA damage and, ultimately, the demise of cells. This interference occurs due to the hindrance of macromolecular biosynthesis, which is caused by the intercalation of doxorubicin with DNA. This process involves the utilisation of the sugar components and the cyclohexane ring of doxorubicin. The research findings indicate that doxorubicin has binding affinity towards both mitochondrial and nuclear DNA, resulting in the subsequent elimination of tumour cells

(Denel-Bobrowska & Marczak, 2017). The significance lies in the poisoning of topoisomerase II and the resulting DNA damage, given that cancer cells exhibit greater susceptibility to DNA breaks in comparison to normal cells. Moreover, doxorubicin possesses the ability to generate a substantial quantity of Reactive Oxygen Species (ROS), such as hydrogen peroxide (H_2O_2) and superoxide anions (O_2^-), which have the potential to be transformed into free radicals (OH). This phenomenon induces oxidative stress, ultimately resulting in the apoptosis of tumour cells, wherein cellular membrane lipids, proteins, and DNA are detrimentally affected (Moiseeva, September 2018; van der Zanden et al., 2021).

Doxorubicin is commonly utilized as a first therapeutic intervention for a variety of cancer forms. However, the therapeutic efficacy of the treatment is compromised due to the presence of adverse effects, such as renal toxicity, cardiotoxicity, and gonadotoxicity (Mohan et al., 2021). Doxorubicin is associated with many limitations, such as its non-specific mechanism of action, insufficient dispersion, and restricted solubility. Furthermore, a significant number of its negative consequences are contingent upon the dosage administered, and its effectiveness in inhibiting tumour growth is primarily observable at elevated dosages. Increased dosages of doxorubicin have the potential to cause gonadotoxicity, which may result in infertility because of testicular and ovarian toxicity. Testicular toxicity is characterized by various physiological changes, including a drop in testicular weight, a reduction in testosterone levels, and a decline in testicular lipid content. These alterations can ultimately lead to impaired sperm motility and the development of zinc insufficiency within the testicles. Likewise, the occurrence of ovarian toxicity can lead to a reduction in the size of the ovaries (Çeribaşı et al., 2012; Silva et al., 2018). In addition, it should be noted that elevated dosages of doxorubicin have the potential to induce irreversible cardiotoxic

effects, hence making it inappropriate for patients with reduced cardiac function, particularly among the older patient demographic. (Abdelaziz et al., 2019; Umlauf & Horký, 2002).

2.2 Organometallic Compounds

Coordination complexes known as organometallic compounds are characterised by the presence of at least one bond between a metal atom and a carbon atom. Additionally, these compounds have the ability to form bonds between the metal atom and hydrogen atoms (Gasser et al., 2011). Prominent within the realm of petrochemical catalysis are several types of organometallic compounds, including metallocenes, half-sandwich complexes, carbenes, CO ligands, and alpha ligands. It is noteworthy that these compounds also demonstrate characteristics that are well-suited for medical applications in the treatment of several disorders (Beller, 2012; Kitanovic et al., 2014).

Figure 7 Types of Organometallic Compounds(Gasser et al., 2011)

Nevertheless, the metal ions in biological environments are subject to reactivity, prompting cells and tissues to effectively regulate their metal ion levels. There is a correlation between disturbances in metal ion concentrations and the occurrence of certain illnesses, such as cancer. As a result, there has been a significant focus on metal-containing compounds due to their potential as agents for combating cancer. This is because these compounds have the ability to interfere with the exact regulation of metal ions. The identification of cisplatin, scientifically referred to as cis-[Pt(II)(NH3)2Cl2], marked a notable advancement in the application of metal compounds for the treatment

of cancer. This achievement generated enthusiasm for exploring platinum(II) and other metal-based complexes as innovative approaches to combat cancer (Pedro Martins, 2014).

2.3 Ferrocene

During the early 1950s, the fortuitous discovery of ferrocene was made by Kealy and Pauson, researchers at Duquesne University, by the reaction of C5H5BrMg with FeCl3 (Hamera, 2015). Ferrocene demonstrates remarkable structural and electrical characteristics (Astruc, 2017). Significantly, it has exceptional thermal stability up to a temperature of 400°C and displays resistance to light, oxygen, and moisture. Ferrocene, characterised by its iron centre exhibiting the saturated electrical configuration akin to krypton, may be readily subjected to standard functionalization techniques and has good solubility in a wide range of commonly used organic solvents. The Cp rings present in ferrocenes possess a partial negative charge, so conferring upon them electron-donating properties. This property enables electrophilic substitution reactions to take place (Dai et al., 2003). Ferrocene has a favourable bioisosteric property with aryl and heteroaryl groups due to its low toxicity (Larik et al., 2017; Patra & Gasser, 2017). In contrast to a saturated calomel electrode, ferrocene also exhibits a moderate and reversible oxidation around +0.4 V., it has been demonstrated that the ferrocenium/ferrocene pair (Fc+/Fc) possesses a wide range of redox capabilities, making it a highly adaptable system for the advancement of switchable functional systems. (Fabbrizzi, 2020). The inter-ring separation in ferrocene, estimated to be around 3 Å, facilitates the occurrence of hydrogen bonding (HB) (Moriuchi, 2022)) and potentially enables other noncovalent interactions between the connected groups on the two cyclopentadienyl (Cp) rings (Kovač et al., 2022). The physicochemical properties of ferrocene render it a powerful pharmacophore that exhibits advantageous

impacts on biological systems. Ferrocene compounds have been found to possess a range of pharmacological activities, including antileishmanial, antifungal, anticancer, and antitumor effects (Hottin et al., 2012).
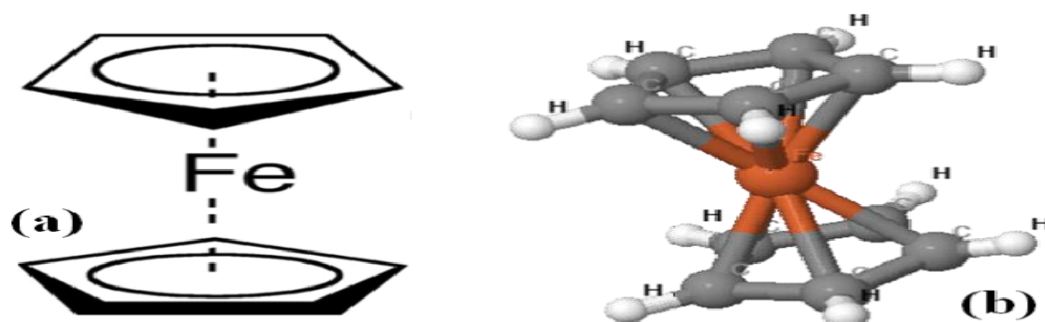
Figure 8 Structure of Ferrocene (Visconti et al., 2017)

The iron (Fe) oxidation state is often linked to the anticancer activities of ferrocenyl derivatives. Iron (II) compounds generally demonstrate greater efficacy in comparison to iron (III) derivatives, primarily due to their ability to cause conformational alterations in receptor proteins. It is noteworthy that some chemicals have significant electrostatic interactions with DNA in their oxidised form, as opposed to their reduced form. The electrostatic interaction described above pertains to the interaction between the phosphate groups that are negatively charged of nucleotides and the $Fe+3$ ions found in the ferrocenyl moiety (Hillard et al., 2006).

2.4 Thiourea

The thiourea functional group plays a crucial role in certain anticancer drugs, such as sorafenib, which is a multikinase inhibitor comprising a diarylthiourea derivative, and tenovin-1, a benzylthiourea molecule that works as a reversible inhibitor of class III HDAC. Additionally, previous studies have indicated that thiourea molecules possessing (hetero)aryl end groups that are enhanced with electron-negative substituents have the potential to elicit various biological effects beyond cytotoxicity.

37

These effects encompass antibacterial, (Bielenica et al., 2015; Maalik et al., 2019), antiviral, antimycobacterial (Doğan et al., 2020; Kollu et al., 2021), antioxidant, and anti-inflammatory effects, and central nervous system activation properties (Kaymakçıoğlu et al., 2005; Stefanska et al., 2012).

The importance of halogenated phenyl-containing heterocyclic thiourea derivatives has been established in their role as effective anticancer medicines targeting solid tumours. The aforementioned chemicals, including 1,3,4-thiadiazine, piperidine, quinazoline, and thiazole derivatives, exert their biological effects through the inhibition of vascular endothelial growth factor receptor 2, epidermal growth factor receptor kinase, or acetylcholinesterase (Mowafy et al., 2016; Ragab et al., 2019; Turan-Zitouni et al., 2016). Furthermore, the nitrophenyl group present in the thiourea derivative has demonstrated considerable potential as a cytotoxic agent against a range of solid tumours, including lung, colorectal, prostate, and breast cancer. This cytotoxic action is attributed to its ability to inhibit the mitogen-activated protein kinase enzyme known as MK-2 (Ghorab et al., 2016; Liu et al., 2015).
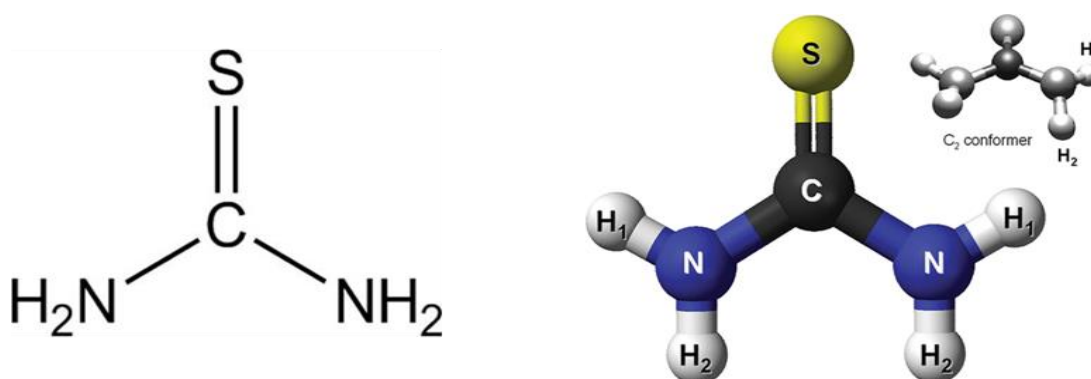
Figure 9 Structure of Thiourea (Puzzarini, 2012)

Thiourea compounds arise from the substitution of an oxygen atom in the urea moiety with a sulphur atom, resulting in distinct properties attributed to the disparate electronegativities of sulphur and oxygen atoms. The presence of the thio-carbonyl

group in thiourea compounds is of significant importance in determining their various biological activities, as it has a direct impact on their lipophilic/hydrophilic characteristics and electrical properties (Lal Bhatia et al., 2016; Saeed et al., 2010).

The reactivity of outgoing substituents and the resulting biological activity of thiourea derivative compounds are influenced by the presence of the thio-carbonyl moiety. The relevance of various derivatives of ferrocenyl thiourea lies in their recognised role as anticancer drugs, mostly due to their ability to inhibit receptor tyrosine kinases (RTKs), protein tyrosine kinases (PTKs), and NADH oxidases (Li et al., 2010; Lv et al., 2010). Various compounds of thiourea have demonstrated bioactivity against infectious illnesses, leukaemias, and solid tumours. The compounds encompassed in this category consist of N-nitrosoureas, benzoylureas, diarylsulphonylureas, and aroylthioureas (Satyen Saha, 2021).

One promising approach to augment the likelihood of DNA damage and cellular death involves incorporating a ferrocenyl moiety into compounds such as thiourea that interact with DNA. This arrangement places the ferrocene moiety in a close position to the DNA, which may enhance the probability of DNA damage and eventual cellular apoptosis. (Li et al., 2020).

2.5 1-(4-ferroceneyl phenyl)-3-(4-nitrobenzyl) thiourea

In the 1970s, Brynes and colleagues conducted a study to explore the possibility of ferrocenyl derivative chemicals as medicines for combating cancer. The study findings indicated that ferrocenyl compounds with amide or amine functional groups

demonstrated anti-cancer properties specifically targeting P-388 leukaemia inside the lymphocytic system (Fiorina et al., 1978).
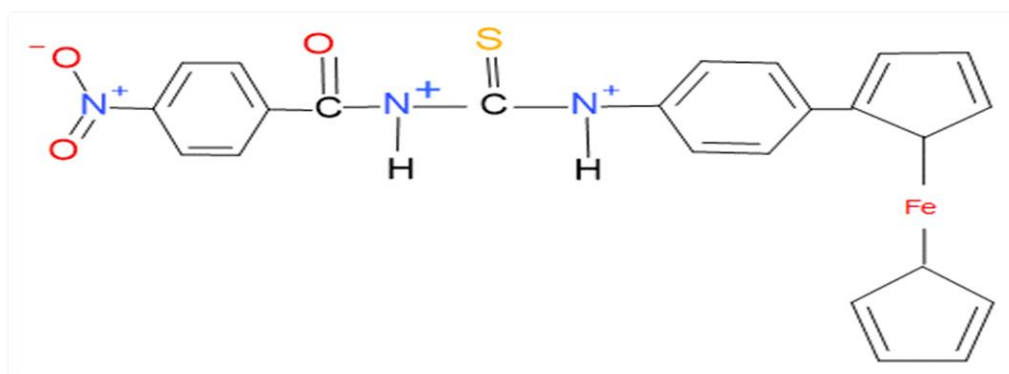
Figure 10 Structure of 1-(4-ferroceneyl phenyl)-3-(4-nitrobenzyl) thiourea

The mechanism of action of thiourea compounds incorporating ferrocene involves the selective targeting of the cell membrane, topoisomerase enzyme II, and DNA. These compounds demonstrate a robust affinity for DNA, forming bonds by both covalent and non-covalent interactions. The major mechanism employed by these agents entails the induction of DNA damage or breaking via electrostatic forces, intercalation, and groove binding. This process finally culminates in cell cycle arrest and the infliction of irreparable harm to the cell genome, ultimately leading to apoptosis (Parveen et al., 2019).

The mechanism of action of thiourea including ferrocene is also correlated with its antioxidant capabilities. Disrupted redox signalling in cancer cells results in genomic instability and DNA mutations, thereby triggering the activation of pro-cancer signalling pathways. The NH moiety located in the central part of the ferrocene structure demonstrates a pronounced capacity to effectively remove reactive oxygen species (ROS). Considering the significance of ROS signalling pathways as a pivotal approach in the advancement of cancer therapy, the integration of ferrocene into thiourea compounds plays a vital role in preserving the equilibrium of redox reactions by effectively eliminating surplus ROS (Satyen Saha, 2021).

The findings of a research investigation pertaining to ferrocifen, a chemical belonging to the Fe(II) category, indicate that the mechanism of action of ferrocifens involves the modulation of the receptor protein's conformation. It is postulated that upon its interaction to the oestrogen receptor (ER), ferrocifen exhibits affinity for a certain DNA region, leading to the dimerization of ferrocifen upon ER binding. Subsequently, the dimerized entities exhibit adherence to particular DNA loci. In the context of electron transfer, it has been observed that the ferrocenium ion in vivo or the ferrocifen-ER complex may give rise to the production of reactive oxygen species (ROS), namely hydroxyl radicals (OH). The creation of reactive oxygen species (ROS) has the capacity to elicit DNA damage and play a role in the promotion of anticancer effects through the generation of radical metabolites that exert deleterious effects on cancer cells. The investigation of complexes comprising thiourea has also been undertaken to examine diverse biological functionalities (Ali et al., 2015). Comprehending the unique ways by which molecular drugs interact with DNA is of paramount importance in the development of targeted treatments and novel therapeutic strategies (Asghar et al., 2017). Small molecules commonly engage in noncovalent interactions with DNA, employing three distinct binding strategies: intercalative binding, groove binding, and electrostatic interactions. The intercalative binding mechanism is regarded as the most stable of these options due to the wedging of the intercalating molecule's surface between the aromatic and heterocyclic DNA base pairs (Singh et al., 2021; Strekowski & Wilson, 2007; Verheijen et al., 2000). According to the findings of the study, it is indicated that the primary amine of N6 lactam, in conjunction with the ferrocenyl moiety, plays a pivotal role in the inhibition of Topo II. Furthermore, it demonstrates a higher level of poisoning activity when compared to the compound that lacks the

ferrocene component, as the latter does not exhibit any discernible effect (Larik et al., 2017; Spencer et al., 2011).

2.6 Nanotechnology in Biomedicine

The field of traditional cancer chemotherapy has notable challenges, such as the development of drug resistance in cancer cells that have undergone mutations, as well as the constraints posed by chemotherapeutic drugs that exhibit inadequate stability and solubility at the intended location inside the body. To surmount these hurdles, it is imperative to make progress in the field of drug delivery systems, with a focus on enhancing specificity, reducing toxicity, and shortening the length of treatment. (Xiao et al., 2019; Yau et al., 2021).
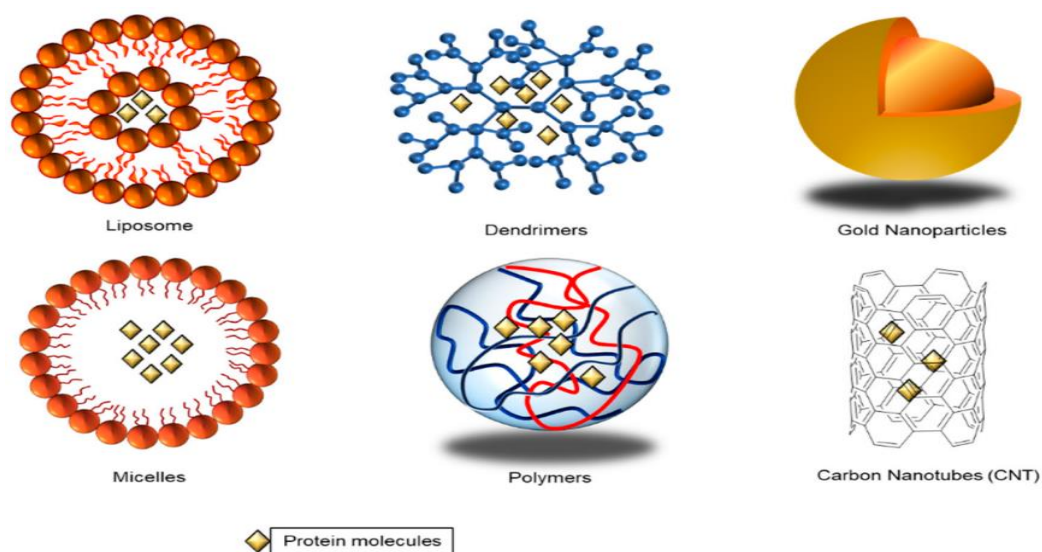
Figure 11 Types of Nanoparticles (Yau et al., 2021)

In order to tackle these obstacles, the application of nanotechnology in the medical industry has been utilised to develop nanoparticles, which exhibit significant promise in addressing these concerns (Liu, 2012). Nanoparticles, which typically exhibit dimensions within the range of 1 to 100 nm, possess the capability to enhance the therapeutic efficacy of drugs when combined with them (Holban & Grumezescu, 2016).

Nanoparticles present numerous benefits, such as heightened bioactivity, extended medication efficacy, improved cellular permeability, modifiable release kinetics, and diminished adverse effects on healthy organs (Yau et al., 2021). In addition to nanoparticles, nanotechnology has seen progress in the development of additional nanocarriers such as protein-based nanocarriers, dendrimers, micelles, and liposomes. These carriers can incorporate pharmaceuticals into their structure. However, it is worth noting that organic nanocarriers, like liposomes, can have sizes larger than 100 nm and may not always fall within the classification of nanoparticles. (López-Dávila et al., 2012).

The management of acute myeloid leukaemia (AML) frequently entails the administration of drugs via intravenous route. However, this approach can result in fast drug clearance and non-specific impacts. In order to address these issues, researchers have devised nanoparticulate systems that possess prolonged circulation durations and the capacity to specifically target malignant cells in the bone marrow. There are currently multiple nano-sized formulations available for the treatment of acute myeloid leukaemia (AML). One such formulation is Vyxeos, which has been approved by the FDA. Vyxeos is a liposomal formulation that contains daunorubicin and cytarabine, and it was granted approval for AML therapy in the year 2017 (Briot et al., 2018).

2.7 Liposomal Nanoparticle for Treatment of AML

The discovery of liposomes is attributed to Dr. Alec D. Bangham, who conducted research at the Babraham Institute located at the University of Cambridge in 1964. (Bangham et al., 1965). The etymology of the name "liposome" can be traced back to its Greek origins, specifically the combination of the word "lipos," denoting fat, and "soma," referring to body (Kumar et al., 2010). Liposomes are diminutive spherical synthetic vesicles consisting of one or more concentric lipid bilayers encircling an

aqueous centre. The particle sizes of liposomes can exhibit a range of 30 nanometers to several micrometers, with their properties being influenced by various aspects such as size, lipid composition, manufacturing technique, and surface charge (Akbarzadeh et al., 2013).
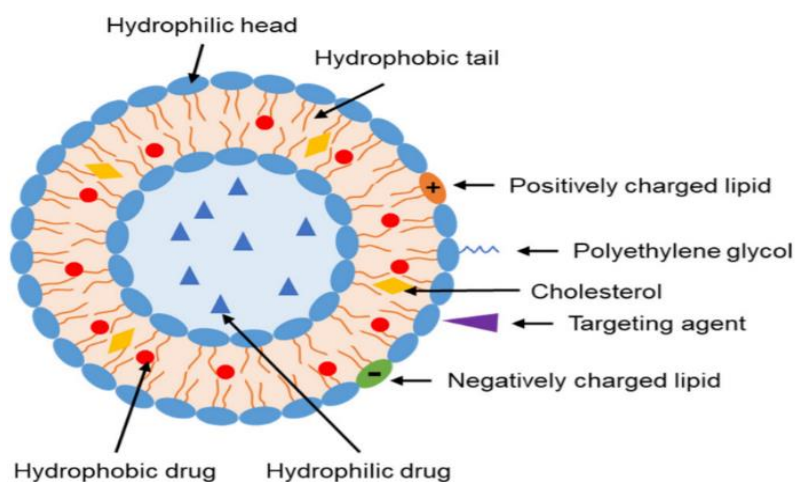
Figure 12 Structure of Liposome (Duong et al., 2023)

Liposomes can be classified according to their lamellarity, size, and manner of formation. Unilamellar vesicles generally exhibit sizes within the range of 50 to 250 nm and are characterized by the presence of a solitary lipid bilayer that encloses an aqueous core. On the other hand, multilamellar vesicles exhibit the presence of several concentric lipid bilayers and generally possess sizes ranging from 1 to 5 micrometres, like the layered structure of an onion. Liposomes are generated through the self-assembly of amphiphilic molecules, resulting in the formation of stable encapsulated structures in an aqueous environment. The phospholipids' hydrophilic head groups are directed towards the watery core, while the hydrophobic fatty acid chains are directed towards the interior, resulting in the formation of a hydrophobic region. Liposomes exhibit a range of sizes spanning from 1 nm to multiple microns; nevertheless, in order to be suitable for therapeutic purposes, liposomes must adhere to the submicron ultra-

filterable category, often characterized by a size smaller than 200 nm (Alavi & Hamidi, 2019).

There are two main categories in which liposome production methods can be classified: passive loading techniques and active loading approaches. Passive loading procedures include mechanical dispersion, solvent dispersion, and detergent removal methods. On the other hand, active loading procedures are dependent on the utilization of disparities in potential across the liposome membrane and the establishment of a pH gradient in order to facilitate the loading of premade liposomes with medicinal molecules. (Powers & Nosoudi, 2019). Liposomes possess the capacity to encapsulate a diverse range of therapeutic and diagnostic substances, hence providing a higher drug payload per particle and protecting the pharmaceuticals from metabolic processes. The lipophilicity of specific medications is a critical factor in determining their positioning within the liposome structure (Bangham, 1993).

Liposomes have been widely regarded as promising options for drug administration owing to their advantageous attributes, such as little toxicity, compatibility with biological systems, and capacity to degrade naturally. Liposomes possess certain characteristics that render them highly advantageous in the pharmaceutical sector, particularly in augmenting the intracellular transportation of anticancer medications. This is mostly attributed to their ability to extend the duration of the enclosed drug's presence within cancerous cells. Liposomes possess the potential to mitigate off-target negative effects by enhancing the pharmacological and pharmacokinetic characteristics of anticancer drugs (Deshpande et al., 2013; Riaz et al., 2018).

2.8 Components of Liposomes

2.8.1 Cholesterol
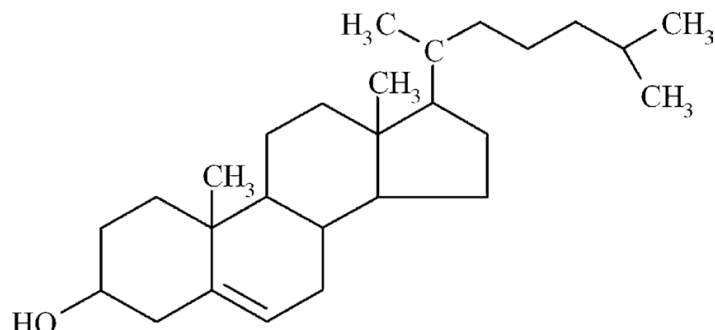
Figure 13 Structure of Cholesterol (Raczynski et al., 2006)

Cholesterol is involved in the modulation of lipid membrane fluidity and polarity, leading to a decrease in permeability and a reduction in the leakage of medication from liposomes. The assessment of cholesterol incorporation into lipid bilayers can be conducted by analysing alterations in the thermotropic profile by methods such as differential scanning calorimetry (DSC). For example, the inclusion of cholesterol at a concentration of 30% prevents the phase transition of diacylphospholipids and enhances the stability of the lipid bilayer. Cholesterol impedes the process of phospholipid acyl chain crystallisation and introduces steric hindrance, hence decreasing the permeability of the lipid membrane to certain solutes (Daraee et al., 2016; Kohli et al., 2014).

2.8.2 Phospholipids

Phospholipids are frequently employed in the manufacture of liposomes owing to their crucial function in biological membranes. Lipids can be easily acquired from abundant natural sources such as egg yolk and soybeans, resulting in a cost-effective approach due to their widespread availability in the natural environment. Nevertheless, the utilisation of natural sources in this context yields a combination of phospholipids that

exhibit disparities in both the head group and the acyl chain. Consequently, such variances can give rise to instability issues in liposomal formulations during their storage and use. An alternative approach is chemical synthesis, which enables the production of synthetic phospholipids with well-defined structures and uniform physicochemical properties. However, the extensive application of synthetic phospholipids is limited due to their relatively high production cost. The amphipathic molecules under consideration possess a hydrophilic head group and two aliphatic side chains that are linked together by a glycerol link.
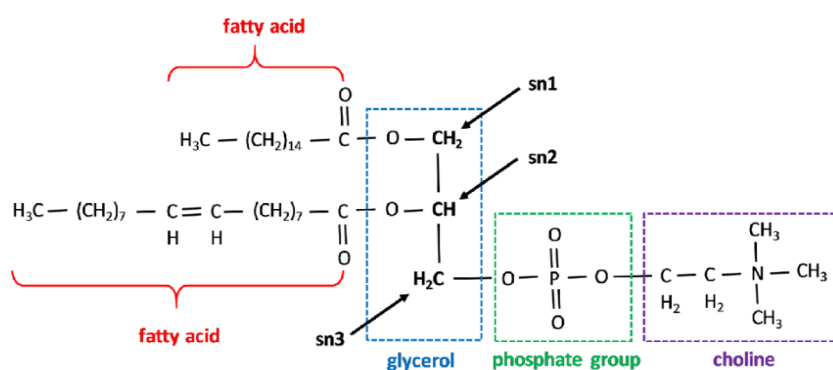
Figure 14 Structure of Phospholipid (MacDonald et al., 2019)

The determination of phospholipid type is contingent upon the makeup of the polar group, encompassing phosphatidylserine (PS), phosphatidylcholine (PC), phosphatidylglycerol (PG), phosphatidylethanolamine (PE), or phosphatidic acid (PA). Phospholipids can be further categorised within each specific group, taking into consideration the length of the fatty acid chain and the level of saturation. The diverse range of phospholipids is attributed to the interaction between the phosphate head group and various polar constituents, leading to the emergence of specific physicochemical properties for each phospholipid variant (Li et al., 2015). Liposomal nanoparticles are predominantly composed of phospholipids that contain glycerol, which are widely employed in their manufacturing.

Chapter 3: Materials and Methods

3.1 Materials

1,2-Dioleoyl-sn-glycero-3-phosphocholine (DOPC), Dipalmitoyl phosphatidyl choline (DPPC) lipid, Cholesterol, Polyethylene glycol (PEG-1000), ethanol was purchased from Sigma-Aldrich USA. FITU was obtained from Quaid-e-Azam university, Islamabad. Wister male rats were purchased from Animal House of ASAB (Atta-ur-Rahman school of Applied Biosciences), National University of science & technology (NUST), Islamabad. Deionized water was used throughout the study.

3.2 Preparation of Liposomal Nanoparticles

3.2.1 Synthesis of Uncoated Liposomal Nanoparticles

Liposomes were generated by employing a lipid composition consisting of DPPC, DOPC, and cholesterol in a molar ratio of 2:2:1. The lipids were carefully measured and subsequently dissolved in ethanol to produce a solution with a concentration of 100 M. Two separate solutions were produced using ethanol as the solvent, with a concentration of 200 µM for both FITU and doxorubicin. A total volume of 500 µL for each drug solution was combined with the lipid solution in order to generate FITU nanoparticles and doxorubicin nanoparticles. To synthesise FITU+Dox nanoparticles, a mixture of 250 µL of FITU solution and 250 µL of doxorubicin solution was combined with the lipid solution. Subsequently, the combination underwent sonication for a duration of 40 minutes at a frequency of 80 MHz. Following this, the water phase and lipid phase were individually heated in a water bath until they attained a temperature of 60°C. The aqueous phase and lipid phase were mixed and subjected to continuous stirring for a duration of 10 minutes at a rotational speed of 90 revolutions

per minute (RPM). Subsequently, the combination underwent sonication for an additional duration of 40 minutes at a frequency of 50 MHz. Subsequently, the ethanol removal was accomplished through the implementation of a rotary evaporation technique conducted at a temperature surpassing the phase transition point, specifically at 50°C (Farooq et al., 2022; Meng et al., 2016). The unentrapped drug was detached through dialysis tube with size 2 Inf Dia 18/32 – 14.3mm and with a pore size of 12-14000 Daltons.

3.2.2 Synthesis of PEG Coated Liposomal Nanoparticles

In order to produce PEG-coated F-NPs, a comparable methodology to that employed for uncoated NPs was implemented, with supplementary stages. Similarly, ethanol was used to prepare solutions of lipids and medication solutions with a concentration of 200 µM. Once the lipid phase had been subjected to sonication, a volume of 500 µL of the drug solution was combined with the lipid solution. Subsequently, the aqueous phase was introduced, and the resultant solution was treated to the process of rotary evaporation. The NP's including FITU, doxorubicin, and FITU+Dox was subsequently coated by diluting each to a final volume of 50 mL. Following that, a solution containing 0.25% PEG was gradually added dropwise with constant stirring. The resulting mixture was then subjected to rotary evaporation until the solution volume reached 10 mL. Dialysis tubing was utilised for the purpose of eliminating any unentrapped drug (Stiufiuc et al., 2013).

3.3 Characterization of Liposomal Nanoparticles

To assess and examine the encapsulation efficiency, particle size, surface charge, and drug release kinetics further characterizations of uncoated and PEG-coated FITU NP'S's, dox NP'S's and FITU+Dox NP'S's were carried out

3.3.1 UV-Vis spectroscopy

UV-Visible spectroscopy is a widely employed analytical method wherein the absorption or transmission of specific wavelengths of ultraviolet (UV) or visible light by a specimen is quantitatively determined relative to a reference or blank. The attribute under consideration can be influenced by the composition of the sample, hence offering valuable information regarding the constituents and their respective concentrations within the sample. The phenomenon of Surface Plasmon Resonance (SPR) is widely recognized in the scientific community, wherein nanoparticles have the ability to absorb light spanning the visible to near-infrared spectrum (NIR). This absorption is attributed to the collective oscillation of surface electrons within the nanoparticles. UV/Vis spectroscopy is a widely employed technique for the characterization of materials by assessing their absorption properties.

A beam of light is split in half in a UV-Vis spectrophotometer such that one half is directed through the cuvette containing the material being studied and the other half is directed to a cuvette containing the solvent alone (reference). A spectrum that depicts the whole range of wavelength vs its absorption at a given wavelength can be produced by measuring absorption both at that wavelength and at the appropriate range. Lambda max is the absorption maximum at a certain wavelength. It monitors molecular electronic transitions and abides by the Beer Lambert Law. For comparing the spectra of various chemicals, the absorbance value known as the molar absorptivity is utilised, which is proportionate to the molar concentration in the cuvette (Zuber et al., 2016). According to Beer-Lambert Law

$$\mathbf{A = \varepsilon Lc}$$

Molar absorptivity $\varepsilon = A/cl$ (where A= absorbance, c= sample concentration in moles/ liter and L= length of light path through the cuvette in cm). This law makes UVVs absorption spectroscopy useful for quantitative analysis.

Spectro UV-Vis Dual Beam PC Scanning Spectrophotometer, model number Spectro UVS-2800, was used to carry out the analysis at resolution of 1nm.

3.3.2 Zeta potential

The Stern layer is a region consisting of ions with opposite charges that are strongly attached to the surface of nanoparticles, leading to the establishment of an overall electric charge inside a solution containing ions. In addition to this, there exists a secondary outer layer characterised by a dispersion of ions that exhibit weak associations. The combination of these two layers is commonly known as the electrical double layer. In the context of the diffuse layer, ions have a tendency to separate into two distinct groups based on their behaviour during the movement of nanoparticles. Specifically, some ions accompany the nanoparticle in its motion, while others remain within the surrounding dispersion in bulk. This phenomenon occurs regardless of whether the particle's movement is driven by Brownian diffusion or an externally applied force. The zeta potential, associated with the surface charge of the nanoparticle, denotes the electrostatic potential at the interface of a "slipping plane." Zeta potential measurements encompass the application of an electric field to the sample, utilising laser Doppler velocimetry (LDV) to quantify the motion of nanoparticles, or electrophoretic mobility. The utilisation of the Henry equation is employed for the calculation of the zeta potential. (Clogston & Patri, 2011).

$$Ue = \frac{2\varepsilon \, zf \, (\kappa\alpha)}{3 \, n}$$

Zeta potential is a measurement of the liposomes' electrical charge on their surface. It is thought that this characteristic of liposomes represents a basic physical characteristic governing electrostatic interaction between particles in suspension. According on their charge characteristics, liposomes can be categorised as cationic, anion, or neutral. The effectiveness of liposome encapsulation, stability, and distribution in target cells and organs are all influenced by its surface charge.

The zeta potential, which represents the surface charge, was evaluated by the utilisation of Dynamic Light Scattering (DLS) employing the Malvern Zeta Sizer Ver. 7.12.

3.3.3 Fourier Transform Infrared Spectroscopy (FTIR)

The Fourier-transform infrared (FTIR) analysis technique utilises infrared radiation to examine samples, providing useful insights into the identification of organic, inorganic, and polymeric constituents. Modifications in the composition of the material can be readily discerned by observing variations in the characteristic absorption band patterns. Fourier Transform Infrared Spectroscopy (FTIR) is utilised for a multitude of objectives, including the identification and characterization of compounds that are not yet known, the detection of additives, the identification of contaminants, and the evaluation of degradation and oxidation processes. A standard Fourier Transform Infrared (FTIR) spectrometer has various essential components, including a source, sample cell, reader, amplifier, analog-to-digital (A/D) converter, and computer. The radiation emitted by the source traverses the interferometer and then arrives at the detector. The signal is amplified by the amplifier and then digitised by the A/D converter, prior to being transmitted to the computer for the purpose of Fourier processing. The sample allows for the transmission of infrared radiation within the range of approximately 10,000 to 100 cm-1, where a portion of the radiation is absorbed while the remainder continues to propagate. The provided sample demonstrates the

conversion of absorbed energy into either vibrational or rotational energy. The obtained signal, encompassing a spectrum spanning from 4000 to 400 cm-1, illustrates the chemical composition of the analysed samples. (Taha et al., 2013).

FTIR analysis of DPPC, cholesterol, FITU liposomal NP's and PEG coated FITU-liposomal NP's was carried out. A pellet of KBr was prepared for every sample and analyzed by using FTIR Spectrophotometer, equipped with software OMNIC™ Version 6.0a; Thermo Fisher Scientific, Waltham, MA, USA).

3.3.4 Scanning Electron Microscopy (SEM)

The technique of scanning electron microscopy (SEM) distinguishes itself from optical microscopy by utilising an electron beam instead of a light beam to examine the object. Within a scanning electron microscope (SEM), a concentrated beam of electrons is emitted from an electron gun positioned at the uppermost part of the apparatus. There exist two fundamental categories of electron guns: thermionic and field emission guns. The former process induces a robust electric field that facilitates the extraction of electrons from atoms, whereas the later method involves the heating of the filament to a point where electron emission occurs. In scanning electron microscopy (SEM), high-energy electron beams are employed to do a surface scan of the sample. In contrast to conventional light microscopes, scanning electron microscopes (SEMs) employ electrons to generate images with significantly enhanced magnification. Upon the collision of the electron beam with the surface of the specimen, an interaction occurs between the beam and the specimen, leading to the emission of three distinct categories of electrons, namely backscattered (or primary), secondary, and Auger electrons, in addition to the generation of X-rays.

The scanning electron microscope (SEM) predominantly relies on the detection and analysis of secondary electrons, which facilitate the generation of high-resolution visual representations that can effectively expose minute details measuring between 1 and 5 nanometers in size. The utilisation of backscattered electrons is also employed in this process for the purpose of image formation. The electron beam is deflected both vertically and horizontally by scanning coils located within the electron column. This enables the raster scanning of a rectangular region on the surface of the specimen. Electronic equipment have the capability to detect and enhance signals, subsequently presenting the outcomes in the form of images on a cathode ray tube. The microscope is effectively coordinated with the raster scanning process, resulting in a visual representation that displays the spatial distribution of the signal amplitude originating from the scanned area of the specimen.

In the context of scanning electron microscopy (SEM), the electron beam necessitates a channel to establish a connection with the ground in order to effectively scan the surface of specimens and facilitate conventional imaging. Frequently, non-conductive solid specimens are coated with conductive materials using techniques such as low vacuum sputter coating or high vacuum evaporation. This measure is implemented in order to mitigate the accumulation of static electric charge on the specimen upon electron exposure. In contrast to the limited magnification capability of a light microscope, which reaches a maximum of 10,000, the scanning electron microscope (SEM) has the ability to magnify objects up to 300,000 times, thereby enabling the acquisition of intricate and comprehensive three-dimensional visual representations (Joshi & Bhattacharyya, 2008).

The visualisation of each individual nanoparticle (Np) was achieved by carefully distributing a 200 μL sample onto a coverslip with a micropipette. Following this, a thin layer of gold was applied onto the surface of the slide using a sputter coater for a duration of 50 seconds. The nanoparticles were imaged using a VEGA3 LMU Scanning Electron Microscope, (Tescan, Czech Republic).

3.3.5 Encapsulation Efficiency

When determining whether liposomes can be effectively synthesised, encapsulation efficiency is a crucial indicator of the drug content of the liposomes. The bioavailability and in vivo effectiveness of liposomes are closely correlated with their encapsulation effectiveness. After centrifuging a nanoparticle formulation at 4500 rpm for an hour, the supernatant was collected, and the amount of medication contained was assessed using a UV spectrophotometer. A graph of concentration and absorbance at 290 nm were displayed on the standardised calibration curve of various drug millimolar doses dissolved in ethanol.

$$E.E = \frac{Total\ Drug\ Added - Free\ Drug\ in\ the\ Supernatant}{Total\ Drug} \ x\ 100$$

3.3.6 Drug Release Kinetics

FITU-loaded NP's and PEG-coated FITU-loaded NP's solutions totalling 3 mL each were deposited separately into a 15 mL centrifuge tube, where they underwent a 10-minute, 4500 rpm, 25 °C centrifugation process. On the other hand, FITU loaded NP'S's and PEG-coated FITU loaded NP'S's solutions each received 3 mL of phosphate buffer saline. After centrifugation, the supernatant was made available for 330nm UV spectrophotometer examination. The same course of action was taken after 1, 2, 4, 6, 8, 12, 14, and 16 hours. An empty nanoparticle solution was employed as a control for the analysis.

3.4 In vitro Assay

In vitro is Latin for "within the glass" under controlled environment. In vitro assay for ferrocene incorporated thiourea has been conducted to determine the cytotoxicity, antioxidant, and enzymatic activity.

3.4.1 Cytotoxicity Assay

3.4.1.1 Brine Shrimp Assay

The brine shrimp lethality bioassay is a rapid and uncomplicated approach used to evaluate the cytotoxic properties of bioactive compounds. The present assay is founded upon the capacity of test compounds to induce mortality in Artemia salina, commonly known as brine shrimp. The test in question was originally introduced by Michael et al. and has since undergone further refinement by other researchers. The practise of assessing the potential toxicity of heavy metals, pesticides, and pharmaceuticals, specifically natural plant extracts, is widely utilised. The assay functions as a preliminary measure in toxicity testing prior to advancing to investigations employing mammalian animal models (Wu, 2014).

Protocol

The sea water used to hatch brine shripm eggs. Sea water was prepared by combining 17 g of sea salt with 500mL of distilled water. The seawater's pH was kept in the range of 8 and 8.5. Afterwards, for two to three hours, sea water was oxygenated using a magnetic stirrer. Brine shrimp eggs weighing 10 mg were dissolved in water and incubated for 24 hours at 37 °C. Following 24 hours, phototactic movement was used by the newly born nauplii (larvae of brine shrimp) to migrate in the lit half. They were then taken away using a 1mL pipette.

On a 96-well plate, 10 brine shrimps were counted under a microscope and placed in each well. Triplicates of ethanol were used as the positive control, while triplicates of saline were used as the negative control. Different dilutions of FITU, doxorubicin and FITU+Dox (80%, 60%, 40%) and their NP's (100%, 80%, 60%) were applied. After 24 hours, the number of alive and dead shrimps were counted to determine the % mortality using the formula:

$$Mortality(\%) = \frac{Mean\ dead\ shrimps\ in\ sample}{Total\ shrimps\ in\ sample}\ x100$$

The percentage mortality values obtained were plotted as graphs.

3.4.1.2 Hemolytic Assay

The in vitro hemolysis assay assesses haemoglobin release in the plasma (as a marker of red blood cell lysis) after test agent exposure. Human blood is combined with serial dilutions of the substance, which is then incubated for 45 minutes at 37°C. After centrifuging the cells, the absorbance of the supernatant, which contains plasma and lysed erythrocytes, is calculated. Using a standard curve of lysed erythrocytes, the percentage of lysis is computed.

Protocol

The evaluation of hemolysis was conducted in the hemolytic assay for FITU, doxorubicin, FITU+Dox, and their respective nanoparticles. In the first step, a blood sample was obtained from a male participant who exhibited no signs of illness, and subsequently treated with ethylenediaminetetraacetic acid (EDTA). The blood cells were suspended in phosphate-buffered saline (PBS) by means of centrifugation followed by repeated washing. Different concentrations of FITU, doxorubicin, and the combination of FITU and doxorubicin (at 80%, 60%, and 40% concentrations) were synthesized, alongside their corresponding lipid nanoparticle Np's counterparts (at

100%, 80%, and 60% concentrations). The solutions were subjected to incubation with blood samples at a temperature of 37°C for a duration of 4 hours. The assay includes a negative control (phosphate-buffered saline) and a positive control (Triton-X100). After the incubation period, the samples underwent centrifugation, and the resulting supernatant was subjected to analysis at a wavelength of 550 nm using a Thermoscientific Multiskan Sky microplate reader. This analysis was performed in order to determine the percentage of hemolysis.

$$Percentage\ Hemolysis = \frac{Abs\ of\ test\ sample}{Abs\ of\ positive\ control}\ x\ 100$$

3.4.2 Anti-oxidant Assay

3.4.2.1 Total Antioxidant Capacity

The assessment of total antioxidant capacity (TAC) serves as a beneficial approach to evaluate the capability of biological samples in scavenging free radicals, hence offering a comprehensive evaluation of their antioxidant composition. The TAC assays have numerous benefits, such as their straightforwardness, cost-effectiveness per sample, promptness in generating results, and the adaptability to be carried out by manual, semi-automated, or fully automated means. The measurement of antioxidant capacity is conducted using the phosphate-molybdenum (VI) to phosphate-molybdenum reduction method in the total antioxidant test (V).

Protocol

The experiment commenced with accurately measuring the quantities of ingredients. A mixture containing 1.679 grammes of NaH2PO4 and 0.247 grammes of (NH4)2MoO4 was dissolved in 50 millilitres of distilled water. Subsequently, 1.63 millilitres of H2SO4 were added to the solution, resulting in the formation of the TAC reagent. In

the antioxidant assay, water was employed as the negative control, while ascorbic acid was utilised as the positive control at a dosage of 1 mg/mL. Three replicates of each dilution of FITU, doxorubicin, FITU+Dox (at concentrations of 80%, 60%, and 40%), and NP's (at concentrations of 100%, 80%, and 60%) were dispensed into a 96-well plate. Subsequently, 180 µl of the TAC reagent was added. The experimental conditions encompassed the use of ascorbic acid and water as control substances. Following a 90-minute period of incubation and subsequent cooling, the absorbance was quantified at a wavelength of 695 nm while maintaining a temperature of 95 °C. The TAC value was determined by employing the subsequent formula:

$$Ascorbic\ Acid\ Equivalence = \frac{Absorbance\ of\ sample}{2.651} \ x\ 100$$

3.4.2.2 DPPH (1,1-diphenyl-2-picrylhydrazyl) Free Radical Scavenging Activity

The DPPH (2,2-diphenyl-1-picryl-hydrazyl-hydrate) free radical analysis method is an antioxidant assay that functions based on the principle of electron transfer. At the outset, it produces a solution with a violet hue when dissolved in methanol. Nevertheless, upon the introduction of an antioxidant molecule, the previously stable free radical undergoes a reduction process, leading to the creation of a methanol solution devoid of colour.

Protocol

FITU and its nanoparticles were tested for their ability to scavenge free radicals using the 96-well plate approach. 3.9 mg of solid DPPH was dissolved in 100ml of methanol to create 0.1mM of DPPH stock solution. The stock solution of DPPH was diluted in methanol in order to get an optical density of 0.96 (±0.03) as the desired objective. The negative control in this experiment was represented by distilled water, whereas a positive control solution was created using ascorbic acid at a concentration of 3 mg/mL. In each reaction, a volume of 190 µL of a 0.1 mM DPPH solution was mixed with a

volume of 10 µL of different drug dilutions (80%, 60%, 40%) and their respective lipid nanoparticles (100%, 80%, 60%). The reaction mixtures were subjected to incubation in a light-free environment at a temperature of 37°C for a duration of 30 minutes. Following that, the measurement of absorbance at a wavelength of 517 nm was conducted utilizing a Thermoscientific Multiskan Sky microplate reader. The IC50 values were established by employing the GraphPad Prism IC50checker programmed version 5. Additionally, the free radical scavenging potential of every sample was assessed using the formula shown below:

$$\textbf{\textit{Percentage Scavenging}}$$
$$= \frac{\textbf{\textit{Absorbance of control}} - \textbf{\textit{Absorbance of test sample}}}{\textbf{\textit{Absorbance of Control}}} \textbf{\textit{x}}\textbf{100}$$

3.4.2.3 Total Reducing Power Assay

The methodology employed to evaluate reducing power is grounded on the principle that substances possessing a reduction potential can undergo a reaction with potassium ferricyanide (Fe^{3+}) resulting in the formation of potassium ferrocyanide (Fe^{2+}). Following this, the ferrocyanide can react with ferric chloride, resulting in the formation of a complex consisting of ferric and ferrous ions. With a few minor modifications, the technique outlined by (Oyaizu, 1986) was used to assess the reducing power capability of test compounds.

Protocol

1g of $K_3Fe(CN)_6$ was dissolved in distilled water to create 1% potassium ferricyanide. 10g of trichloroacetic acid in 100ml of distilled water was added to produce 10% trichloroacetic acid (TCA). 0.1g of $FeCl_3$ was dissolved in 100ml of distilled water to produce 0.1% $FeCl_3$. The pH was set at 6.8 for preparing the 0.2M phosphate buffer.

The positive control in this experiment was a solution of ascorbic acid with a concentration of 3 mg/mL, while the negative control was distilled water.

In an Eppendorf tube, a volume of 500 µL of potassium ferricyanide was introduced subsequent to its combination with 640 µL of a phosphate buffer with a concentration of 0.2M. Additionally, 60 µL of each dilution of the medicines (80%, 60%, 40%) and their corresponding lipid nanoparticle formulations (100%, 80%, 60%) were included. The negative control in this experiment was represented by distilled water, whereas the positive control was represented with ascorbic acid. Following a 20-minute incubation period at a temperature of 50°C, the mixture was subsequently combined with 500 µL of trichloroacetic acid. The resulting mixture was then subjected to centrifugation at a speed of 3000 revolutions per minute for a duration of 10 minutes. The uppermost layer, measuring 500 µL, was separated and subsequently, an additional 100 µL of ferric chloride was introduced into a separate Eppendorf tube. Subsequently, a volume of 200 µL from the aforementioned solution was carefully dispensed into each well of a 96-well plate. The measurement of absorbance was conducted at a wavelength of 700 nm using a Thermoscientific Multiskan Sky microplate reader. The calculation of ascorbic acid equivalence was performed utilising the subsequent formula:

$$Ascorbic\ Acid\ Equivalence = \frac{Absorbance\ of\ sample}{2.705}\ x100$$

3.5 In vivo Assay

In vivo means "among the living." It describes the tests, and experiments that scientists carry out on or within an organism. In vivo assay for ferrocene incorporated thiourea has been conducted.

3.5.1 Development of Animal Model

Female wistar rats weighing 100-150g and 7 weeks old were acquired from ASAB animal house. The animals were randomly divided into groups and exposed to a one-week acclimatisation phase with free access to food and water. Conventional cages were used to house the rats. The cages were filled with new sawdust that was replenished every two days. The temperature was kept at 27°C ± 2°C, while the humidity was kept at 600% ± 5%. For each type of leukemia model, rats were split into seven groups of five rats each and one normal group. Throughout the model designing and treatment phase, rat's weights were monitored weekly. Rats handling and care were controlled by FDA (Food and Drug Administration) standards for appropriate laboratory practise in 1978.

3.5.2 Positive Control

Five rats were placed in positive control group. No induction of leukemia and no treatment were given to rats, and they were dissected at the end and their test values were taken as standard.

3.5.3 Induction of Leukemia

Normal rats were kept without exposure to any chemical while other groups were given benzene via IV injection. Benzene injections were made by combining benzene isopropanol and water in a (1:2:1) ratio. A stock solution was made by combining 0.5mL benzene, 1mL isopropanol, and 0.5mL water in a constant proportion. During four weeks on alternate days, 100µl of this stock was administered intravenously.

3.5.4 Treatment Plan

To assess to ani-leukemic effect of drug as single therapy and as a co-therapy with doxorubicin as well as their nanoparticles, they were administered intravenously to each group on alternate days for four weeks, and the dose given was 100µl.

No.	Groups	No. of Rats	Mode of administration of Drug and Benzene	Dose of drug
1	Control	5	-	-
2	Diseased	5	IV	-
3	Free FITU	5	IV	5mg/kg
4	Free Doxorubicin	5	IV	5mg/kg
5	FITU + DOX	5	IV	5mg/kg
6	FITU NP's	5	IV	100µl from stock sol.
7	FITU+DOXNP's	5	IV	100µl from stock sol.
8	Dox NP's	5	IV	100µl from stock sol.
9	Blank NP's	5	IV	100µl from stock sol.

Table 1 Dosing of Rats

3.5.5 Morphology of Blood

Blood smears were made from fresh blood for morphological study every week and at the time of dissections. A blood drop was placed on glass slides, then a cover slip was placed at 45 degrees on the blood dot to produce a smear, which was then air dried. The stains were remedied by submerging them in methanol that had been cooled, for a

duration of 3 minutes, and subsequently permitting them to undergo air drying. Subsequently, the smears underwent a staining process using Giemsa staining solution for a duration of 10 minutes. This was followed by a comprehensive rinsing with distilled water and a subsequent round of air drying. Subsequently, the slides were subjected to microscopic examination, employing a 100X lens for the purpose of analysing the cellular morphology.

3.5.6 Serological Testing

Blood was taken from direct cardiac puncture and collected in EDTA tubes and serum tubes for serological tests such as CBC, LFT's, RFT's.

3.5.7 Dissection and Histopathological Examination

Rats were dissected after treatment, and each organ's size, shape, and colour was observed. 5µm section of each organ was taken and placed into PBS solution and stored in liquid nitrogen. For histological examination organs slides were prepared and stained with hematoxylin and eosin (HE) stain. The structural modifications were examined using a biological microscope, model LB-200. A Labomed biological microscope equipped with Pixel Pro software was used to acquire images at a 100x magnification. Based on the histological grading criteria, the pathological grading and score were completed.

Chapter 4: Results

4.1 Physical characterization of Ferrocene and Doxorubicin NP's and PEGylated NP's

NPs of Doxorubicin, FITU and FITU+Dox was formed through thin film hydration method. A bilayer vesicle of phospholipid was formed by utilizing DPPC (a kind of phospholipid together with lecithin, made up of two C16 palmitic acid groups), DOPC (is a phospholipid in which the phosphatidyl acyl groups i.e. oleoyl attached at position 1 and 2) and cholesterol. After synthesis they were coated with PEG, which resulted in broad peaks.
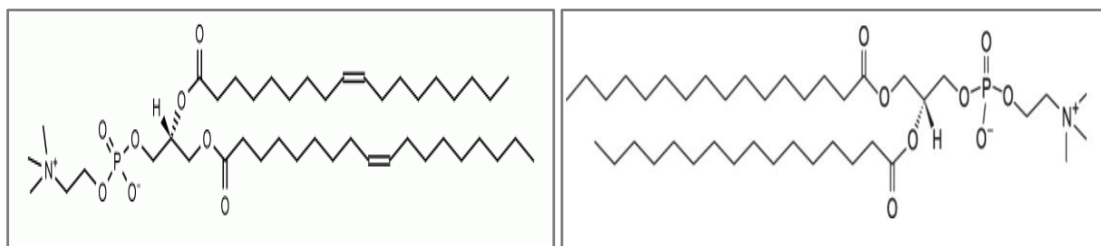
Figure 15 Structure of (a)DOPC (b) DPPC

4.1.1 UV-Visible Spectroscopy

The results of UV-VIS absorption spectroscopy displayed the peaks of cholesterol at 207nm, PEG-1000 at 250nm, DOPC at 240nm, DPPC at 220nm. DOX showed peaks at 233nm and 480nm, FITU showed peaks at 246nm and 440nm. The blank Np had peak at 230nm. The shift in the peaks of DOX-Np, FITU-Np and FITU+DOX-Np depicts the successful conjugation of cholesterol, PEG-1000, and entrapment of drugs in the nanoparticles.

Figure 16 UV-Visible spectrum of DPPC, DOPC, Cholesterol, PEG-1000, FITU, DOX Blank-Np, DOX-Np, FITU-Np and FITU+DOX-Np.

4.1.2 Zeta Potential

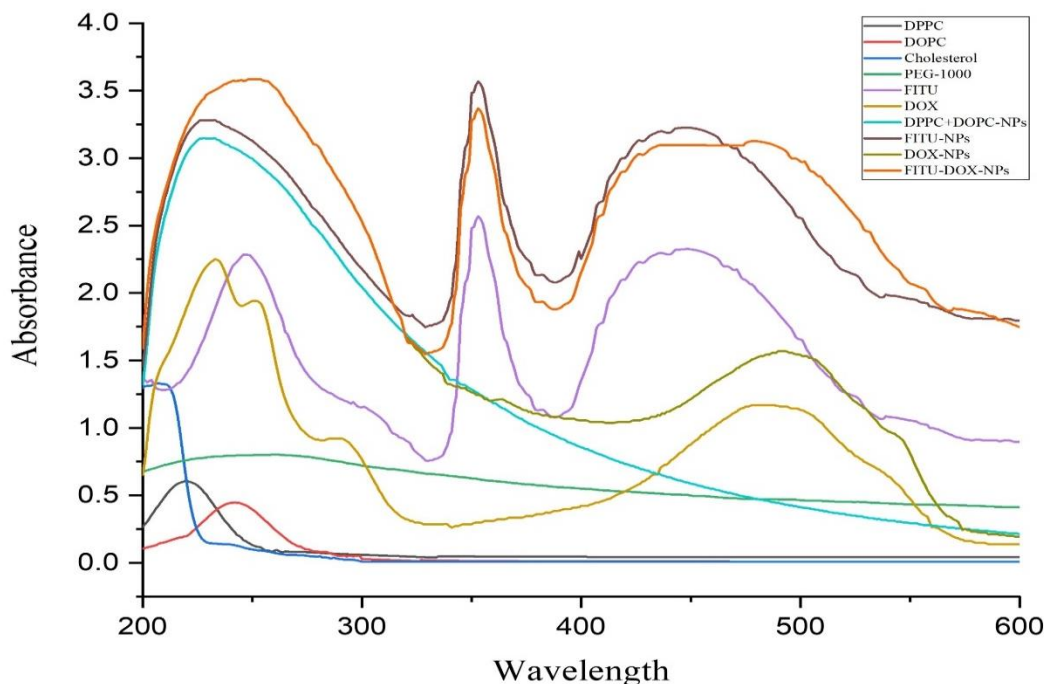| Compound	Zeta Potential (mV)
Blank Np	-4.45
DOX-Np	-6.25
FITU-NP	-8.45
FITU+DOX-Np	-10.35

Table 2 Zeta Potential of Blank-Np, DOX-Np, FITU-Np and FITU+DOX-Np

The average Zeta potential of Blank-Np, DOX-Np, FITU-Np, and FITU+DOX-Np was found to be -4.45, -6.25, -8.45 and -10.35 mV respectively.

4.1.3 Fourier Transform Infrared Spectroscopy (FTIR) Analysis

The FTIR spectrum of DPPC indicated peaks at 2919/cm (C-H stretch), 1632/cm (R-NH2, Amines), 1115/cm (C-O stretch), 720/cm (RCH2CH3), 1215/cm (P-0 stretch). The DOPC indicated peaks at 1372/cm (-C(CH3)2- stretch), 1304/cm (P-0 stretch), 2896/cm (CH3 stretch), 2896/cm (-CH3/-CH2 stretch), 1054/cm (P-O-C stretch). Cholesterol indicated peaks or bands at 2850/cm (C-H stretch), 3417/cm (O-H stretch),

1375/cm (C-O-H stretch), 873/cm (Tri-substituted Aromatics). The PEG-1000 indicated a peak at around 1200/cm (C-O stretch) and 2850/cm (C-H stretch),1639/cm (C=C stretch). The DOX indicated peaks at 1314/cm (C-O stretch), 1490/cm (C=C ring stetch), 3181/cm (N-H stretch), 3435/cm (O-H stretch), 1045/cm (C-O-C stretch). FITU exhibited peaks at 3093/cm (C-H stretch), 1105/cm (C-C stretch), 1589/cm (C=C stretch), 3379/cm (N-H stretch), 1670/cm (C=O stretch), 1250/cm (C=S stretch), 1063/cm (N-C-N stretch). The spectra peaks of drug loaded Np and Blank Np are coated with Peg 1000. Hence, the polymer coating has masked their individual peaks. By integrating drug and PEG 1000, the structural changes in lipid biomolecules were demonstrated by changes in infrared bands.
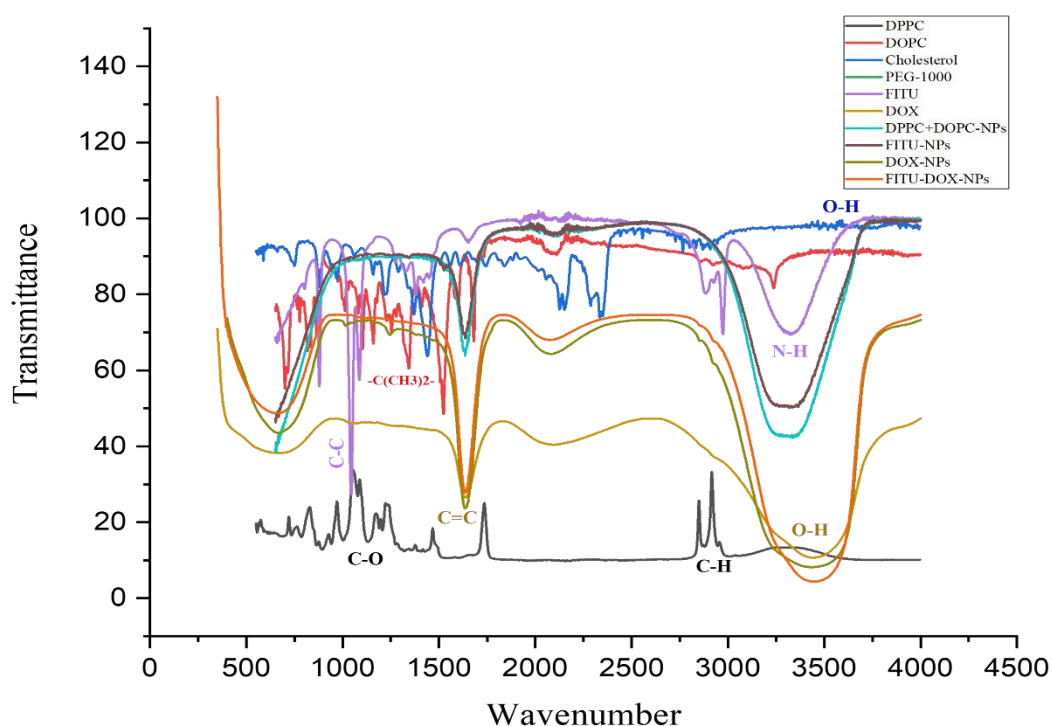

Figure 17 FTIR Spectrum of DPPC, DOPC, Cholesterol, PEG-1000, FITU, DOX Blank-Np, DOX-Np, FITU-Np and FITU+DOX-Np.

4.1.4 Particle Size and Area Distribution

The dimensions of DOX-Np, FITU-Np, and FITU+DOX-Np were evaluated using Scanning Electron Microscopy (SEM), and the dispersion of nanoparticle regions was measured using ImageJ software. The scanning electron microscopy (SEM) pictures exhibited the presence of spherical nanoparticles, with mean diameters measuring 34 nm, 78 nm, 87 nm, and 99 nm for DOX-Np, FITU-Np, and FITU+DOX-Np, respectively.
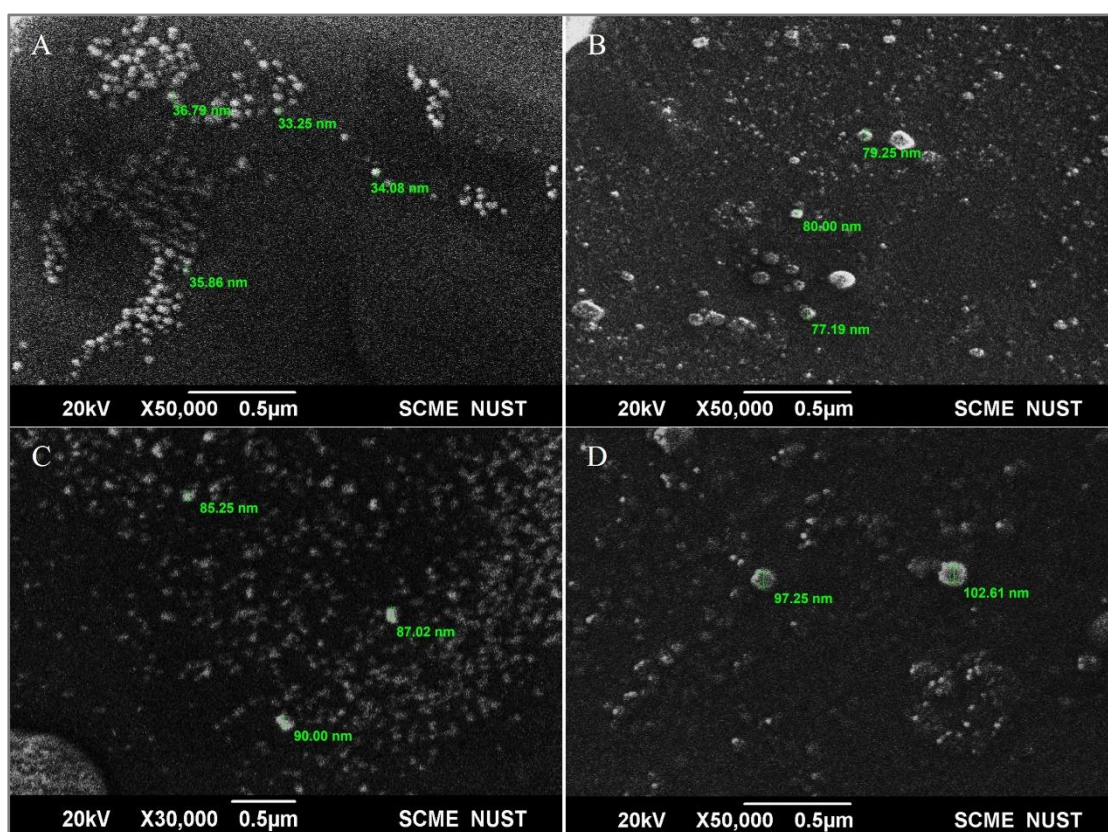

Figure 18 SEM Images of (A) Blank-Np (B) DOX-Np (C) FITU-Np (D) FITU+DOX-Np

4.1.5 Drug Encapsulation Efficiency

The encapsulation efficiency of DOX-Np, FITU-Np and FITU+DOX-Np was found to be 77, 73, and 74 % respectively explaining the entrapment of drug in nanoparticles respectively.

4.1.6 Drug Release Kinetics

The release of drug from Np were noted up to 16 hours suggesting the sustain released of drug with time. This long stay of drug helps in achieving high bioavailability and eventually leads to high efficacy in treating the diseases.
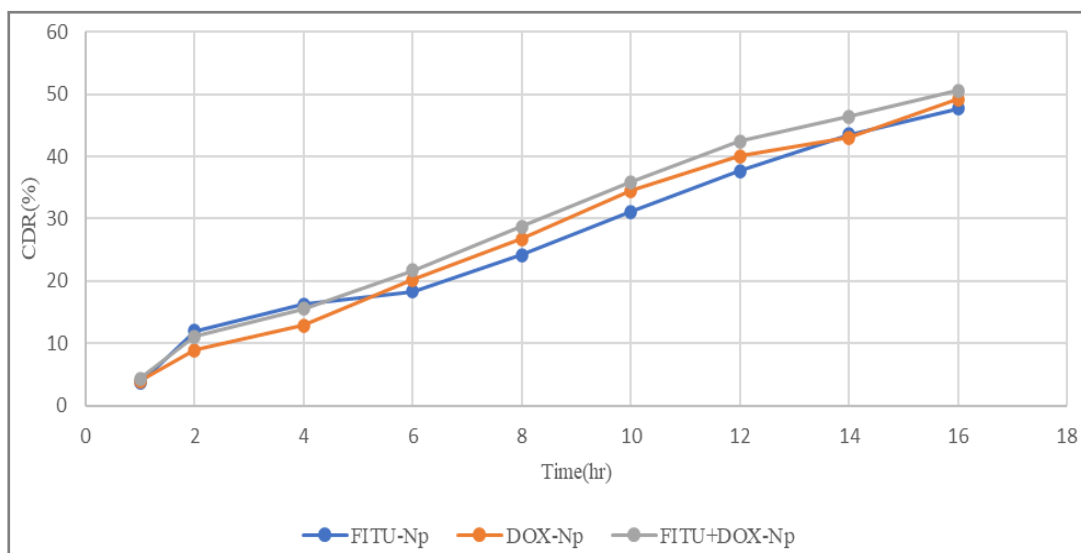
Figure 19 Comparative Drug Release Graph of FITU-Np, DOX-Np, FITU+DOX-Np

4.2 In-Vitro Assay

4.2.1 Cytotoxicity Assay

4.2.1.1 Brine shrimp Assay

The percentage mortality of DOX-Np, FITU-Np and FITU+DOX-Np at different concentrations were significant as compared to DOX, FITU and FITU+DOX respectively, as shown in figure. The LC50 calculated for DOX, DOX-Np, FITU, FITU-Np, FITU+DOX and FITU+DOX-Np were 1807.7µg/ml, 2375.3µg/ml, 2056.0µg/ml, 2994.7 µg/ml, 1865.9µg/ml and 3300.9µg/ml respectively, showed that drugs their nanoparticles were non-toxic according to criteria (Zheng & Bossier, 2023).
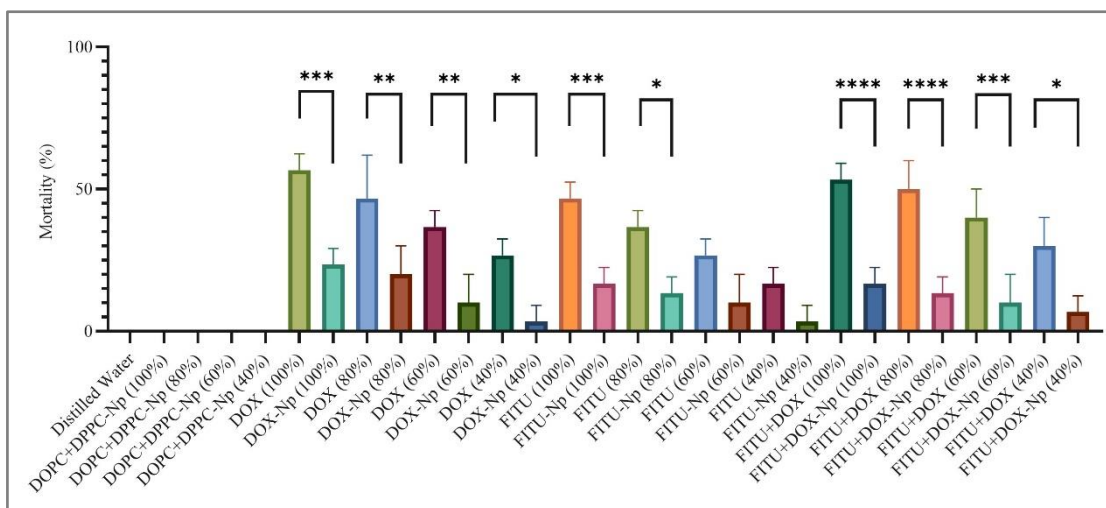
Figure 20 Brine Shrimp Assay

4.2.1.2 Hemolytic Assay

The percentage hemolysis of DOX-Np, FITU-Np and FITU+DOX-Np at different concentrations were significant as compared to DOX, FITU and FITU+DOX respectively, as shown in figure. The LC50 calculated for DOX, DOX-Np, FITU, FITU-Np, FITU+DOX and FITU+DOX-Np were 5869.8µg/ml, 7838.6µg/ml, 8499.7µg/ml, 9173.5µg/ml, 7888.9µg/ml and 7356.0µg/ml respectively, showed that drugs their nanoparticles were non-toxic according to criteria (Zheng & Bossier, 2023). According to ASTM F 756-00 standards (Dobrovolskaia et al., 2008) the designed nanoparticles were hence suitable for IV route and are biocompatible as they are less hemolytic than free drug.
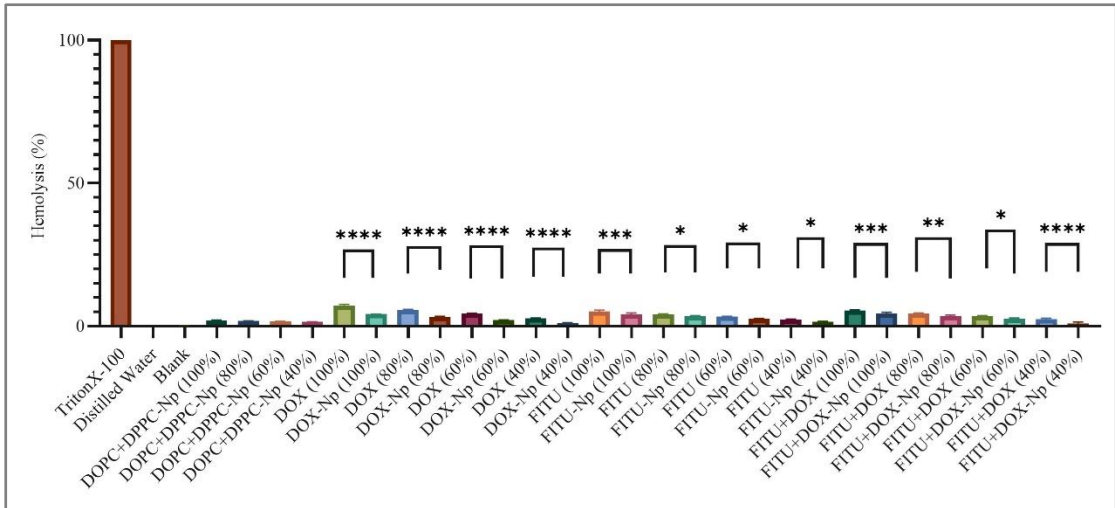
Figure 21 Hemolytic Assay

4.2.2 Antioxidant Assay

4.2.2.1 Total Antioxidant Capacity

The TAC of DOX-Np, FITU-Np and FITU+DOX-Np at different concentrations were significant (P<0.0001) in comparison to free drug as shown in figure which states that Np are biocompatible.
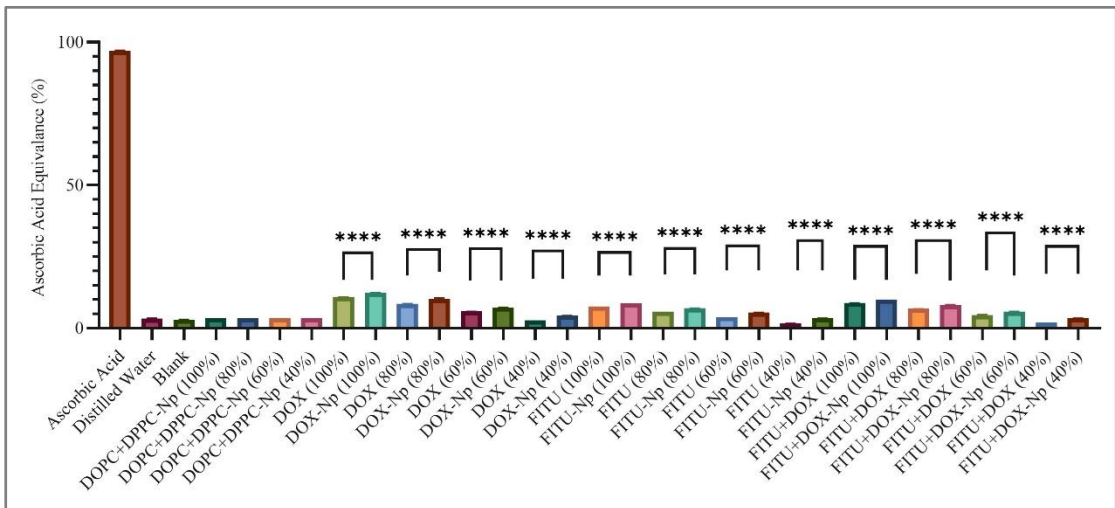
Figure 22 Total Antioxidant Assay

4.2.2.2 DPPH (1,1-diphenyl-2-picrylhydrazyl) Free Radical Scavenging Activity

The DPPH scavenging activity of DOX-Np, FITU-Np and FITU+DOX-Np at different concentrations were significant when compared to their free drugs respectively (P< 0.001).
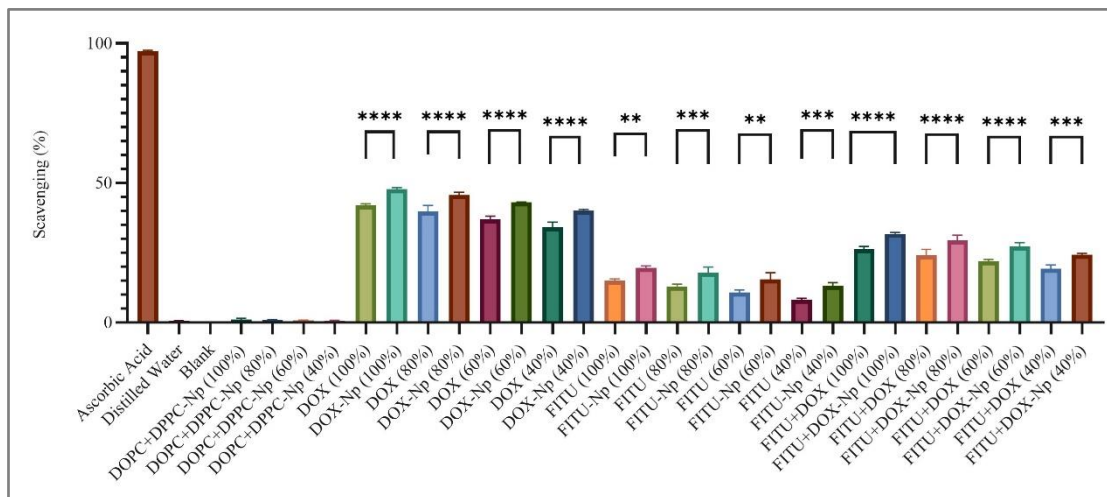
Figure 23 DPPH Assay

4.2.2.3 Total Reducing Power Assay

The TRP value of DOX-Np, FITU-Np and FITU+DOX-Np at different concentrations were more significant as compared to free drug (P < 0.0001) as shown in figure 24.
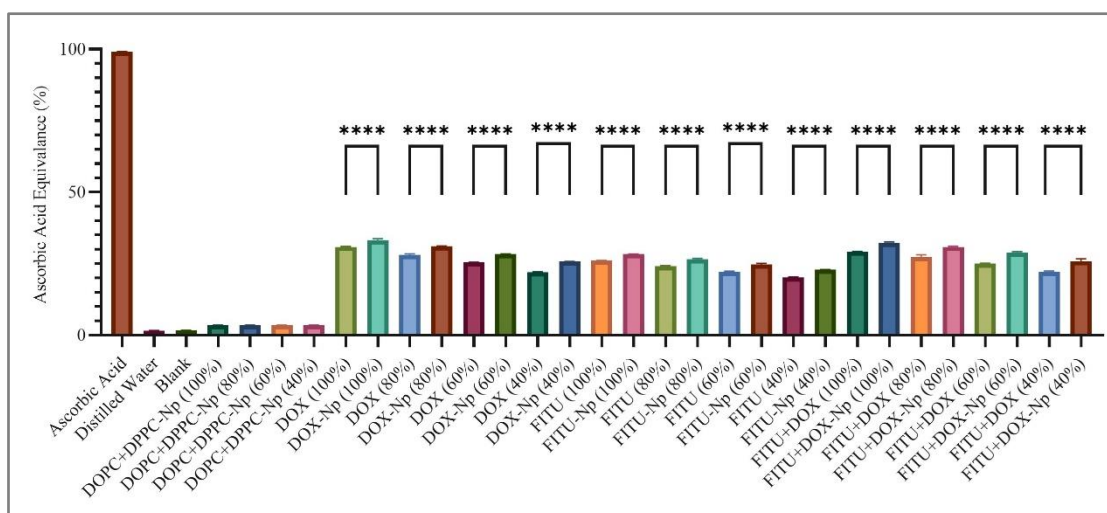
Figure 24 Total Reducing Power Assay

4.3 In vivo Assay

4.3.1 Body and Organ weights Analysis

4.3.1.1 Body Weights

During the period of acclimatization body weight of all the rats increased. In the induction period the body weights of all the rats decreased over the time as compared to control group. The diseased group showed significant decline in body weights as compared to control group when t-test was applied ($P < 0.05$) as shown in figure 25. During the treatment period, significant increase in the body weights was observed in all treatment groups.
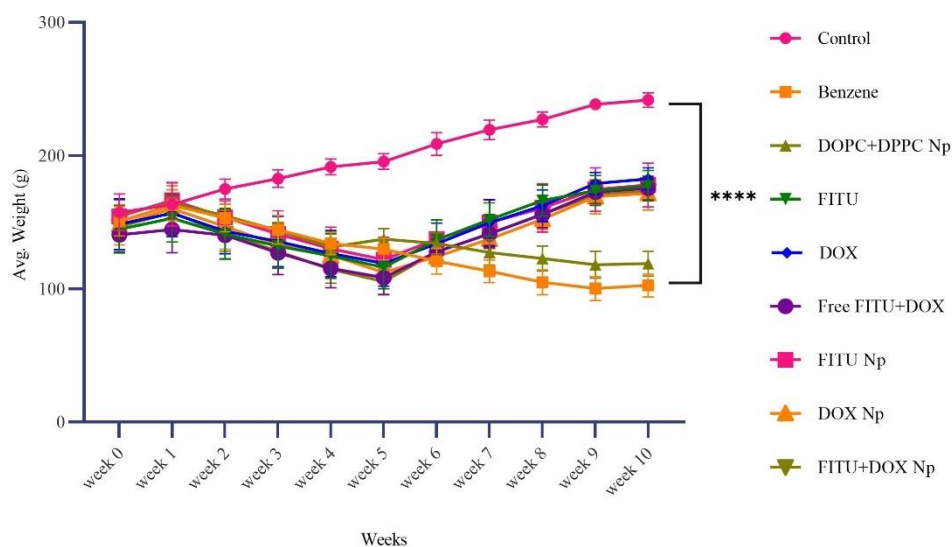
Figure 25 Weight Analysis of Body Weights of Control, Diseased and Treatment Groups.

4.3.1.2 Organ weights

The organ weights were obtained at the time of dissections, which showed significant increase in organ weights in diseased group as compared to control. While one way ANOVA analysis displayed that treatment groups showed significant decrease in body weights of liver, heart and kidney as compared to disease group which is evident from graph as shown in figure 26.
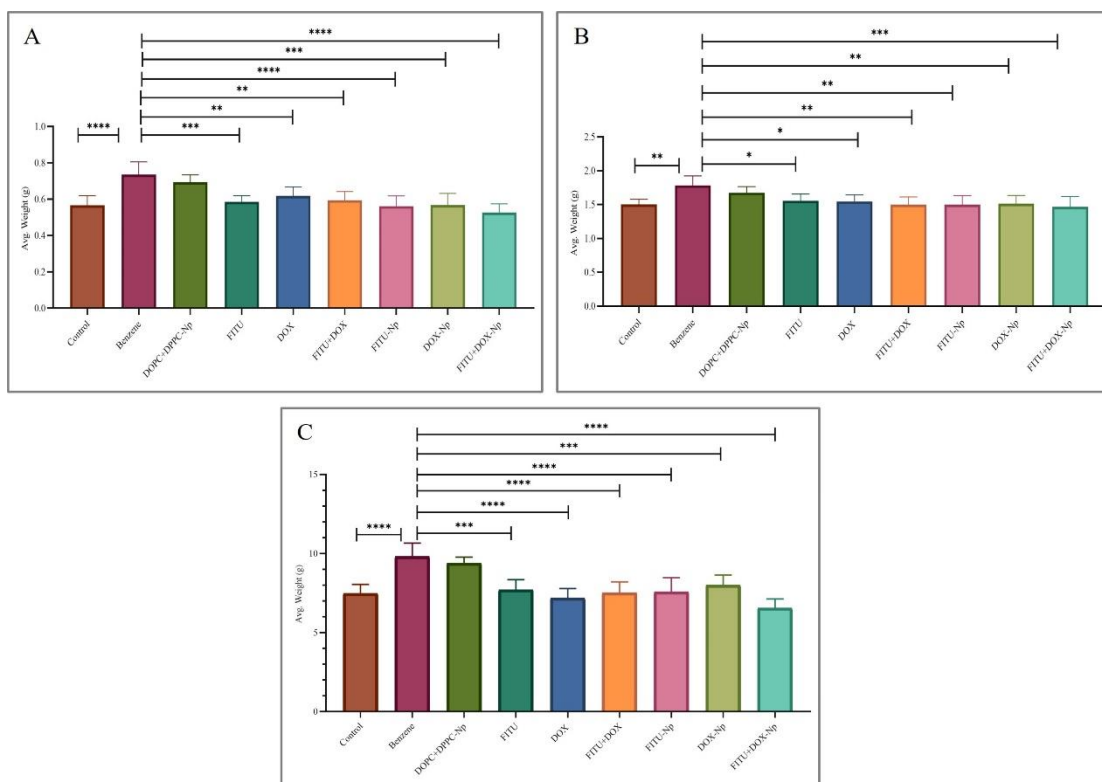
Figure 26 A) Heart weight B) Kidney weight C) Liver weight significance.

4.3.2 Serological Analysis

4.3.2.1 Liver Function Test

The results of liver function test including alkaline phosphatase (ALP), aspartate aminotransferase (AST), alanine transaminsae (ALT) showed significant increase in the serum levels when benzene was given for induction. However, treatment groups showed significant decrease in serum level of ALP, AST, and ALP. The nanoparticles showed more significant results as compared to free drug as shown in figure 27.
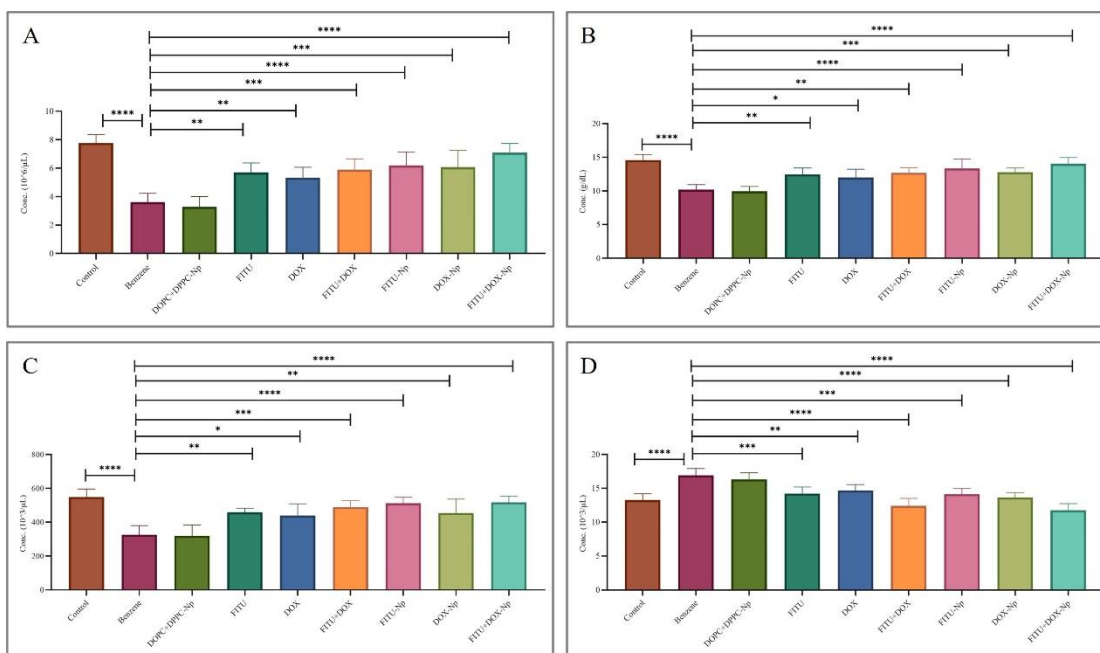
Figure 27 Liver function test (A)ALP (B) ALT (C) AST (D) Total bilirubin

4.3.2.2 Renal Function Test

The results of the liver function test, which included the measurement of creatinine, urea, and uric acid, revealed a significant increase in serum levels after the administration of benzene. In contrast, the experimental groups demonstrated a significant decrease in the concentrations of creatinine, urea, and uric acid in the serum. Significantly, the nanoparticles exhibited more prominent effects in comparison to the free drug, as depicted in figure 28.
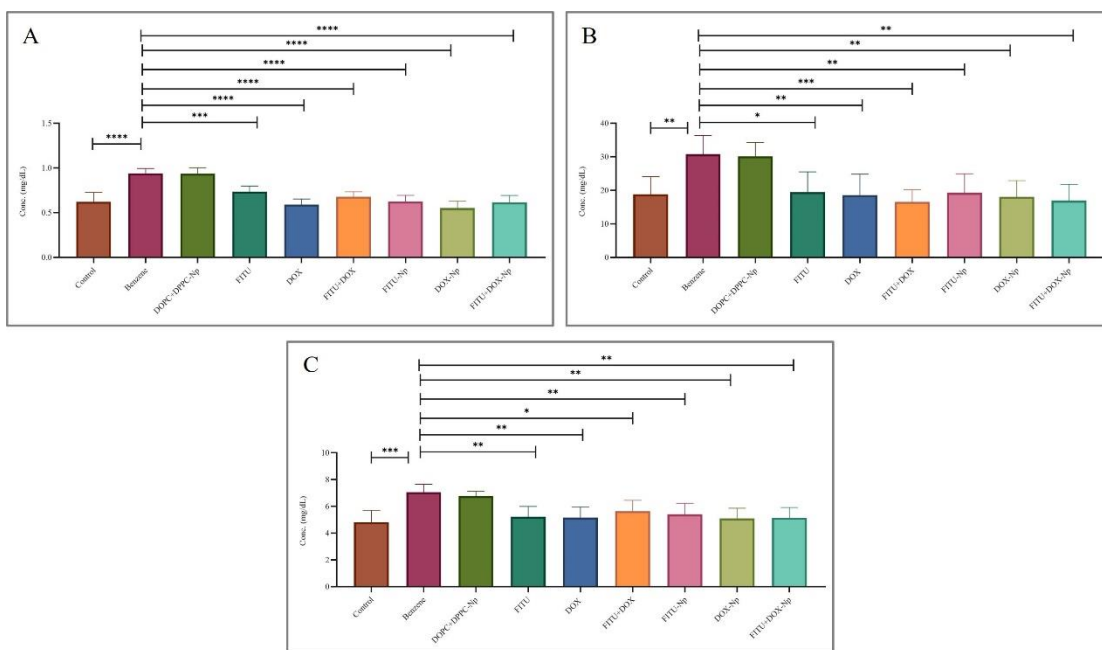
Figure 28 Renal function test (A) Creatinine (B) Urea (C) Uric acid

4.3.3 Haematological Analysis

Blood samples from rats were subjected to a comprehensive analysis known as a complete blood count. The findings demonstrated a reduction in the levels of red blood cells (RBCs), haemoglobin (Hb), and platelet count as a result of benzene exposure. In contrast, the levels of white blood cells (WBCs), such as lymphocytes, basophils, monocytes, neutrophils, and eosinophils, demonstrated an elevation after the administration of benzene.
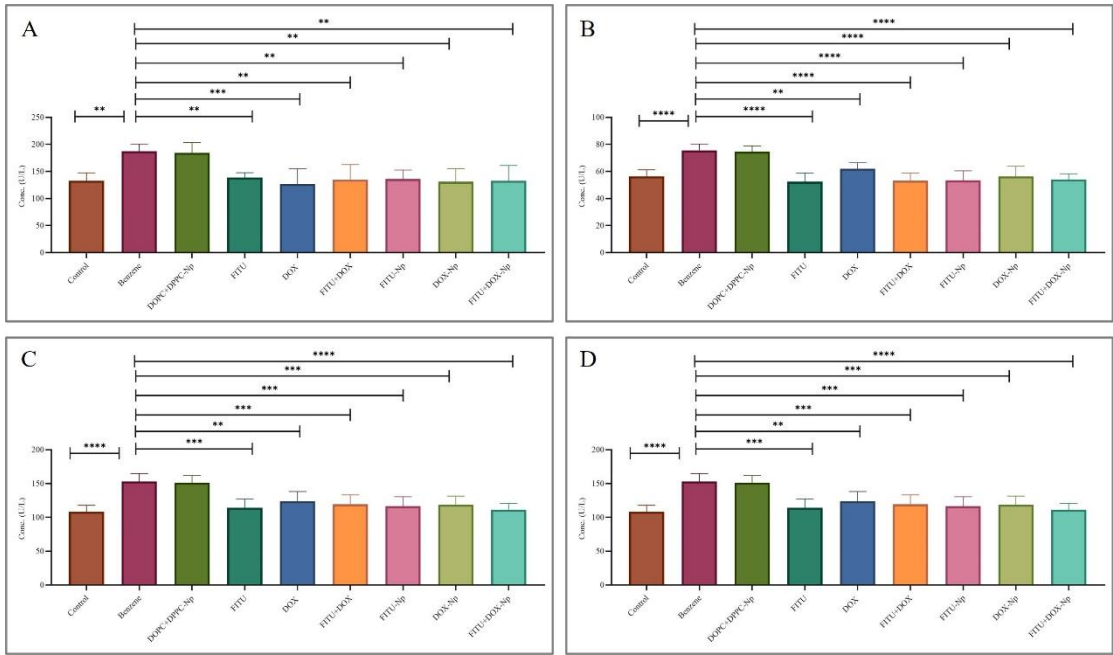
Figure 29 Complete Blood Count (A) Red blood cells (B) Hemoglobin (C) Platelets
(D) White blood cells
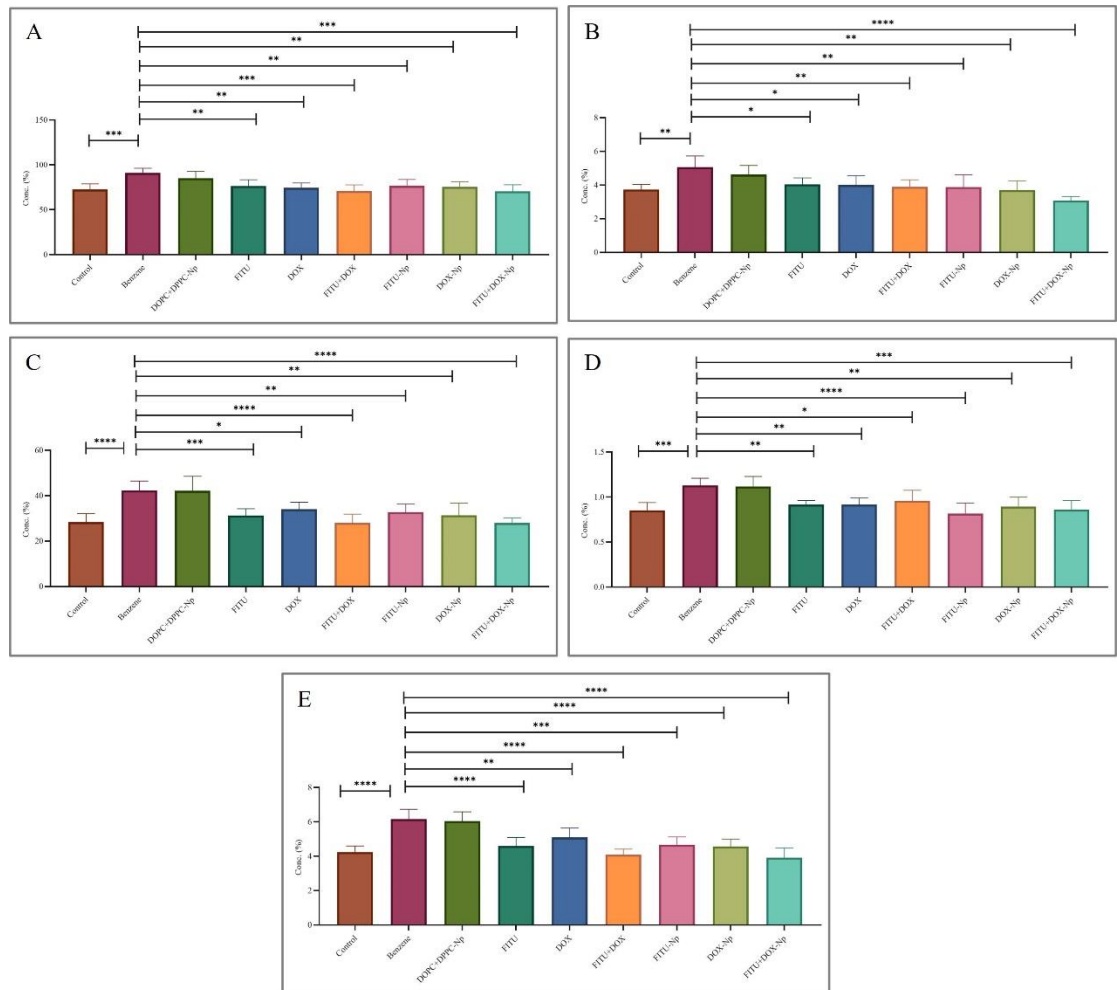
Figure 30 WBC's differential count (A) Lymphocytes (B) Monocytes (C) Neutrophils
(D) Basophils (E) Eosinophils

The treatment groups showed considerable increase in RBC's, Hb and platelets while WBC's count was restored towards normal.

4.3.4 Morphological Analysis

The blood smear slides examination depicted increased number of myeloblasts with immature chromatin and cytoplasmic granules in case of diseased group showing the reminiscent of acute myeloid leukemia. However, with treatment the cells showed improved morphology, the treatment with liposomal nanoparticles depicted better results having normal cell morphology as shown in figure 31.
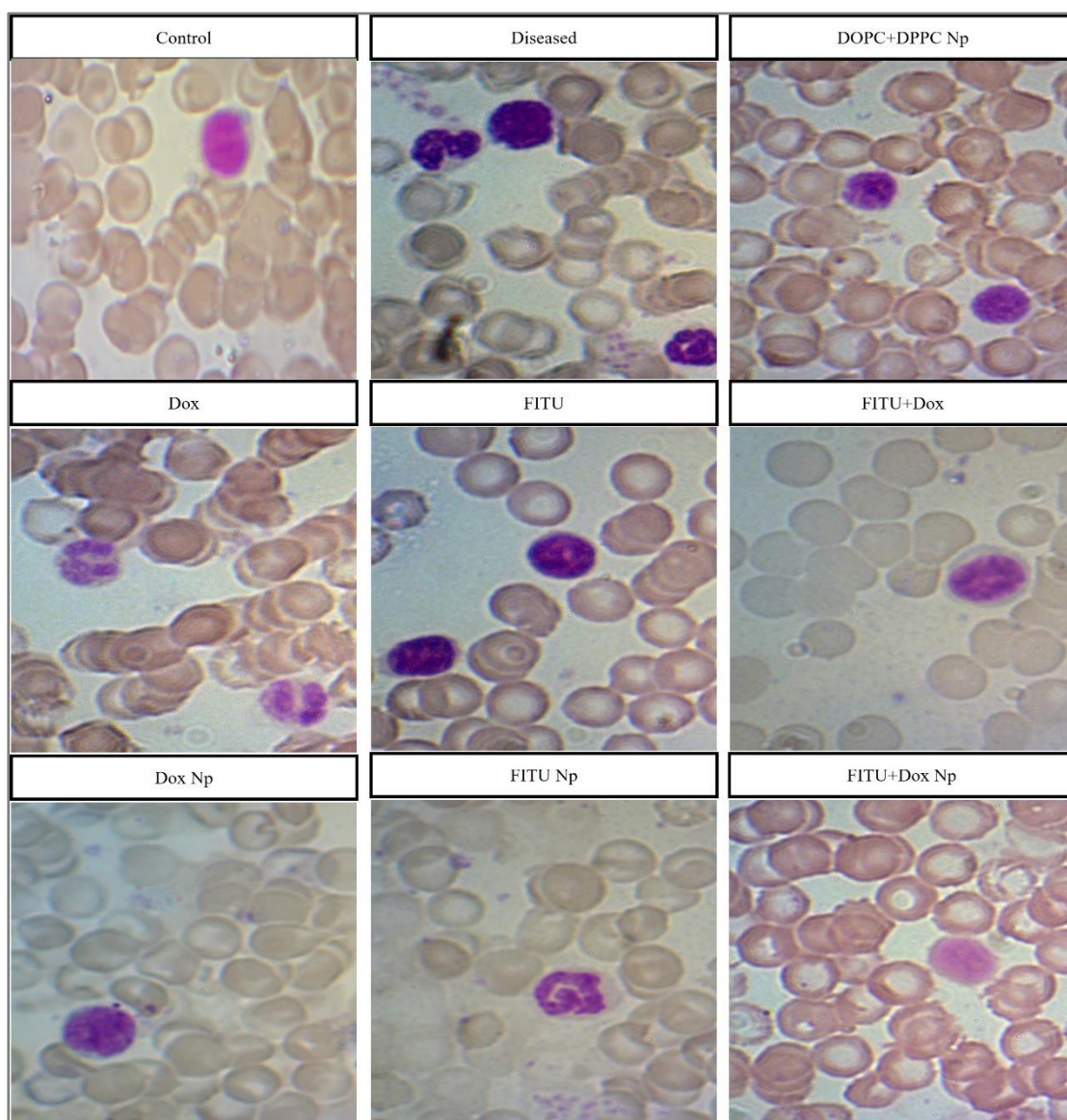
Figure 31 Blood Morphology

4.3.5 Histopathological Analysis

4.3.5.1 Histopathology of Liver

The liver from control group showed normal morphology i.e having normal hepatocytes and portal tracts. In the diseased group, necrosis of hepatocytes, disintegration of plasma membrane, protrusion of cytoplasm along with extramedullary hematopoiesis was observed. Treatment groups showed, normal cell integrity with no infiltration and necrosis. The results of liposomal nanoparticles were more significant.
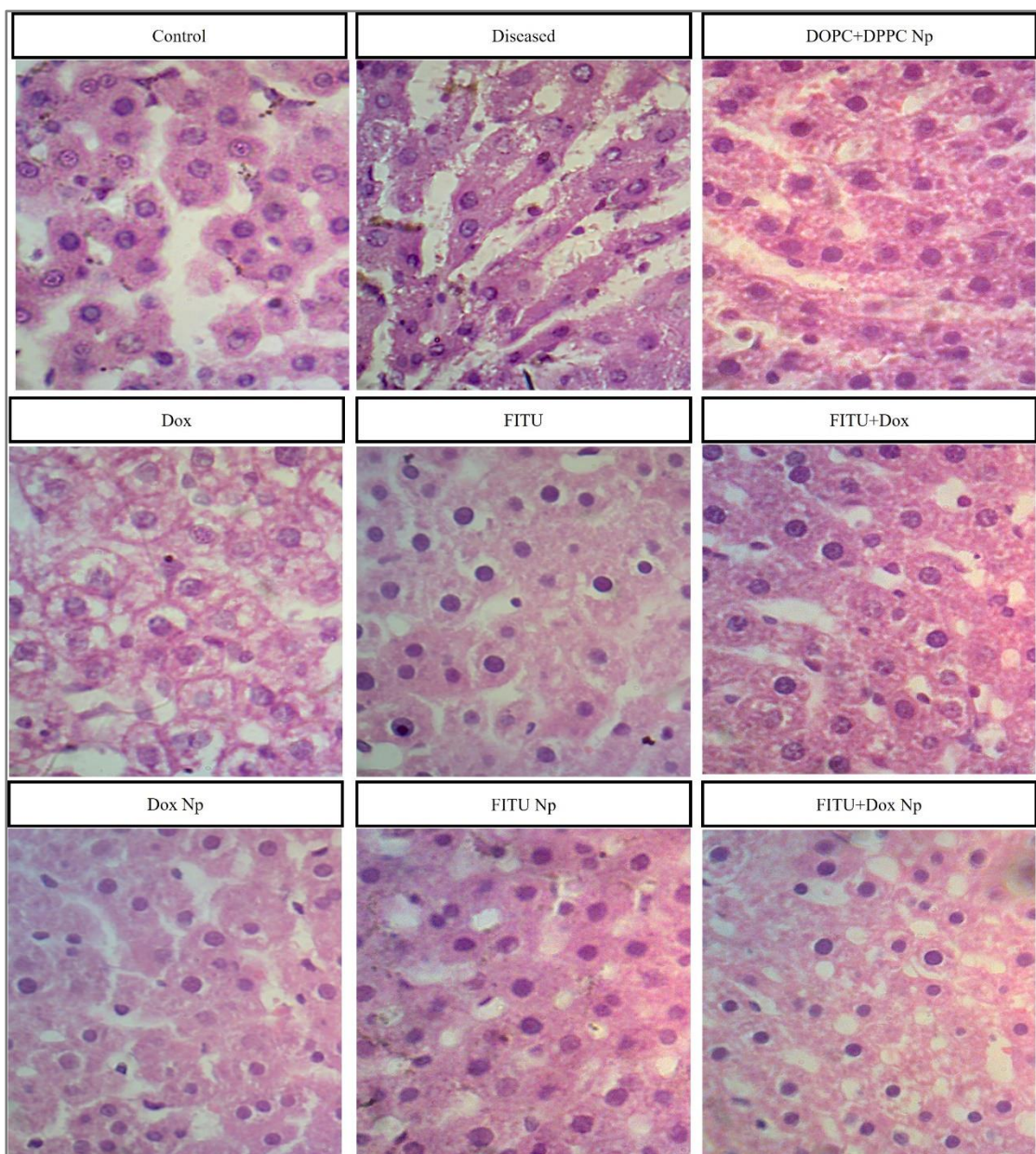
Figure 32 Histopathology of Liver

4.3.5.2 Histopathology of Kidney

Control group showed intact structure with normal glomerulus, proximal tubule, and distal tubule. However, diseased group exhibited dilation, inflammation, tubular necrosis, hypertrophy of glomerulus and large space of Bowman's capsule. Analysis of treatment groups showed reduced inflammation, and normal glomerulus. Liposomal groups showed more improved results in comparison to free drug.
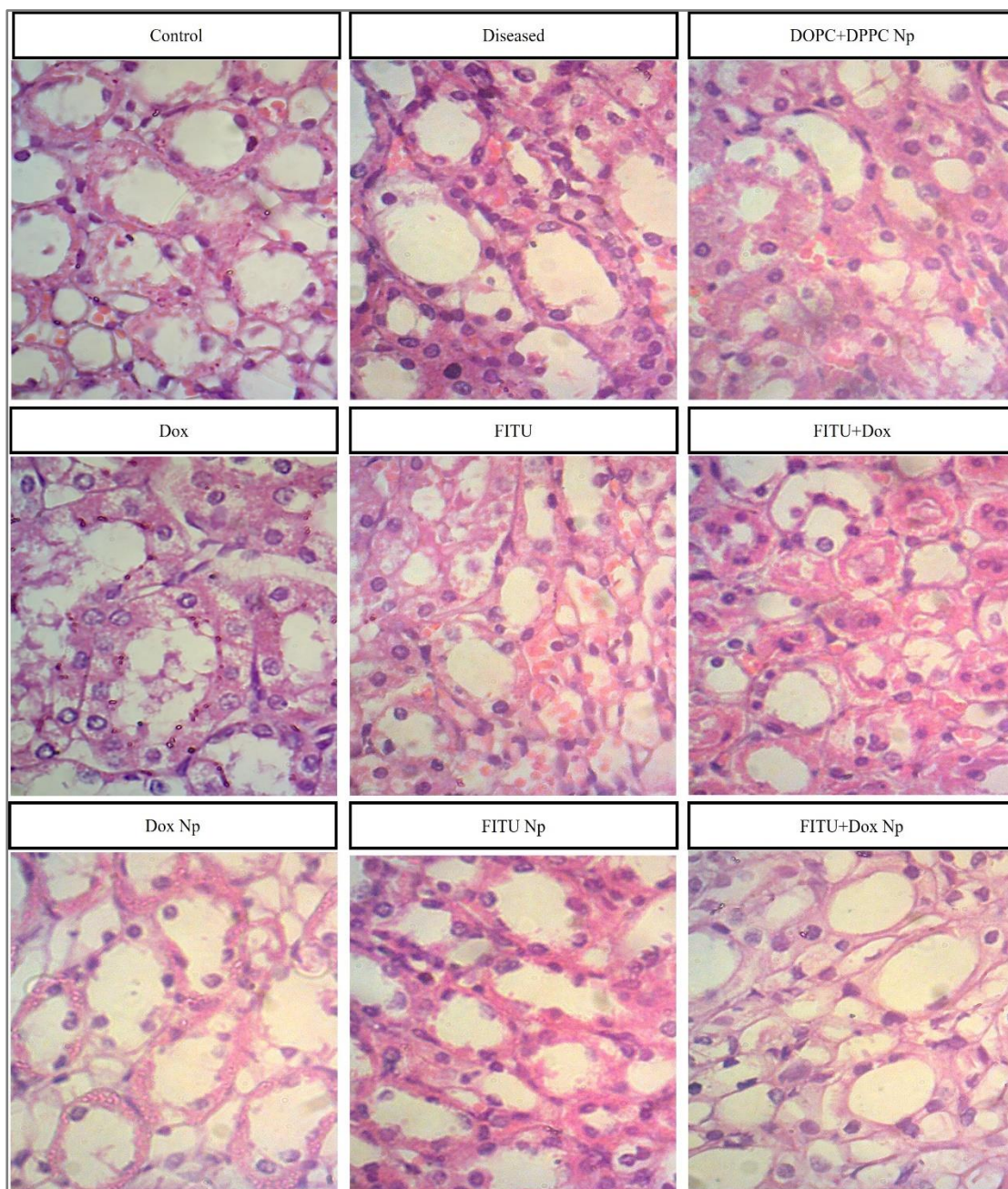
Figure 33 Histopathology of Kidney

4.3.5.3 Histopathology of Heart

The control group showed normal cardiac muscles arrangement with no necrosis, infiltration, and inflammation. Infiltration of mononuclear cells was observed in diseased group along with disarrangement of cardiac tissues and inflammation. The Dox treated group showed haemorrhage, necrosis, cellular infiltration. Other treatment groups restore the cardiac structure and show improvement in histopathological results. The liposomal nanoparticles results were more significant.
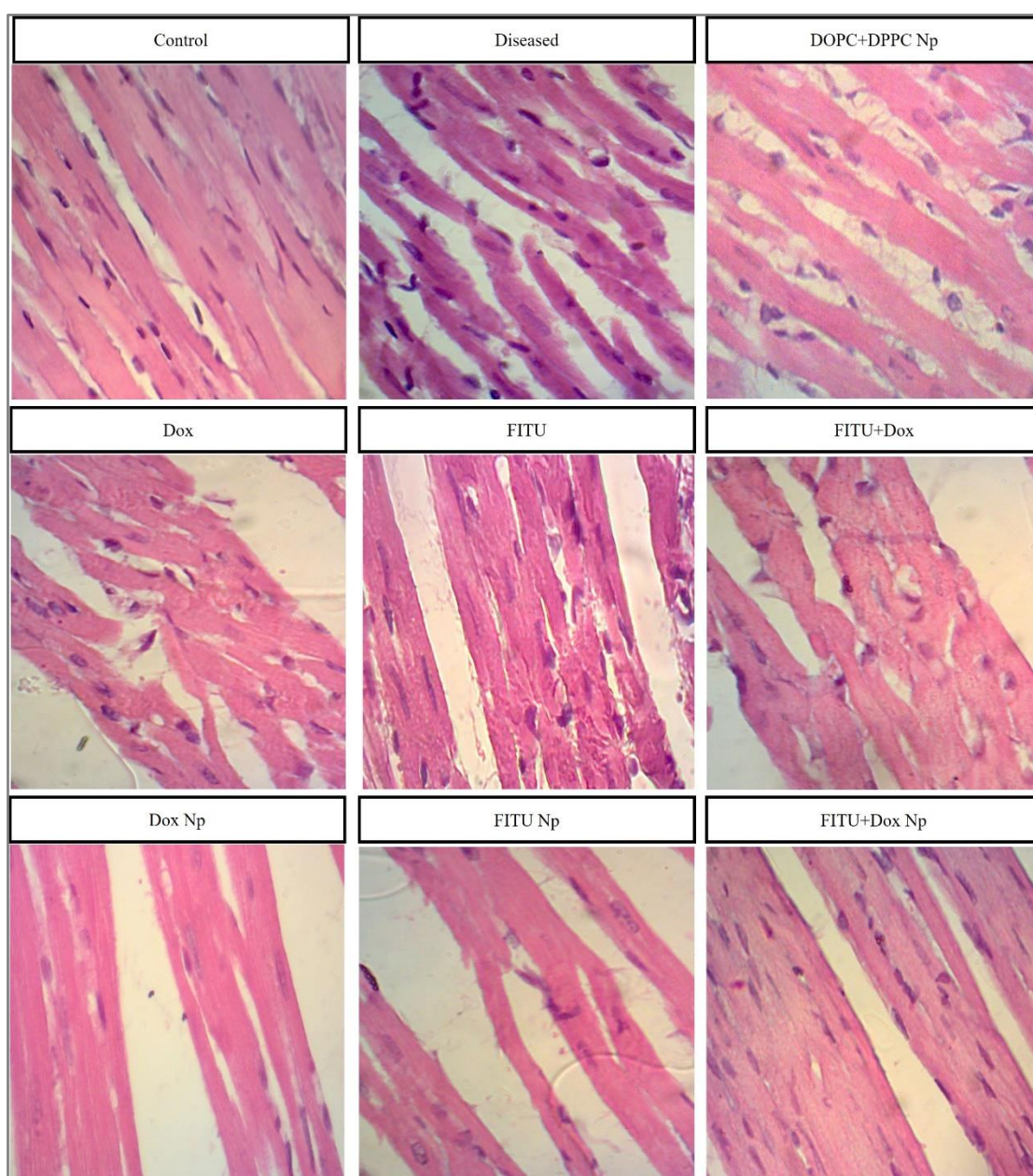
Figure 34 Histopathology of Heart

Chapter 5: Discussion

Even with advancement in treatment of acute myeloid leukemia through novel therapeutic agents, improving chemotherapy and supportive care acute myeloid leukaemia still is a life-threatening disease. Conventional chemotherapies have been proven futile and causing multi-drug resistance. New treatment strategies for acute myeloid leukemia with high efficacy and less side effects are essential (Issa et al., 2023). The management of acute myeloid leukaemia continues to be a significant obstacle in terms of ensuring both safety and efficacy. Within this particular context, the use of nano-drug delivery has arisen as a crucial methodology in the advancement of targeted drug delivery systems. The primary objective of such systems is to reduce the occurrence of adverse effects, maximise the availability of drugs at the intended location, and improve patient adherence to treatment protocols (Kalepu & Nekkanti, 2015; Wang, 2023; Zahra et al., 2023). Lipid nanoparticles are good carriers for drug delivery at target site because of their high encapsulation efficacy, enhanced stability, and increased circulation time (Farooq et al., 2022).

Although DOX is used as a standard drug for treatment of leukemia however, it's therapeutic potential is limited because of its cardiotoxicity, and hepatotoxicity (Abdel Moneim et al., 2023). FITU complex shows prominent biochemical activity due to the presence of the thiocarbonyl group, amine group and ferrocene moiety. Its mechanism of action is similarly related to antioxidant capabilities. However, the bioavailability of the FITU drug is questionable because of the hydrophobic nature of the drug (Larik et al., 2017).

In this study, PEG coated Np's for FITU drug, DOX drug and combination of FITU+DOX were successfully designed and studied against acute myeloid leukemia

model of rats. The characterization of Np's was done and efficient conjugation of drug with their respective nanoparticles were represented in the results of UV-analysis and FTIR analysis which showed significant masking in peaks and shift in band, with PEG coating thus increasing the stability of designed Np (Allen et al., 2002). According to the Zeta Potential data, developed Np have neutral potentials between 0 and 10 mV. The stability of Np is determined by the zeta potential; a larger positive charge is needed to prevent NP aggregation (Anwar et al., 2020). The SEM analysis of FITU-Np, DOX-Np and FITU+DOX-Np showed increased particle size as compared to Blank-Np thus indicating effective loading of drug in the designed Np (Farooq et al., 2022; Maryam et al., 2023).The encapsulation efficiency of DOX-Np, FITU-Np and FITU+DOX-Np was found to be 77%, 73%, and 74% respectively explaining the entrapment of drug in nanoparticles respectively and results from drug release kinetics explained the sustained drug delivery from the Np (Zhao et al., 2017).

The results of in-vitro assay (cytotoxicity, antioxidant) showed that DOX, FITU, FITU+DOX, DOX-Np, FITU-Np, FITU+DOX-Np have antioxidant activity and non-toxic property (Gabizon et al., 2003; Hussain et al., 2014).

The animal model of AML was designed by induction through benzene, (Snyder, 2012) the successful induction was confirmed by blood morphology which depicted increased myeloblast and increased white blood cells including lymphocytes, monocytes, neutrophils, basophils, and eosinophils (Hendrik et al., 2011).

The decline in body weights of rats was observed which was presumed because of the production of toxic substances by rapidly dividing cells which effect the speed and efficacy of normal body metabolism (Smith et al., 2015). Nonetheless, treatment with DOX, FITU, FITU+DOX, DOX-Np, FITU-Np, FITU+DOX-Np restored the body weights. Also, the organ weights of leukemic rats were significantly increased which is

indicative of inflammation and hypertrophy because of infiltration of malignant blast cells (Gamal Abdul, 2013; Kang et al., 2019). However, these weights were significantly returned to normal ranges after treatment with DOX, FITU, FITU+DOX, DOX-Np, FITU-Np, FITU+DOX-Np.

Liver function test including ALT, AST, ALP, and total bilirubin revealed an increased levels of them because of the toxicity caused by metabolites of benzene (Akinlolu et al., 2018; Golabi-Habashi et al., 2021; Mathews et al., 2008). The treatment with DOX, FITU, FITU+DOX, DOX-Np, FITU-Np, FITU+DOX-Np significantly reverses the hepatotoxicity because of the antioxidant property of the compounds. The renal function test including urea, creatinine, and uric acid were also increased in diseased group (El-Shakour et al., 2015; Lahoti et al., 2010; Rasool et al., 2015). The levels were restored to normal on treatment with DOX, FITU, FITU+DOX, DOX-Np, FITU-Np, FITU+DOX-Np.

In leukemic rats' complete blood count revealed decrease in red blood cells (RBC's), haemoglobin (Hb), platelets, which indicates anemia. This is because abnormal WBCs prevent the bone marrow from producing RBCs and PLTs (Qian & Wen-jun, 2013; Vucinic et al., 2021). An abnormally high level of white blood cells (WBC) has been linked to the induction of AML. A shorter duration of relapse and a lower survival rate are both related to a larger lymphocyte count at the time of diagnosis of AML (Zhang et al., 2021). However, treatment with DOX, FITU, FITU+DOX, DOX-Np, FITU-Np, FITU+DOX-Np restored the RBC's, Hb, and platelets count towards normal and improved the WBC's differential count in treated groups.

Morphological analysis showed reduced and immature RBCs and increased number of myeloblasts with immature chromatin and cytoplasmic granules (Döhner et al., 2010; Ladines-Castro et al., 2016; Zhu et al., 2023). Treatment with DOX, FITU,

FITU+DOX, DOX-Np, FITU-Np, FITU+DOX-Np, however, reduced blast cell numbers while also restoring the normal shape of leukocytes in treated rats. The histopathological findings of liver, kidney and heart showed inflammation and infiltration of malignant blast cells (Bukhari et al., 2022; Walsh et al., 2021), which were reversed on treatment with DOX, FITU, FITU+DOX, DOX-Np, FITU-Np, FITU+DOX-Np.

Chapter 6: Conclusion

In an innovative approach to cancer therapy, specifically targeting leukemia, researchers have developed a method to encapsulate FITU and doxorubicin (DOX) within liposomal nanoparticles. This encapsulation is a strategic response to the limitations that these drugs face when administered individually.The conventional administration of FITU and DOX has been hampered by challenges that restrict their clinical efficacy. For FITU, the issue lies in its bioavailability, which dictates the extent and rate at which the active medicinal ingredient enters systemic circulation, thereby reaching the site of action. On the other hand, DOX is notorious for its cardiotoxicity, a severe side effect that limits its therapeutic window.

Liposomal nanoparticles present a solution, serving as a delivery vehicle that enhances the drugs' bioavailability. These spherical vesicles, composed of phospholipid bilayers, are adept at encapsulating medicinal compounds, thereby improving the circulation time and stability of the drugs. Furthermore, their site-specific delivery capabilities mean they can direct the drugs to the targeted area while avoiding the exposure of non-target tissues, significantly reducing the likelihood of adverse side effects. The co-encapsulation within these liposomes has demonstrated promising improvements in several clinical parameters. Blood morphology, which encompasses the size, shape, and number of blood cells, showed improvements, indicating a healthier systemic state. Additionally, the activity of hepatic and renal enzymes was modulated, suggesting protective effects on the liver and kidneys, which are often compromised by cancer therapies. Crucially, a reduction in organ inflammation was observed, an encouraging sign that points towards the anti-inflammatory potential of the therapy. These enhancements suggest that the co-administered drugs may possess significant anti-leukemic potential, whether used alone or in combination therapy. The improvements

in key biomarkers reflect a systemic therapeutic benefit, underscoring the potential of this novel approach to leukemia treatment. The study paves the way for further research, with the designed animal model serving as a foundation for the exploration of disease and drug parameters. The liposomal formulation used DOPC (dioleoylphosphatidylcholine) and DPPC (dipalmitoylphosphatidylcholine) for the synthesis of the nanoparticles. However, researchers suggest that alternative lipids could be explored for potentially improved drug encapsulation efficiency. Moreover, the use of other forms of PEGylation, which involves coating the nanoparticles with polyethylene glycol (PEG), could be investigated to enhance the internalization and circulation time of the nanoparticles, thereby further improving the targeted delivery and therapeutic profile of the drugs. The conclusion of this study is not an endpoint but a gateway to extensive research, with the aim of developing a deeper understanding of leukemia and refining drug delivery systems for better clinical outcomes.

Chapter 7: Future Prospect

This study was designed to overcome the issues associated with drugs i.e bioavailability of FITU and side effects associated with doxorubicin by encapsulating them in liposomal nanoparticles which increase their circulation time, stability, and site-specific delivery to avoid unwanted side effects. The designed animal model could be used for further studies of disease and drug parameters. The lipids used in this study were DOPC and DPPC for synthesis of liposomal nanoparticles, which could be replaced by other lipids for improved drug encapsulation. Alternatively, other PEG for coating could also be used for better internalization and improved circulation time of nanoparticles. Moreover, further studies should be conducted for better understanding of leukemia and drugs.

References

Abdel Moneim, A., Ezzat, A., Salem, F. E. H., Kassab, R., & El-Yamany, N. A. (2023). Protective effect of virgin coconut oil against doxorubicin-mediated hepatotoxicity in rats. *Advances in Basic and Applied Sciences*, *1*(1), 46-54. https://doi.org/10.21608/abas.2023.195721.1009

Abdelaziz, M. H., Salah El-Din, E. Y., El-Dakdoky, M. H., & Ahmed, T. A. (2019). The impact of mesenchymal stem cells on doxorubicin-induced testicular toxicity and progeny outcome of male prepubertal rats [https://doi.org/10.1002/bdr2.1535]. *Birth Defects Research*, *111*(13), 906-919. https://doi.org/https://doi.org/10.1002/bdr2.1535

Adams, J. M., & Cory, S. (2007). The Bcl-2 apoptotic switch in cancer development and therapy. *Oncogene*, *26*(9), 1324-1337. https://doi.org/10.1038/sj.onc.1210220

Akbarzadeh, A., Rezaei-Sadabady, R., Davaran, S., Joo, S. W., Zarghami, N., Hanifehpour, Y., Samiei, M., Kouhi, M., & Nejati-Koshki, K. (2013). Liposome: classification, preparation, and applications. *Nanoscale Research Letters*, *8*(1), 102. https://doi.org/10.1186/1556-276X-8-102

Akinlolu, A., Salau, B., Odewabi, A., Biliaminu, S., & Abdulazeez, I. (2018). Plasma hepatic enzymes as biopredictors of type, metastasis, and prognostication of hematological malignancies [Original Article]. *Journal of Medical Sciences*, *38*(1), 24-28. https://doi.org/10.4103/jmedsci.jmedsci_13_17

Alavi, M., & Hamidi, M. (2019). Passive and active targeting in cancer therapy by liposomes and lipid nanoparticles. *34*(1). https://doi.org/doi:10.1515/dmpt-2018-0032 (Drug Metabolism and Personalized Therapy)

Ali, S., Yasin, G., Zuhra, Z., Wu, Z., Butler, I. S., Badshah, A., & Din, I. u. (2015). Ferrocene-Based Bioactive Bimetallic Thiourea Complexes: Synthesis and Spectroscopic Studies. *Bioinorganic Chemistry and Applications*, *2015*, 386587. https://doi.org/10.1155/2015/386587

Allen, C., Dos Santos, N., Gallagher, R., Chiu, G. N. C., Shu, Y., Li, W. M., Johnstone, S. A., Janoff, A. S., Mayer, L. D., Webb, M. S., & Bally, M. B. (2002). Controlling the Physical Behavior and Biological Performance of Liposome Formulations Through Use of Surface Grafted Poly(ethylene Glycol). *Bioscience Reports*, *22*(2), 225-250. https://doi.org/10.1023/a:1020186505848

Anwar, M., Muhammad, F., Akhtar, B., ur Rehman, S., & Saleemi, M. K. (2020). Nephroprotective effects of curcumin loaded chitosan nanoparticles in cypermethrin induced renal toxicity in rabbits. *Environmental Science and Pollution Research*, *27*(13), 14771-14779. https://doi.org/10.1007/s11356-020-08051-5

Arber, D. A., Orazi, A., Hasserjian, R., Thiele, J., Borowitz, M. J., Le Beau, M. M., Bloomfield, C. D., Cazzola, M., & Vardiman, J. W. (2016). The 2016 revision to the World Health Organization classification of myeloid neoplasms and acute leukemia. *Blood*, *127*(20), 2391-2405. https://doi.org/https://doi.org/10.1182/blood-2016-03-643544

Asghar, F., Badshah, A., Lal, B., Zubair, S., Fatima, S., & Butler, I. S. (2017). Facile synthesis of fluoro, methoxy, and methyl substituted ferrocene-based urea complexes as potential therapeutic agents. *Bioorganic Chemistry*, *72*, 215-227. https://doi.org/https://doi.org/10.1016/j.bioorg.2017.04.016

Astruc, D. (2017). Why is Ferrocene so Exceptional? [https://doi.org/10.1002/ejic.201600983]. *European Journal of Inorganic Chemistry*, *2017*(1), 6-29. https://doi.org/https://doi.org/10.1002/ejic.201600983

Baeriswyl, V., & Christofori, G. (2009). The angiogenic switch in carcinogenesis. *Seminars in Cancer Biology*, *19*(5), 329-337. https://doi.org/https://doi.org/10.1016/j.semcancer.2009.05.003

Bangham, A. D. (1993). Liposomes: the Babraham connection. *Chemistry and Physics of Lipids*, *64*(1), 275-285. https://doi.org/https://doi.org/10.1016/0009-3084(93)90071-A

Bangham, A. D., Standish, M. M., & Watkins, J. C. (1965). Diffusion of univalent ions across the lamellae of swollen phospholipids. *Journal of Molecular Biology*, *13*(1), 238-IN227. https://doi.org/https://doi.org/10.1016/S0022-2836(65)80093-6

Beller, M. B., H. . (2012). *Organometallics as catalysts in the fine chemical industry.* . Springer.

Bielenica, A., Stefańska, J., Stępień, K., Napiórkowska, A., Augustynowicz-Kopeć, E., Sanna, G., Madeddu, S., Boi, S., Giliberti, G., Wrzosek, M., & Struga, M. (2015). Synthesis, cytotoxicity and antimicrobial activity of thiourea derivatives incorporating 3-(trifluoromethyl)phenyl moiety. *European Journal of Medicinal Chemistry*, *101*, 111-125. https://doi.org/https://doi.org/10.1016/j.ejmech.2015.06.027

Bispo, J. A. B., Pinheiro, P. S., & Kobetz, E. K. (2020). Epidemiology and Etiology of Leukemia and Lymphoma. *Cold Spring Harbor perspectives in medicine*, *10*(6), a034819. https://doi.org/10.1101/cshperspect.a034819

Blackburn, L. M., Bender, S., & Brown, S. (2019). Acute Leukemia: Diagnosis and Treatment. *Seminars in Oncology Nursing*, *35*(6), 150950. https://doi.org/https://doi.org/10.1016/j.soncn.2019.150950

Blasco, M. A. (2005). Telomeres and human disease: ageing, cancer and beyond. *Nature Reviews Genetics*, *6*(8), 611-622. https://doi.org/10.1038/nrg1656

Briot, T., Roger, E., Thépot, S., & Lagarce, F. (2018). Advances in treatment formulations for acute myeloid leukemia. *Drug Discovery Today*, *23*(12), 1936-1949. https://doi.org/https://doi.org/10.1016/j.drudis.2018.05.040

Brooks, C. L., & Gu, W. (2011). p53 regulation by ubiquitin. *FEBS Letters*, *585*(18), 2803-2809. https://doi.org/https://doi.org/10.1016/j.febslet.2011.05.022

Bukhari, S., Siddique, M. H., Naeem, A., Khan, I., Ali, Z., Essa, A., Fazal, F., Anis, R. A., Moran, L., Sultan, A., Murtaza, I., Vanhara, P., & Anees, M. (2022). Combined efficacy of Cinnamomum zeylanicum and doxorubicin against leukemia through regulation of TRAIL and NF-kappa B pathways in rat model. *Molecular Biology Reports*, *49*(7), 6495-6507. https://doi.org/10.1007/s11033-022-07478-y

Burnett, A. K., Russell, N. H., Hills, R. K., Hunter, A. E., Kjeldsen, L., Yin, J., Gibson, B. E. S., Wheatley, K., & Milligan, D. (2013). Optimization of Chemotherapy for Younger Patients With Acute Myeloid Leukemia: Results of the Medical Research Council AML15 Trial. *Journal of Clinical Oncology*, *31*(27), 3360-3368. https://doi.org/10.1200/JCO.2012.47.4874

Cancer Genome Atlas Research, N., Ley, T. J., Miller, C., Ding, L., Raphael, B. J., Mungall, A. J., Robertson, A. G., Hoadley, K., Triche, T. J., Jr., Laird, P. W., Baty, J. D., Fulton, L. L., Fulton, R., Heath, S. E., Kalicki-Veizer, J., Kandoth, C., Klco, J. M., Koboldt, D. C., Kanchi, K.-L., . . . Eley, G. (2013). Genomic and epigenomic landscapes of adult de novo acute myeloid leukemia. *The New England Journal Of Medicine*, *368*(22), 2059-2074. https://doi.org/10.1056/NEJMoa1301689

Çeribaşı, A. O., Sakin, F., Türk, G., Sönmez, M., & Ateşşahin, A. (2012). Impact of ellagic acid on adriamycin-induced testicular histopathological lesions, apoptosis, lipid peroxidation and sperm damages. *Experimental and Toxicologic Pathology*, *64*(7), 717-724. https://doi.org/https://doi.org/10.1016/j.etp.2011.01.006

Cho, J. Y. (2008). Suppressive effect of hydroquinone, a benzene metabolite, on in vitro inflammatory responses mediated by macrophages, monocytes, and lymphocytes. *Mediators of inflammation*, *2008*, 298010-298010. https://doi.org/10.1155/2008/298010

Christiansen, D. H., Andersen, M. K., Desta, F., & Pedersen-Bjergaard, J. (2005). Mutations of genes in the receptor tyrosine kinase (RTK)/RAS-BRAF signal transduction pathway in

therapy-related myelodysplasia and acute myeloid leukemia. *Leukemia*, *19*(12), 2232-2240. https://doi.org/10.1038/sj.leu.2404009

Chulián, S., Martínez-Rubio, Á., Rosa, M., & Pérez-García, V. M. (2022). Mathematical models of leukaemia and its treatment: a review. *SeMA Journal*, *79*(3), 441-486. https://doi.org/10.1007/s40324-022-00296-z

Clogston, J. D., & Patri, A. K. (2011). Zeta Potential Measurement. In S. E. McNeil (Ed.), *Characterization of Nanoparticles Intended for Drug Delivery* (pp. 63-70). Humana Press. https://doi.org/10.1007/978-1-60327-198-1_6

Dai, L.-X., Tu, T., You, S.-L., Deng, W.-P., & Hou, X.-L. (2003). Asymmetric Catalysis with Chiral Ferrocene Ligands. *Accounts of Chemical Research*, *36*(9), 659-667. https://doi.org/10.1021/ar020153m

Daraee, H., Etemadi, A., Kouhi, M., Alimirzalu, S., & Akbarzadeh, A. (2016). Application of liposomes in medicine and drug delivery. *Artificial Cells, Nanomedicine, and Biotechnology*, *44*(1), 381-391. https://doi.org/10.3109/21691401.2014.953633

Denel-Bobrowska, M., & Marczak, A. (2017). Structural modifications in the sugar moiety as a key to improving the anticancer effectiveness of doxorubicin. *Life Sciences*, *178*, 1-8. https://doi.org/https://doi.org/10.1016/j.lfs.2017.04.009

Deshpande, P. P., Biswas, S., & Torchilin, V. P. (2013). Current trends in the use of liposomes for tumor targeting. *Nanomedicine*, *8*(9), 1509-1528. https://doi.org/10.2217/nnm.13.118

Dobrovolskaia, M., Clogston, J., Neun, B., Hall, J., Patri, A., & McNeil, S. (2008). Method for Analysis of Nanoparticle Hemolytic Properties In Vitro. *Nano letters*, *8*, 2180-2187. https://doi.org/10.1021/nl0805615

Doğan, Ş. D., Gündüz, M. G., Doğan, H., Krishna, V. S., Lherbet, C., & Sriram, D. (2020). Design and synthesis of thiourea-based derivatives as Mycobacterium tuberculosis growth and enoyl acyl carrier protein reductase (InhA) inhibitors. *European Journal of Medicinal Chemistry*, *199*, 112402. https://doi.org/https://doi.org/10.1016/j.ejmech.2020.112402

Döhner, H., Estey, E. H., Amadori, S., Appelbaum, F. R., Büchner, T., Burnett, A. K., Dombret, H., Fenaux, P., Grimwade, D., Larson, R. A., Lo-Coco, F., Naoe, T., Niederwieser, D., Ossenkoppele, G. J., Sanz, M. A., Sierra, J., Tallman, M. S., Löwenberg, B., & Bloomfield, C. D. (2010). Diagnosis and management of acute myeloid leukemia in adults: recommendations from an international expert panel, on behalf of the European LeukemiaNet. *Blood*, *115*(3), 453-474. https://doi.org/10.1182/blood-2009-07-235358

Döhner, H., Wei, A. H., Appelbaum, F. R., Craddock, C., DiNardo, C. D., Dombret, H., Ebert, B. L., Fenaux, P., Godley, L. A., Hasserjian, R. P., Larson, R. A., Levine, R. L., Miyazaki, Y., Niederwieser, D., Ossenkoppele, G., Röllig, C., Sierra, J., Stein, E. M., Tallman, M. S., . . . Löwenberg, B. (2022). Diagnosis and management of AML in adults: 2022 recommendations from an international expert panel on behalf of the ELN. *Blood*, *140*(12), 1345-1377. https://doi.org/https://doi.org/10.1182/blood.2022016867

Döhner, H., Wei, A. H., & Löwenberg, B. (2021). Towards precision medicine for AML. *Nature Reviews Clinical Oncology*, *18*(9), 577-590. https://doi.org/10.1038/s41571-021-00509-w

Dumas, P.-Y., Bertoli, S., Bérard, E., Leguay, T., Tavitian, S., Galtier, J., Alric, C., Bidet, A., Delabesse, E., Rieu, J. B., Vial, J.-P., Vergez, F., Lechevalier, N., Luquet, I., Klein, E., Sarry, A., Rey, H., de Grande, A.-C., Despas, F., . . . Récher, C. (2020). Delivering HDAC over 3 or 5 days as consolidation in AML impacts health care resource consumption but not outcome. *Blood advances*, *4*(16), 3840-3849. https://doi.org/10.1182/bloodadvances.2020002511

Duong, V.-A., Nguyen, T.-T.-L., & Maeng, H.-J. (2023). Recent Advances in Intranasal Liposomes for Drug, Gene, and Vaccine Delivery. *Pharmaceutics*, *15*(1).

Eid, M. M. A., Rashed, A. N. Z., Bulbul, A. A.-M., & Podder, E. (2021). Mono-Rectangular Core Photonic Crystal Fiber (MRC-PCF) for Skin and Blood Cancer Detection. *Plasmonics*, *16*(3), 717-727. https://doi.org/10.1007/s11468-020-01334-0

El-Shakour, A. A., El-Ebiarie, A. S., Ibrahim, Y. H., Moneim, A. E. A., & El-Mekawy, A. (2015). Effect of exposure to Benzene on oxidative stress and the functions of liver and kidney of male Albino Rat. *Journal of Environmental and Occupational Science*, *4*, 34-39.

Estey, E. (2016). Acute myeloid leukemia: 2016 Update on risk-stratification and management [https://doi.org/10.1002/ajh.24439]. *American Journal of Hematology*, *91*(8), 824-846. https://doi.org/https://doi.org/10.1002/ajh.24439

Fabbrizzi, L. (2020). The ferrocenium/ferrocene couple: a versatile redox switch. *ChemTexts*, *6*(4), 22. https://doi.org/10.1007/s40828-020-00119-6

Farooq, A., Iqbal, A., Rana, N. F., Fatima, M., Maryam, T., Batool, F., Rehman, Z., Menaa, F., Azhar, S., Nawaz, A., Amin, F., Mohammedsaleh, Z. M., & Alrdahe, S. S. (2022). A Novel Sprague-Dawley Rat Model Presents Improved NASH/NAFLD Symptoms with PEG Coated Vitexin Liposomes. *International Journal of Molecular Sciences*, *23*(6).

Fiorina, V. J., Dubois, R. J., & Brynes, S. (1978). Ferrocenyl polyamines as agents for the chemoimmunotherapy of cancer. *Journal of Medicinal Chemistry*, *21*(4), 393-395. https://doi.org/10.1021/jm00202a016

Gabizon, A., Shmeeda, H., & Barenholz, Y. (2003). Pharmacokinetics of Pegylated Liposomal Doxorubicin. *Clinical Pharmacokinetics*, *42*(5), 419-436. https://doi.org/10.2165/00003088-200342050-00002

Galluzzi, L., & Kroemer, G. (2008). Necroptosis: A Specialized Pathway of Programmed Necrosis. *Cell*, *135*(7), 1161-1163. https://doi.org/https://doi.org/10.1016/j.cell.2008.12.004

Gamal Abdul, H. (2013). Acute Leukemia Clinical Presentation. In G. Margarita & B. Gueorgui (Eds.), *Leukemia* (pp. Ch. 3). IntechOpen. https://doi.org/10.5772/53531

Gasser, G., Ott, I., & Metzler-Nolte, N. (2011). Organometallic Anticancer Compounds. *Journal of Medicinal Chemistry*, *54*(1), 3-25. https://doi.org/10.1021/jm100020w

Ghorab, M. M., Alsaid, M. S., Al-Dosary, M. S., Nissan, Y. M., & Attia, S. M. (2016). Design, synthesis and anticancer activity of some novel thioureido-benzenesulfonamides incorporated biologically active moieties. *Chemistry Central Journal*, *10*(1), 19. https://doi.org/10.1186/s13065-016-0161-4

Golabi-Habashi, N., Salimi, A., & Malekinejad, H. (2021). Quercetin attenuated the Benzene-induced hemato- and hepatotoxicity in mice. *Toxicology Reports*, *8*, 1569-1575. https://doi.org/https://doi.org/10.1016/j.toxrep.2021.08.001

Gutschner, T., & Diederichs, S. (2012). The hallmarks of cancer. *RNA Biology*, *9*(6), 703-719. https://doi.org/10.4161/rna.20481

Hamera, R. (2015). Ferrocene. *Synlett*, *26*, 2047 - 2048.

Hameroff, S. (2022). Consciousness, Cognition and the Neuronal Cytoskeleton – A New Paradigm Needed in Neuroscience. *Frontiers in Molecular Neuroscience*, *15*, 869935. https://doi.org/10.3389/fnmol.2022.869935

Hanahan, D., & Weinberg, R. A. (2000). The Hallmarks of Cancer. *Cell*, *100*(1), 57-70. https://doi.org/https://doi.org/10.1016/S0092-8674(00)81683-9

Hanahan, D., & Weinberg, Robert A. (2011). Hallmarks of Cancer: The Next Generation. *Cell*, *144*(5), 646-674. https://doi.org/https://doi.org/10.1016/j.cell.2011.02.013

Hanušová, V., Boušová, I., & Skálová, L. (2011). Possibilities to increase the effectiveness of doxorubicin in cancer cells killing. *Drug Metabolism Reviews*, *43*(4), 540-557. https://doi.org/10.3109/03602532.2011.609174

Hartmut Döhner, M. D., Daniel J. Weisdorf, M.D., and Clara D. Bloomfield, M.D. (2015). Acute Myeloid Leukemia. *The New England Journal Of Medicine*. https://www.nejm.org/doi/10.1056/NEJMra1406184?url_ver=Z39.88-2003&rfr_id=ori:rid:crossref.org&rfr_dat=cr_pub%20%200pubmed

Henderson, A. P., Bleasdale, C., Delaney, K., Lindstrom, A. B., Rappaport, S. M., Waidyanatha, S., Watson, W. P., & Golding, B. T. (2005). Evidence for the formation of Michael adducts from reactions of (E,E)-muconaldehyde with glutathione and other thiols. *Bioorganic Chemistry*, *33*(5), 363-373. https://doi.org/https://doi.org/10.1016/j.bioorg.2005.05.004

Hendrik, J. M. d. J., Peter, J. M. V., Eveline, S. J. M. d. B., Jan Jacob, S., Gert, O., Edo, V., & Gerwin, H. (2011). Prognostic impact of white blood cell count in intermediate risk acute myeloid leukemia: relevance of mutated NPM1 and FLT3-ITD. *Haematologica*, *96*(9), 1310-1317. https://doi.org/10.3324/haematol.2011.040592

Henson, J. D., Cao, Y., Huschtscha, L. I., Chang, A. C., Au, A. Y. M., Pickett, H. A., & Reddel, R. R. (2009). DNA C-circles are specific and quantifiable markers of alternative-lengthening-of-telomeres activity. *Nature Biotechnology*, *27*(12), 1181-1185. https://doi.org/10.1038/nbt.1587

Hillard, E., Vessières, A., Thouin, L., Jaouen, G., & Amatore, C. (2006). Ferrocene-Mediated Proton-Coupled Electron Transfer in a Series of Ferrocifen-Type Breast-Cancer Drug Candidates [https://doi.org/10.1002/anie.200502925]. *Angewandte Chemie International Edition*, *45*(2), 285-290. https://doi.org/https://doi.org/10.1002/anie.200502925

Hilmer, S. N., Cogger, V. C., Muller, M., & Le Couteur, D. G. (2004). THE HEPATIC PHARMACOKINETICS OF DOXORUBICIN AND LIPOSOMAL DOXORUBICIN. *Drug Metabolism and Disposition*, *32*(8), 794. https://doi.org/10.1124/dmd.32.8.794

Holban, A., & Grumezescu, A. (2016). *Nanoarchitectonics for Smart Delivery and Drug Targeting*.

Hottin, A., Dubar, F., Steenackers, A., Delannoy, P., Biot, C., & Behr, J.-B. (2012). Iminosugar–ferrocene conjugates as potential anticancer agents [10.1039/C2OB25727K]. *Organic & Biomolecular Chemistry*, *10*(29), 5592-5597. https://doi.org/10.1039/C2OB25727K

Huls, G., Chitu, D. A., Havelange, V., Jongen-Lavrencic, M., van de Loosdrecht, A. A., Biemond, B. J., Sinnige, H., Hodossy, B., Graux, C., Kooy, R. v. M., de Weerdt, O., Breems, D., Klein, S., Kuball, J., Deeren, D., Terpstra, W., Vekemans, M.-C., Ossenkoppele, G. J., Vellenga, E., . . . the Dutch-Belgian Hemato-Oncology Cooperative, G. (2019). Azacitidine maintenance after intensive chemotherapy improves DFS in older AML patients. *Blood*, *133*(13), 1457-1464. https://doi.org/10.1182/blood-2018-10-879866

Hussain, S., Badshah, A., Lal, B., Hussain, R. A., Ali, S., Tahir, M. N., & Altaf, A. A. (2014). New supramolecular ferrocene incorporated N,N′-disubstituted thioureas: synthesis, characterization, DNA binding, and antioxidant studies. *Journal of Coordination Chemistry*, *67*(12), 2148-2159. https://doi.org/10.1080/00958972.2014.934819

Ibrahim, M., Abuwatfa, W. H., Awad, N. S., Sabouni, R., & Husseini, G. A. (2022). Encapsulation, Release, and Cytotoxicity of Doxorubicin Loaded in Liposomes, Micelles, and Metal-Organic Frameworks: A Review. *Pharmaceutics*, *14*(2).

Iskander, K., & Jaiswal, A. K. (2005). Quinone oxidoreductases in protection against myelogenous hyperplasia and benzene toxicity. *Chemico-Biological Interactions*, *153-154*, 147-157. https://doi.org/https://doi.org/10.1016/j.cbi.2005.03.019

Issa, H., Swart, L. E., Rasouli, M., Ashtiani, M., Nakjang, S., Jyotsana, N., Schuschel, K., Heuser, M., Blair, H., & Heidenreich, O. (2023). Nanoparticle-mediated targeting of the fusion gene RUNX1/ETO in t(8;21)-positive acute myeloid leukaemia. *Leukemia*, *37*(4), 820-834. https://doi.org/10.1038/s41375-023-01854-8

Jaramillo, S., Benner, A., Krauter, J., Martin, H., Kindler, T., Bentz, M., Salih, H. R., Held, G., Köhne, C. H., Götze, K., Lübbert, M., Kündgen, A., Brossart, P., Wattad, M., Salwender, H., Hertenstein, B., Nachbaur, D., Wulf, G., Horst, H. A., . . . for the German-Austrian Acute Myeloid Leukemia Study, G. (2017). Condensed versus standard schedule of high-dose cytarabine consolidation therapy with pegfilgrastim growth factor support in acute myeloid leukemia. *Blood Cancer Journal*, *7*(5), e564-e564. https://doi.org/10.1038/bcj.2017.45

Jawad, B., Poudel, L., Podgornik, R., Steinmetz, N. F., & Ching, W.-Y. (2019). Molecular mechanism and binding free energy of doxorubicin intercalation in DNA [10.1039/C8CP06776G]. *Physical Chemistry Chemical Physics*, *21*(7), 3877-3893. https://doi.org/10.1039/C8CP06776G

Jentzsch, M., Grimm, J., Bill, M., Brauer, D., Backhaus, D., Goldmann, K., Schulz, J., Niederwieser, D., Platzbecker, U., & Schwind, S. (2021). ELN risk stratification and outcomes in secondary and therapy-related AML patients consolidated with allogeneic stem cell transplantation. *Bone Marrow Transplantation*, *56*(4), 936-945. https://doi.org/10.1038/s41409-020-01129-1

Joshi, M., & Bhattacharyya, A. (2008). Characterization techniques for nanotechnology applications in textiles. *Indian Journal of Fibre and Textile Research*, *33*, 304-317.

Kalepu, S., & Nekkanti, V. (2015). Insoluble drug delivery strategies: review of recent advances and business prospects. *Acta Pharmaceutica Sinica B*, *5*(5), 442-453. https://doi.org/https://doi.org/10.1016/j.apsb.2015.07.003

Kang, Y., Assuncao, B. L., Denduluri, S., McCurdy, S., Luger, S., Lefebvre, B., Carver, J., & Scherrer-Crosbie, M. (2019). Symptomatic Heart Failure in Acute Leukemia Patients Treated With Anthracyclines. *JACC: CardioOncology*, *1*(2), 208-217. https://doi.org/https://doi.org/10.1016/j.jaccao.2019.10.008

Kaymakçıoğlu, B. K., Rollas, S., Körceğez, E., & Arıcıoğlu, F. (2005). Synthesis and biological evaluation of new N-substituted-N'-(3,5-di/1,3,5-trimethylpyrazole-4-yl)thiourea/urea derivatives. *European Journal of Pharmaceutical Sciences*, *26*(1), 97-103. https://doi.org/https://doi.org/10.1016/j.ejps.2005.05.005

Kayser, S., Döhner, K., Krauter, J., Köhne, C.-H., Horst, H. A., Held, G., von Lilienfeld-Toal, M., Wilhelm, S., Kündgen, A., Götze, K., Rummel, M., Nachbaur, D., Schlegelberger, B., Göhring, G., Späth, D., Morlok, C., Zucknick, M., Ganser, A., Döhner, H., . . . AMLSG, f. t. G.-A. (2011). The impact of therapy-related acute myeloid leukemia (AML) on outcome in 2853 adult patients with newly diagnosed AML. *Blood*, *117*(7), 2137-2145. https://doi.org/10.1182/blood-2010-08-301713

Khalade, A., Jaakkola, M. S., Pukkala, E., & Jaakkola, J. J. K. (2010). Exposure to benzene at work and the risk of leukemia: a systematic review and meta-analysis. *Environmental Health*, *9*(1), 31. https://doi.org/10.1186/1476-069X-9-31

Kitanovic, I., Can, S., Alborzinia, H., Kitanovic, A., Pierroz, V., Leonidova, A., Pinto, A., Spingler, B., Ferrari, S., Molteni, R., Steffen, A., Metzler-Nolte, N., Wölfl, S., & Gasser, G. (2014). A Deadly Organometallic Luminescent Probe: Anticancer Activity of a ReI Bisquinoline Complex [https://doi.org/10.1002/chem.201304012]. *Chemistry – A European Journal*, *20*(9), 2496-2507. https://doi.org/https://doi.org/10.1002/chem.201304012

Kohli, A. G., Kierstead, P. H., Venditto, V. J., Walsh, C. L., & Szoka, F. C. (2014). Designer lipids for drug delivery: From heads to tails. *Journal of Controlled Release*, *190*, 274-287. https://doi.org/https://doi.org/10.1016/j.jconrel.2014.04.047

Kollu, U., Avula, V. K. R., Vallela, S., Pasupuleti, V. R., Zyryanov, G. V., Neelam, Y. S., & Chamarthi, N. R. (2021). Synthesis, antioxidant activity and bioinformatics studies of L-3-hydroxytyrosine templated N-alkyl/aryl substituted urea/thioureas. *Bioorganic Chemistry*, *111*, 104837. https://doi.org/https://doi.org/10.1016/j.bioorg.2021.104837

Kovač, V., Kodrin, I., Radošević, K., Molčanov, K., Adhikari, B., Kraatz, H.-B., & Barišić, L. (2022). Oxalamide-Bridged Ferrocenes: Conformational and Gelation Properties and In Vitro Antitumor Activity. *Organometallics*, *41*(8), 920-936. https://doi.org/10.1021/acs.organomet.1c00661

Kumar, A., Badde, S., Kamble, R., & Pokharkar, V. (2010). Development and characterization of liposomal drug delivery system for Nimesulide. *International Journal of Pharmacy and Pharmaceutical Sciences*, *2*, 87-89.

Ladines-Castro, W., Barragán-Ibañez, G., Luna-Pérez, M. A., Santoyo-Sánchez, A., Collazo-Jaloma, J., Mendoza-García, E., & Ramos-Peñafiel, C. O. (2016). Morphology of leukaemias. *Revista Médica del Hospital General de México*, *79*(2), 107-113. https://doi.org/https://doi.org/10.1016/j.hgmx.2015.06.007

Lahoti, A., Kantarjian, H., Salahudeen, A. K., Ravandi, F., Cortes, J. E., Faderl, S., O'Brien, S., Wierda, W., & Mattiuzzi, G. N. (2010). Predictors and outcome of acute kidney injury in patients with acute myelogenous leukemia or high-risk myelodysplastic syndrome. *Cancer*, *116*(17), 4063-4068. https://doi.org/10.1002/cncr.25306

Lal Bhatia, D. B., Altaf, A., Badshah, A., Hussain, R. A., & Li, H. (2016). Synthesis, Crystal Structure, Spectral And Electrochemical Characterization, DNA Binding and Antioxidant studies of 1-(2- florobenzoyl)-3-(2-chloro, 4-ferrocenylphenyl) thiourea. *International journal of electrochemical science*, *11*, 1632-1639.

Larik, F. A., Saeed, A., Fattah, T. A., Muqadar, U., & Channar, P. A. (2017). Recent advances in the synthesis, biological activities and various applications of ferrocene derivatives [https://doi.org/10.1002/aoc.3664]. *Applied Organometallic Chemistry*, *31*(8), e3664. https://doi.org/https://doi.org/10.1002/aoc.3664

Levine, B., & Kroemer, G. (2008). Autophagy in the Pathogenesis of Disease. *Cell*, *132*(1), 27-42. https://doi.org/https://doi.org/10.1016/j.cell.2007.12.018

Li, B., Li, Y. Q., Yang, L. J., Chen, S. H., Yu, W., Chen, J. Y., & Liu, W. W. (2009). Decreased T-cell receptor excision DNA circles in peripheral blood mononuclear cells among benzene-exposed workers. *International Journal of Immunogenetics*, *36*(2), 107-111. https://doi.org/https://doi.org/10.1111/j.1744-313X.2009.00832.x

Li, C., Yang, H., Xie, J., Wang, K., Li, J., & Zhang, Q. (2020). Ferrocene-Based Mixed-Valence Metal–Organic Framework as an Efficient and Stable Cathode for Lithium-Ion-Based Dual-Ion Battery. *ACS Applied Materials & Interfaces*, *12*(29), 32719-32725. https://doi.org/10.1021/acsami.0c07729

Li, H.-Q., Yan, T., Yang, Y., Shi, L., Zhou, C.-F., & Zhu, H.-L. (2010). Synthesis and structure–activity relationships of N-benzyl-N-(X-2-hydroxybenzyl)-N'-phenylureas and thioureas as antitumor agents. *Bioorganic & Medicinal Chemistry*, *18*(1), 305-313. https://doi.org/https://doi.org/10.1016/j.bmc.2009.10.054

Li, J., Wang, X., Zhang, T., Wang, C., Huang, Z., Luo, X., & Deng, Y. (2015). A review on phospholipids and their main applications in drug delivery systems. *Asian Journal of Pharmaceutical Sciences*, *10*(2), 81-98. https://doi.org/https://doi.org/10.1016/j.ajps.2014.09.004

Lindsey, R. H., Bender, R. P., & Osheroff, N. (2005). Effects of Benzene Metabolites on DNA Cleavage Mediated by Human Topoisomerase IIα: 1,4-Hydroquinone Is a Topoisomerase II Poison. *Chemical Research in Toxicology*, *18*(4), 761-770. https://doi.org/10.1021/tx049659z

Liu, S. (2012). Epigenetics advancing personalized nanomedicine in cancer therapy. *Advanced Drug Delivery Reviews*, *64*(13), 1532-1543. https://doi.org/https://doi.org/10.1016/j.addr.2012.08.004

Liu, S., Louie, M. C., Rajagopalan, V., Zhou, G., Ponce, E., Nguyen, T., & Green, L. (2015). Synthesis and evaluation of the diarylthiourea analogs as novel anti-cancer agents.

Bioorganic & Medicinal Chemistry Letters, *25*(6), 1301-1305. https://doi.org/https://doi.org/10.1016/j.bmcl.2015.01.042

López-Dávila, V., Seifalian, A. M., & Loizidou, M. (2012). Organic nanocarriers for cancer drug delivery. *Current Opinion in Pharmacology*, *12*(4), 414-419. https://doi.org/https://doi.org/10.1016/j.coph.2012.02.011

Lv, P.-C., Li, H.-Q., Sun, J., Zhou, Y., & Zhu, H.-L. (2010). Synthesis and biological evaluation of pyrazole derivatives containing thiourea skeleton as anticancer agents. *Bioorganic & Medicinal Chemistry*, *18*(13), 4606-4614. https://doi.org/https://doi.org/10.1016/j.bmc.2010.05.034

Maalik, A., Rahim, H., Saleem, M., Fatima, N., Rauf, A., Wadood, A., Malik, M. I., Ahmed, A., Rafique, H., Zafar, M. N., Riaz, M., Rasheed, L., & Mumtaz, A. (2019). Synthesis, antimicrobial, antioxidant, cytotoxic, antiurease and molecular docking studies of N-(3-trifluoromethyl)benzoyl-N'-aryl thiourea derivatives. *Bioorganic Chemistry*, *88*, 102946. https://doi.org/https://doi.org/10.1016/j.bioorg.2019.102946

MacDonald, G., Rajasekaran, S., Caldwell, C., Udenigwe, C., & Macdonald, M. (2019). Potential Roles of Fatty Acids and Lipids in Postharvest Needle Abscission Physiology. *American Journal of Plant Sciences*, *10*, 1069-1089. https://doi.org/10.4236/ajps.2019.106078

Maryam, T., Rana, N. F., Alshahrani, S. M., Batool, F., Fatima, M., Tanweer, T., Alrdahe, S. S., Alanazi, Y. F., Alsharif, I., Alaryani, F. S., Kashif, A. S., & Menaa, F. (2023). Silymarin Encapsulated Liposomal Formulation: An Effective Treatment Modality against Copper Toxicity Associated Liver Dysfunction and Neurobehavioral Abnormalities in Wistar Rats. *Molecules*, *28*(3), 1514. https://www.mdpi.com/1420-3049/28/3/1514

Mathews, E., Laurie, T., O'Riordan, K., & Nabhan, C. (2008). Liver involvement with acute myeloid leukemia. *Case reports in gastroenterology*, *2*(1), 121-124. https://doi.org/10.1159/000120756

Meng, J., Guo, F., Xu, H., Liang, W., Wang, C., & Yang, X.-D. (2016). Combination Therapy using Co-encapsulated Resveratrol and Paclitaxel in Liposomes for Drug Resistance Reversal in Breast Cancer Cells in vivo. *Scientific Reports*, *6*(1), 22390. https://doi.org/10.1038/srep22390

Mohan, U. P., P.B, T. P., Iqbal, S. T. A., & Arunachalam, S. (2021). Mechanisms of doxorubicin-mediated reproductive toxicity – A review. *Reproductive Toxicology*, *102*, 80-89. https://doi.org/https://doi.org/10.1016/j.reprotox.2021.04.003

Moiseeva, A. A. (September 2018). Anthracycline Derivatives and Their Anticancer Activity. *Journal of Nesmeyanov Institute of Organoelement Compounds of the Russian Academy of Sciences*, *2*(1). http://ineosopen.org/io1902r

Moriuchi, T. (2022). Helical Chirality of Ferrocene Moieties in Cyclic Ferrocene-Peptide Conjugates [https://doi.org/10.1002/ejic.202100902]. *European Journal of Inorganic Chemistry*, *2022*(5), e202100902. https://doi.org/https://doi.org/10.1002/ejic.202100902

Mowafy, S., Galanis, A., Doctor, Z. M., Paranal, R. M., Lasheen, D. S., Farag, N. A., Jänne, P. A., & Abouzid, K. A. M. (2016). Toward discovery of mutant EGFR inhibitors; Design, synthesis and in vitro biological evaluation of potent 4-arylamino-6-ureido and thioureido-quinazoline derivatives. *Bioorganic & Medicinal Chemistry*, *24*(16), 3501-3512. https://doi.org/https://doi.org/10.1016/j.bmc.2016.05.063

Oyaizu, S. (1986). Research on browning substances. *nutrition journal*, *44* 307-315. https://doi.org/https://doi.org/10.5264/eiyogakuzashi.44.307

Parveen, S., Arjmand, F., & Tabassum, S. (2019). Development and future prospects of selective organometallic compounds as anticancer drug candidates exhibiting novel modes of action. *European Journal of Medicinal Chemistry*, *175*, 269-286. https://doi.org/https://doi.org/10.1016/j.ejmech.2019.04.062

Patra, M., & Gasser, G. (2017). The medicinal chemistry of ferrocene and its derivatives. *Nature Reviews Chemistry*, *1*(9), 0066. https://doi.org/10.1038/s41570-017-0066

Pedro Martins, M. M., Lidia Coito, Armando J.L. Pombeiro, Pedro Viana Baptista and Alexandra R. Fernandes. (2014). Organometallic Compounds in Cancer Therapy: Past Lessons and Future Directions. *Bentham Science*, *Volume 14*(9). http://www.eurekaselect.com/article/62075

Powers, D., & Nosoudi, N. (2019). Liposomes; from synthesis to targeting macrophages. *Biomedical Research*, *30*. https://doi.org/10.35841/biomedicalresearch.30-19-058

Puzzarini, C. (2012). Molecular Structure of Thiourea. *The Journal of Physical Chemistry A*, *116*(17), 4381-4387. https://doi.org/10.1021/jp301493b

Qian, X., & Wen-jun, L. (2013). Platelet Changes in Acute Leukemia. *Cell Biochemistry and Biophysics*, *67*(3), 1473-1479. https://doi.org/10.1007/s12013-013-9648-y

Raaschou-Nielsen, O., Hvidtfeldt, U. A., Roswall, N., Hertel, O., Poulsen, A. H., & Sørensen, M. (2018). Ambient benzene at the residence and risk for subtypes of childhood leukemia, lymphoma and CNS tumor [https://doi.org/10.1002/ijc.31421]. *International Journal of Cancer*, *143*(6), 1367-1373. https://doi.org/https://doi.org/10.1002/ijc.31421

Raczynski, P., Dawid, A., Pietek, A., & Gburski, Z. (2006). Reorienatational dynamics of cholesterol molecules in thin film surrounded carbon nanotube: Molecular dynamics simulations. *Journal of Molecular Structure - J MOL STRUCT*, *792*, 216-220. https://doi.org/10.1016/j.molstruc.2006.01.064

Ragab, F. A. F., Abdel-Aziz, S. A., Kamel, M., Ouf, A. M. A., & Allam, H. A. (2019). Design, synthesis and biological evaluation of some new 1,3,4-thiadiazine-thiourea derivatives as potential antitumor agents against non-small cell lung cancer cells. *Bioorganic Chemistry*, *93*, 103323. https://doi.org/https://doi.org/10.1016/j.bioorg.2019.103323

Rasool, M., Farooq, S., Malik, A., Shaukat, A., Manan, A., Asif, M., Sani, S., Qazi, M. H., Kamal, M. A., Iqbal, Z., & Hussain, A. (2015). Assessment of circulating biochemical markers and antioxidative status in acute lymphoblastic leukemia (ALL) and acute myeloid leukemia (AML) patients. *Saudi Journal of Biological Sciences*, *22*(1), 106-111. https://doi.org/https://doi.org/10.1016/j.sjbs.2014.09.002

Riaz, M. K., Riaz, M. A., Zhang, X., Lin, C., Wong, K. H., Chen, X., Zhang, G., Lu, A., & Yang, Z. (2018). Surface Functionalization and Targeting Strategies of Liposomes in Solid Tumor Therapy: A Review. *International Journal of Molecular Sciences*, *19*(1).

Rivedal, E., & Witz, G. (2005). Metabolites of benzene are potent inhibitors of gap-junction intercellular communication. *Archives of Toxicology*, *79*(6), 303-311. https://doi.org/10.1007/s00204-004-0638-0

Röllig, C., Kramer, M., Schliemann, C., Mikesch, J.-H., Steffen, B., Krämer, A., Noppeney, R., Schäfer-Eckart, K., Krause, S. W., Hänel, M., Herbst, R., Kunzmann, V., Einsele, H., Jost, E., Brümmendorf, T. H., Scholl, S., Hochhaus, A., Neubauer, A., Sohlbach, K., . . . Bornhäuser, M. (2020). Does time from diagnosis to treatment affect the prognosis of patients with newly diagnosed acute myeloid leukemia? *Blood*, *136*(7), 823-830. https://doi.org/https://doi.org/10.1182/blood.2019004583

Rose-Inman, H., & Kuehl, D. (2014). Acute Leukemia. *Emergency Medicine Clinics of North America*, *32*(3), 579-596. https://doi.org/https://doi.org/10.1016/j.emc.2014.04.004

Ross, D. (2000). THE ROLE OF METABOLISM AND SPECIFIC METABOLITES IN BENZENE-INDUCED TOXICITY: EVIDENCE AND ISSUES. *Journal of Toxicology and Environmental Health, Part A*, *61*(5-6), 357-372. https://doi.org/10.1080/00984100050166361

Rupapara, V., Rustam, F., Aljedaani, W., Shahzad, H. F., Lee, E., & Ashraf, I. (2022). Blood cancer prediction using leukemia microarray gene data and hybrid logistic vector trees model. *Scientific Reports*, *12*(1), 1000. https://doi.org/10.1038/s41598-022-04835-6

Saeed, A., Erben, M., Abbas, D. N., & Flörke, U. (2010). Synthesis, crystal X-ray diffraction structure, vibrational properties and quantum chemical calculations on 1-(4-(4-Fluorobenzamido)phenyl)-3-(4-fluorobenzoyl)thiourea. *Journal of Molecular Structure*, *984*, 240-245. https://doi.org/10.1016/j.molstruc.2010.09.035

Satyen Saha, R. K. K. a. T. V. S. (2021). Photophysics, Photochemical and Substitution Reactions. In (pp. 230). https://doi.org/10.5772/intechopen.84412

Severson, C. (2016). Hematologic Malignancies in Adults. *Canadian Oncology Nursing Journal*, *26*(2), 177-177. https://www.ncbi.nlm.nih.gov/pmc/articles/PMC6516278/

Shephard, E. A., Neal, R. D., Rose, P. W., Walter, F. M., & Hamilton, W. (2016). Symptoms of adult chronic and acute leukaemia before diagnosis: large primary care case-control studies using electronic records. *The British journal of general practice : the journal of the Royal College of General Practitioners*, *66*(644), e182-e188. https://doi.org/10.3399/bjgp16X683989

Silva, R. C., Britto, D. M. C., de Fátima Pereira, W., Brito-Melo, G. E. A., Machado, C. T., & Pedreira, M. M. (2018). Effect of short- and medium-term toxicity of doxorubicin on spermatogenesis in adult Wistar rats. *Reproductive Biology*, *18*(2), 169-176. https://doi.org/https://doi.org/10.1016/j.repbio.2018.03.002

Singh, A., Maiti, S. K., & Barman, P. (2021). Synthesis, characterization, and DNA binding study of ruthenium(II/III) complexes containing ONS donor Schiff base. *Nucleosides, Nucleotides & Nucleic Acids*, *40*(10), 968-984. https://doi.org/10.1080/15257770.2021.1969023

Smith, M. T. (2010). Advances in Understanding Benzene Health Effects and Susceptibility. *Annual Review of Public Health*, *31*(1), 133-148. https://doi.org/10.1146/annurev.publhealth.012809.103646

Smith, Z., Vidal, G., Machiorlatti, M., Vesely, S. K., Frank, S., Asch, A. S., Holter-Chakrabarty, J. L., Khawandanah, M., & Cherry, M. (2015). Prognostic Significance of Weight Loss and BMI during Induction Chemotherapy of Newly Diagnosed Acute Myeloid Leukemia (AML) Patients. *Blood*, *126*(23), 5625. https://doi.org/https://doi.org/10.1182/blood.V126.23.5625.5625

Snyder, R. (2012). Leukemia and benzene. *International journal of environmental research and public health*, *9*(8), 2875-2893. https://doi.org/10.3390/ijerph9082875

Spencer, J., Amin, J., Wang, M., Packham, G., Alwi, S. S. S., Tizzard, G. J., Coles, S. J., Paranal, R. M., Bradner, J. E., & Heightman, T. D. (2011). Synthesis and Biological Evaluation of JAHAs: Ferrocene-Based Histone Deacetylase Inhibitors. *ACS Medicinal Chemistry Letters*, *2*(5), 358-362. https://doi.org/10.1021/ml100295v

Stefanska, J., Szulczyk, D., Koziol, A. E., Miroslaw, B., Kedzierska, E., Fidecka, S., Busonera, B., Sanna, G., Giliberti, G., La Colla, P., & Struga, M. (2012). Disubstituted thiourea derivatives and their activity on CNS: Synthesis and biological evaluation. *European Journal of Medicinal Chemistry*, *55*, 205-213. https://doi.org/https://doi.org/10.1016/j.ejmech.2012.07.020

Stiufiuc, R., Iacovita, C., Nicoara, R., Stiufiuc, G., Florea, A., Achim, M., & Lucaciu, C. M. (2013). One-Step Synthesis of PEGylated Gold Nanoparticles with Tunable Surface Charge. *Journal of Nanomaterials*, *2013*, 146031. https://doi.org/10.1155/2013/146031

Strekowski, L., & Wilson, B. (2007). Noncovalent interactions with DNA: An overview. *Mutation Research/Fundamental and Molecular Mechanisms of Mutagenesis*, *623*(1), 3-13. https://doi.org/https://doi.org/10.1016/j.mrfmmm.2007.03.008

Subramanya, D., & Grivas, P. D. (2008). HPV and Cervical Cancer: Updates on an Established Relationship. *Postgraduate Medicine*, *120*(4), 7-13. https://doi.org/10.3810/pgm.2008.11.1928

Sung, H., Ferlay, J., Siegel, R. L., Laversanne, M., Soerjomataram, I., Jemal, A., & Bray, F. (2021). Global Cancer Statistics 2020: GLOBOCAN Estimates of Incidence and Mortality

Worldwide for 36 Cancers in 185 Countries. *CA: A Cancer Journal for Clinicians*, *71*(3), 209-249. https://doi.org/https://doi.org/10.3322/caac.21660

Taha, M., Hassan, M., Essa, S., & Tartor, Y. (2013). Use of Fourier transform infrared spectroscopy (FTIR) spectroscopy for rapid and accurate identification of Yeasts isolated from human and animals. *International Journal of Veterinary Science and Medicine*, *1*(1), 15-20. https://doi.org/https://doi.org/10.1016/j.ijvsm.2013.03.001

Takami, A. (2018). Hematopoietic stem cell transplantation for acute myeloid leukemia. *International Journal of Hematology*, *107*(5), 513-518. https://doi.org/10.1007/s12185-018-2412-8

Turan-Zitouni, G., Altıntop, M. D., Özdemir, A., Kaplancıklı, Z. A., Çiftçi, G. A., & Temel, H. E. (2016). Synthesis and evaluation of bis-thiazole derivatives as new anticancer agents. *European Journal of Medicinal Chemistry*, *107*, 288-294. https://doi.org/https://doi.org/10.1016/j.ejmech.2015.11.002

Ugai, T., Matsuo, K., Sawada, N., Iwasaki, M., Yamaji, T., Shimazu, T., Sasazuki, S., Inoue, M., & Tsugane, S. (2017). Smoking and subsequent risk of leukemia in Japan: The Japan Public Health Center-based Prospective Study. *Journal of Epidemiology*, *27*(7), 305-310. https://doi.org/https://doi.org/10.1016/j.je.2016.07.005

Umlauf, J., & Horký, M. (2002). Molecular biology of doxorubicin-induced cardiomyopathy. *Experimental and clinical cardiology*, *7*(1), 35-39. https://pubmed.ncbi.nlm.nih.gov/19644577

https://www.ncbi.nlm.nih.gov/pmc/articles/PMC2716188/

van der Zanden, S. Y., Qiao, X., & Neefjes, J. (2021). New insights into the activities and toxicities of the old anticancer drug doxorubicin [https://doi.org/10.1111/febs.15583]. *The FEBS Journal*, *288*(21), 6095-6111. https://doi.org/https://doi.org/10.1111/febs.15583

Verheijen, J. C., van der Marel, G. A., van Boom, J. H., & Metzler-Nolte, N. (2000). Transition Metal Derivatives of Peptide Nucleic Acid (PNA) OligomersSynthesis, Characterization, and DNA Binding. *Bioconjugate Chemistry*, *11*(6), 741-743. https://doi.org/10.1021/bc0000740

Visconti, P., Primiceri, P., Longo, D., Strafella, L., Carlucci, A. P., Lomascolo, M., Creti, A., & Mele, G. (2017). Photo-ignition process of multiwall carbon nanotubes and ferrocene by continuous wave Xe lamp illumination. *Beilstein Journal of Nanotechnology*, *2017*, 134-144. https://doi.org/10.3762/bjnano.8.14

Vucinic, V., Ruhnke, L., Sockel, K., Röhnert, M. A., Backhaus, D., Brauer, D., Franke, G.-N., Niederwieser, D., Bornhäuser, M., Röllig, C., Platzbecker, U., Schwind, S., & Jentzsch, M. (2021). The diagnostic red blood cell distribution width as a prognostic factor in acute myeloid leukemia. *Blood advances*, *5*(24), 5584-5587. https://doi.org/10.1182/bloodadvances.2021005974

Waidyanatha, S., & Rappaport, S. M. (2005). Investigation of cysteinyl protein adducts of benzene diolepoxide. *Chemico-Biological Interactions*, *153-154*, 261-266. https://doi.org/https://doi.org/10.1016/j.cbi.2005.03.033

Walsh, L. R., Yuan, C., Boothe, J. T., Conway, H. E., Mindiola-Romero, A. E., Barrett-Campbell, O. O., Yerrabothala, S., & Lansigan, F. (2021). Acute myeloid leukemia with hepatic infiltration presenting as obstructive jaundice. *Leukemia research reports*, *15*, 100251-100251. https://doi.org/10.1016/j.lrr.2021.100251

Wang, L. (2023). Editorial for Special Issue “Cancer Treatment via Nanotherapy&rdquo. *Nanomaterials*, *13*(7), 1153. https://www.mdpi.com/2079-4991/13/7/1153

Wu, C. (2014). An important player in brine shrimp lethality bioassay: The solvent. *Journal of advanced pharmaceutical technology & research*, *5*(1), 57-58. https://pubmed.ncbi.nlm.nih.gov/24696818

https://www.ncbi.nlm.nih.gov/pmc/articles/PMC3960796/

Xiao, Y., Liu, Q., Clulow, A. J., Li, T., Manohar, M., Gilbert, E. P., de Campo, L., Hawley, A., & Boyd, B. J. (2019). PEGylation and surface functionalization of liposomes containing drug nanocrystals for cell-targeted delivery. *Colloids and Surfaces B: Biointerfaces*, *182*, 110362. https://doi.org/https://doi.org/10.1016/j.colsurfb.2019.110362

Yau, A., Lee, J., & Chen, Y. (2021). Nanomaterials for Protein Delivery in Anticancer Applications. *Pharmaceutics*, *13*(2).

Yilmaz, M., & Christofori, G. (2009). EMT, the cytoskeleton, and cancer cell invasion. *Cancer and Metastasis Reviews*, *28*(1), 15-33. https://doi.org/10.1007/s10555-008-9169-0

Yoon, J.-H., Kwak, W. S., & Ahn, Y.-S. (2018). A brief review of relationship between occupational benzene exposure and hematopoietic cancer. *Annals of Occupational and Environmental Medicine*, *30*(1), 33. https://doi.org/10.1186/s40557-018-0245-9

Zahra, M., Chota, A., Abrahamse, H., & George, B. P. (2023). Efficacy of Green Synthesized Nanoparticles in Photodynamic Therapy: A Therapeutic Approach. *International Journal of Molecular Sciences*, *24*(13), 10931. https://www.mdpi.com/1422-0067/24/13/10931

Zhang, Q., Yang, Q., Weng, Y., Huang, Z., Chen, R., Zhu, Y., Dai, K., Zhang, S., Jiang, S., & Yu, K. (2021). Neutrophil-to-lymphocyte ratio correlates with prognosis and response to chemotherapy in patients with non-M3 de novo acute myeloid leukemia. *Translational cancer research*, *10*(2), 1013-1024. https://doi.org/10.21037/tcr-20-2179

Zhao, Y.-N., Xu, X., Wen, N., Song, R., Meng, Q., Guan, Y., Cheng, S., Cao, D., Dong, Y., Qie, J., Liu, K., & Zhang, Y. (2017). A Drug Carrier for Sustained Zero-Order Release of Peptide Therapeutics. *Scientific Reports*, *7*(1), 5524. https://doi.org/10.1038/s41598-017-05898-6

Zheng, X., & Bossier, P. (2023). Toxicity assessment and anti-Vibrio activity of essential oils: Potential for application in shrimp aquaculture [https://doi.org/10.1111/raq.12795]. *Reviews in Aquaculture*, *n/a*(n/a). https://doi.org/https://doi.org/10.1111/raq.12795

Zhu, H.-H., Qin, Y.-Z., Zhang, Z.-L., Liu, Y.-J., Wen, L.-J., You, M. J., Zhang, C., Such, E., Luo, H., Yuan, H.-J., Zhou, H.-S., Liu, H.-X., Xu, R., Li, J., Li, J.-H., Hao, J.-P., Jin, J., Yu, L., Zhang, J.-Y., . . . Chen, S.-N. (2023). A global study for acute myeloid leukemia with RARG rearrangement. *Blood advances*, *7*(13), 2972-2982. https://doi.org/10.1182/bloodadvances.2022008364

Zuber, A., Purdey, M., Schartner, E., Forbes, C., van der Hoek, B., Giles, D., Abell, A., Monro, T., & Ebendorff-Heidepriem, H. (2016). Detection of gold nanoparticles with different sizes using absorption and fluorescence based method. *Sensors and Actuators B: Chemical*, *227*, 117-127. https://doi.org/https://doi.org/10.1016/j.snb.2015.12.044